Polysaccharides
DOI 10.1007/978-3-319-03751-6_50-1

Advanced Nano-biocomposites Based on Starch

Fengwei Xie[a]*, Eric Pollet[b], Peter J. Halley[a] and Luc Avérous[b]*
[a]Australian Institute for Bioengineering and Nanotechnology, The University of Queensland, Brisbane, QLD, Australia
[b]BioTeam/ICPEES-ECPM, UMR 7515, Université de Strasbourg, Strasbourg, Cedex 2, France

Abstract

Starch as a biopolymer directly extracted from nature has received much attention in recent years due to its strong advantages such as low cost, wide availability, renewability, and total compostability without toxic residues. Starch-based materials always display properties that are less satisfactory than those of traditional polymer materials, which can be ascribed to the inherent characteristics of starch. To make such materials to be truly competitive and to widen its applications, the development of starch-based nano-biocomposites could be a promising solution. This chapter provides the fundamental knowledge related to starch-based nano-biocomposites as well as the most recent developments in this area. Various types of nanofillers that have been used with plasticized starch are discussed such as montmorillonite, cellulose nanowhiskers, and starch nanoparticles. The preparation strategies for starch-based nano-biocomposites with these types of nanofillers and the corresponding dispersion state and related properties are also largely discussed.

Keywords

Starch; Nanocomposites; Biopolymers; Biodegradable polymers; Bioplastics; Nanoclays; Cellulose nanowhiskers; Starch nanoparticles; Carbon nanotubes

Abbreviations

AFM	Atomic force microscopy
BCNW	Bacterial cellulose nanowhisker
CB	Carbon black
CEC	Cationic exchange capacity
CMC	Carboxymethyl cellulose sodium
CNT	Carbon nanotube
CNW	Cellulose nanowhisker
D	Diameter
d_{001}	Interlayer spacing or *d*-spacing
DMA	Dynamic mechanical analysis
DMSO	Dimethyl sulfoxide

---

*Email: f.xie@uq.edu.au

*Email: fwhsieh@gmail.com

*Email: luc.averous@unistra.fr

DP	Degree of polymerization
FTIR	Fourier transform infrared spectroscopy
G’	Elastic modulus (rheology)
GO	Graphite oxide
HA	Hydroxyapatite
IL	Ionic liquid
L	Length
L/D	Length-to-diameter ratio (i.e., aspect ratio)
LCA	Life-cycle assessment
LDH	Layered double hydroxide
MMT	Montmorillonite
MMT–Na$^+$	Sodium montmorillonite
MWCNT	Multiwall carbon nanotube
O	Octahedral sheets
OMMT	Organomodified montmorillonite
OMMT–CS	Cationic starch–organomodified montmorillonite
PBAT	Poly(butylene adipate-*co*-terephthalate)
PBSA	Poly(butylene succinate-*co*-adipate)
PCL	Polycaprolactone
PEG	Polyethylene glycol
PLA	Poly(lactic acid)/polylactide
PVA	Poly(vinyl alcohol)
REX	Reactive extrusion
SEM	Scanning electron microscopy
SME	Specific mechanical energy
SNP	Starch nanoparticles
SSE	Single-screw extruder
SWCNT	Single-wall carbon nanotube
T	Tetrahedral sheets
TEM	Transmission electron microscopy
T_g	Glass transition temperature
TSE	Twin-screw extruder
UV	Ultraviolet
XRD	X-ray diffraction

1 Introduction

The increasing environmental concerns, the strong decrease of the availability on the market of some conventional refinery fractions which are more or less refined (e.g., isoprene, butadiene, bitumen, etc.), the expected shortage of fossil resources (mainly petroleum), and the necessity to develop innovative materials architectures are some of the main drivers to push the use of biobased compounds extracted from the biomass. Following this mainstream, starch, as a natural polymer from renewable resources, has experienced considerable development in the past decades in nonfood and materials applications (Avérous and Halley 2014). Starch has strong advantages such

DOI 10.1007/978-3-319-03751-6_50-1

as low cost, wide availability, renewability, and total compostability without toxic residues. By using conventional polymer processing techniques such as extrusion, native starch (also known as raw starch) in the form of granules can be transformed into a molten state with the presence of low content of "plasticizers" such as water and glycerol. This converted form of starch is known as "plasticized starch," "thermoplastic starch" (although its behavior is not totally thermoplastic but more thermo-mechano-plastic (Martin et al. 2003)), or abbreviated as "TPS," which can be produced into different end-use forms such as extruded, molded, thermoformed, or blown articles (Liu et al. 2009a).

Despite of the advantages mentioned above, starch-based plastic materials are known to have limitations such as poor processability and limited properties (e.g., weak mechanical properties, large evolution of properties during aging, and high water sensitivity). Formulation development could be the major key to solve these crucial problems. To give some examples, various starch-based blends and biocomposites (i.e., with fillers) have been developed, showing improved performance (Avérous 2004; Avérous and Halley 2009; Kalambur and Rizvi 2006a; Tang and Alavi 2011; Wang et al. 2003; Yu et al. 2006a) compared to the neat matrix. Recently, along with the exponential momentum of the development in polymer nanocomposites (Alexandre and Dubois 2000; Crosby and Lee 2007; Paul and Robeson 2008; Pavlidou and Papaspyrides 2008; Sinha Ray and Okamoto 2003; Sinha Ray and Bousmina 2005; Spitalsky et al. 2010), much attention has been focused on the use of nanosized fillers (at least one dimension in the nanometer range, i.e., 1–100 nm) in producing starch-based nano-biocomposite materials. Their nanosize can generate huge areas at the matrix–filler interface, which largely control the global macrostructures and associated global properties of the corresponding materials. Under certain conditions with the tailored nanofiller and/or organomodification of the nanofiller, nanocomposite materials can exhibit drastic improvement in mechanical behavior, thermal stability, flame retardancy, and gas barrier properties (Alexandre and Dubois 2000). Such property enhancement depends on the nature, geometry, surface area, and surface chemistry of the nanofiller (Sinha Ray and Okamoto 2003).

Unlike most conventional synthetic polymers, starch is a biopolymer directly extracted from biomass, which has unique chemical structure and processing behavior. Therefore, the preparation and properties of starch-based nano-biocomposites are inherently dissimilar to those of other polymer nanocomposite systems. Furthermore, the incorporation of appropriately tuned nanoparticles into starch as a biopolymer may not only enhance the conventional material performance of starch-based materials, but it could also provide new functionalities for new applications due to the resulting novel structures and functional groups. While this chapter aims to provide the basic knowledge of starch and starch-based nano-biocomposites, which should be helpful to those new to this area, it touches some of the most recent international research progress on this topic as well.

2 Starch Characteristics

2.1 Structure of Native Starch

The starch granule provides the main way of storing carbon and energy over long periods in green plants (Pérez et al. 2009). Starch granules are mainly found in seeds, roots, and tubers and display different shapes (spherical, lenticular, and polygonal) depending on their origins such as maize (corn), wheat, potato, and rice. In Fig. 1, an overview of starch granule structure is shown, which presents a concentric three-dimensional architecture from the hilum, with a crystallinity varying from 15 % to 45 % depending on the botanical source (Zobel 1988). The starch granule is well

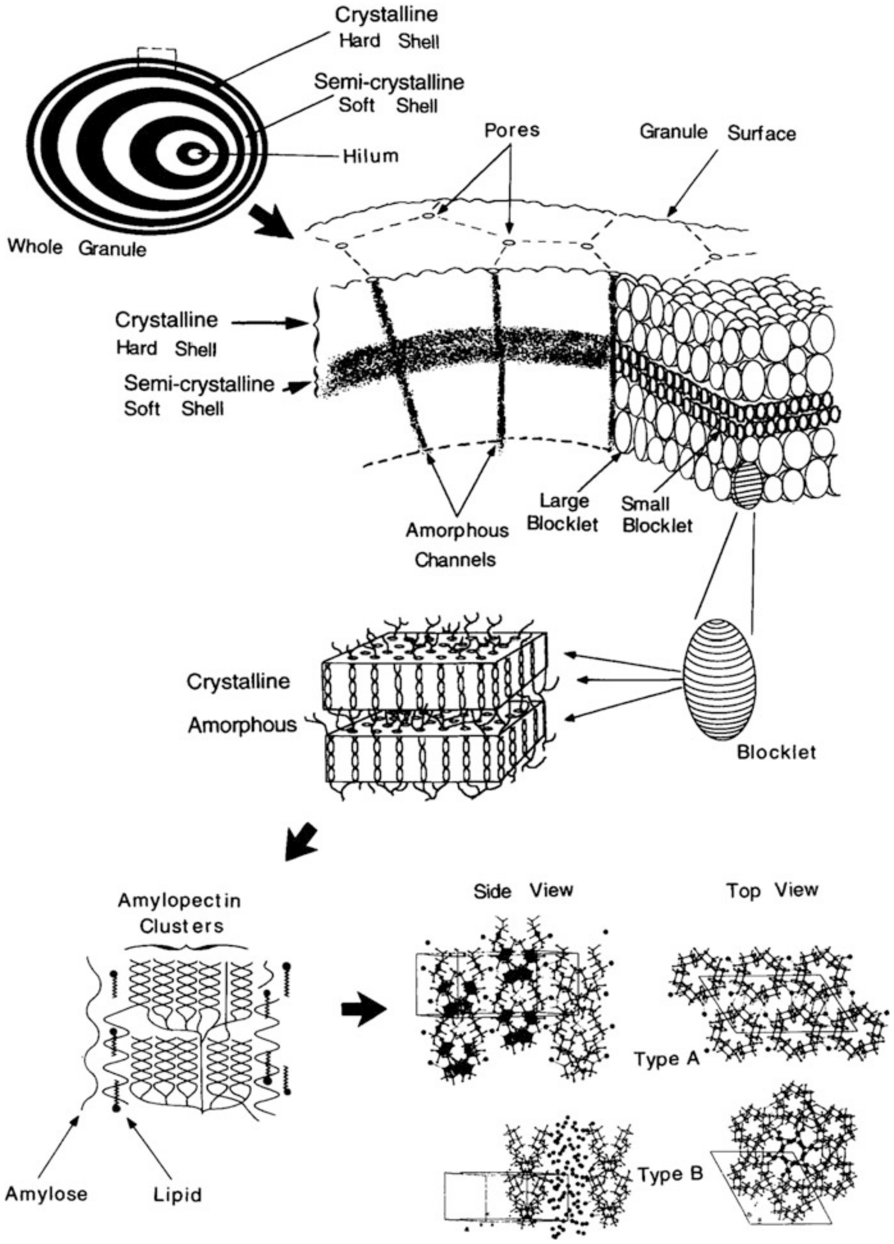

Fig. 1 Overview of starch granule structure. At the lowest level of granule organization (*upper left*), alternating crystalline (*hard*) and semicrystalline (*soft*) shells are shown (*dark and light* colors, respectively). Shells are thinner toward the granule exterior (due to increasing surface area to be added to by constant growth rate) and the hilum is shown off-center. At a higher level of structure, the blocklet structure is shown in association with amorphous radial channels. Blocklet size is smaller in the semicrystalline shells than in the crystalline shells. At the next highest level of structure, one blocklet is shown containing several amorphous crystalline lamellae. In the next diagram, amylopectin is shown in the lamellae. The next image is a reminder of the importance of amylose–lipid (and protein) components in the organization of amylopectin chains. At the highest level of order, crystal structures of the starch polymers are shown (Reprinted from Gallant et al. (1997), Copyright (1997), with permission from Elsevier. Redrawn in Gallant et al. (1997) from Imberty et al. (1988) and Imberty and Perez (1988))

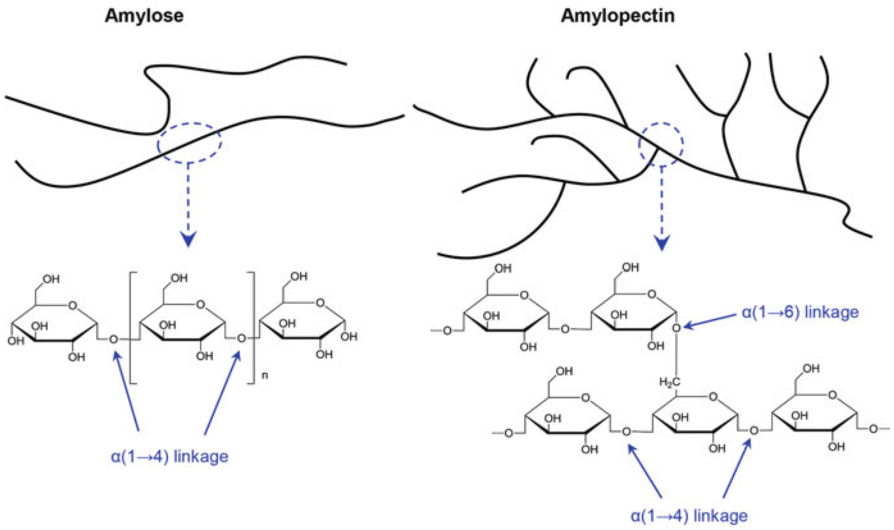

Fig. 2 Chemical structures of amylose and amylopectin molecules of starch

known to possess multilevel structures from macro- to molecular scales, i.e., starch granules (<1–100 μm), alternating amorphous and semicrystalline shells (growth rings) (100–400 nm), crystalline and amorphous lamellae (periodicity) (9–10 nm), and macromolecular chains (∼nm) (Buléon et al. 1998; Jane 2009; Pérez et al. 2009; Pérez and Bertoft 2010).

In molecular level of structure, starch is a polysaccharide consisting of D-glucose units, referred to as homoglucan or glucopyranose. Figure 2 presents the two major biomacromolecules of starch, i.e., amylose and amylopectin. Amylose is a sparsely branched carbohydrate mainly based on α(1–4) bonds with a molar mass of 10^5–10^6 and can have a degree of polymerization (DP) as high as 600 (Pérez et al. 2009). The number of macromolecular configurations based on α(1–6) links is directly proportional to the amylose molar mass (Tako and Hizukuri 2002). The chains show spiral-shaped single or double helices with a rotation on the α(1–4) link and with six glucoses per turn, where the hydroxyl groups are mainly located toward the exterior of the helices. As a result, the core of the helix is mainly hydrophobic. On the other hand, amylopectin is a highly multiple-branched polymer with a high molar mass of 10^7–10^9. It is one of the largest natural polymers on earth (Pérez et al. 2009). Amylopectin is based on α(1–4) (around 95 %) and α(1–6) (around 5 %) links, with constituting branching points localized every 22–70 glucose units, generating a highly branched structure with a lot of pending chains of DP ≈ 15, which are mainly responsible for the materials' crystallinity (between 20 % and 45 %). This specific structure has a profound effect on the physical and biological properties (Pérez et al. 2009; Pérez and Bertoft 2010).

Besides, in starch granules, very small amounts of proteins, lipids, and phosphorus are also found depending on the botanical resource (Jane 2009; Pérez and Bertoft 2010). These components can interact with the carbohydrate chains during processing (e.g., Maillard reaction) and then modify the behavior of the starchy materials.

Depending on the source, amylose content of starch can be varied from <1 % to 83 % (Tan et al. 2007). The so-termed waxy starch contains little or no amylose, whereas high-amylose starch contains >50 % amylose. The amylose content has a great impact on the crystalline structure and degree of crystallinity (Tan et al. 2007), as well as on the thermal, rheological, and processing properties (Li et al. 2011a; Liu et al. 2006, 2011d; Wang et al. 2010a; Xie et al. 2009).

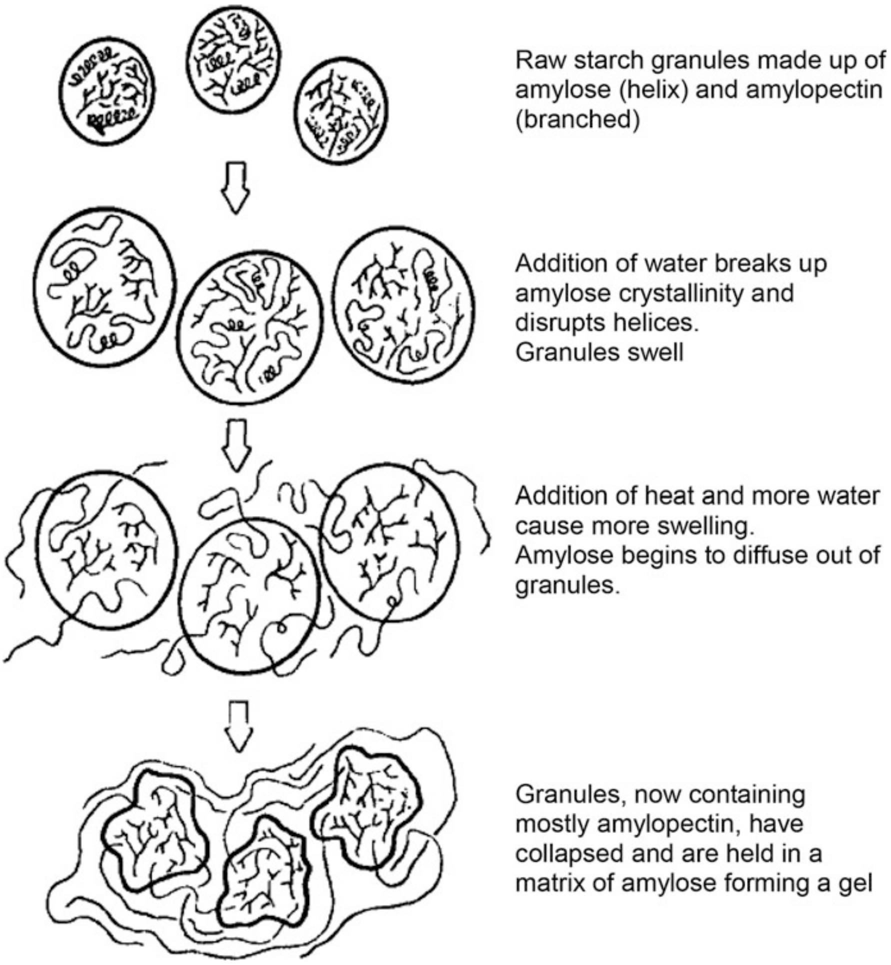

Fig. 3 Mechanism of starch gelatinization (Copyright © 1978 Wiley Periodicals, Inc. Reproduced from Remsen and Clark (1978) with permission)

2.2 Gelatinization/Melting of Native Starch

When native starch granules are heated in water, their semicrystalline nature and three-dimensional architecture are gradually disrupted, resulting in a phase transition from the ordered granular structure into a disordered state in water, which is known as "gelatinization" (Atwell et al. 1988; Lelievre 1974; Ratnayake et al. 2008). The process of gelatinization is schemed in Fig. 3. Gelatinization is an irreversible process that includes, in a broad sense and in time/temperature sequence, granular swelling, native crystalline melting (loss of birefringence, as observed under polarized light), and molecular solubilization (Russo et al. 2009). Full gelatinization of starch under shearless conditions requires excess water, which Wang et al. (1991) have defined as >63 % for waxy maize starch, for example. If the water concentration is too high, the crystallites in starch might be pulled apart by swelling, leaving none to be melted at higher temperature. If the water concentration is limited, the swelling forces will be much less significant and the steric hindrance is high. Thus, complete gelatinization will not occur in the usual temperature range (Lai and Kokini 1991; Liu et al. 2005, 2006). However, as the temperature increases, starch molecules will become progressively more mobile and eventually the crystalline regions will be destructured (Donovan 1979). The process of gelatinization with low water content could more accurately be defined as the "melting" of starch (Lai and Kokini 1991).

DOI 10.1007/978-3-319-03751-6_50-1

The gelatinization/melting behavior of starch is quite different when shear treatment is applied (Xie et al. 2006). With abundant water, shear can enhance the destructuration of starch granules (Chen et al. 2007; Yu et al.2006b). When the water content is limited, shear can assist the melting of crystallites (Wang et al. 2010a; Xie et al. 2008; Xue et al. 2008). The significance of such studies is that most processing techniques for starch involve shear treatment. In extrusion processing (which will be discussed below in Sect. 3.1), shear forces can physically destructure starch granules, allowing faster transfer and distribution of water into the material (Burros et al. 1987). Therefore, during extrusion, the loss of the crystallinity is not only caused by the water penetration but also by mechanical disruption due to the intense shear fields within the extruder (Barron et al. 2001; Wang and Zheng 1995; Zheng and Wang 1994; Zheng et al. 1995).

3 Starch-Based Materials

3.1 Processing Techniques

The techniques that have been used to process starch polymers, such as solution casting, internal mixing, extrusion, injection molding, and compression molding, are similar to those widely used for conventional synthetic thermoplastics. Solution casting has been frequently utilized in the literature as a method to prepare starch-based films for research purposes. However, this technique suffers from disadvantages such as low efficiency and the difficulty in scaling up from the lab scale to the industry and not being considered as a “green process” due to the use of toxic organic solvents and the great consumption of energy for solvent evaporation. Alternatively, extrusion processing is more aligned to modern industrial production. A single-screw extruder (SSE) can handle the high viscosity of starch and provide high processing pressure for continuous metering of starch through a die shape. A twin-screw extruder (TSE) has large operational flexibility (individual barrel zone temperature control, multiple feeding/injection, and screw configuration for different degree of mixing/kneading) and is useful to intensive mixing and compounding of other components into starch plastics. Another advantage of TSE is to allow the decoupling of the die flow and the mechanical treatment. In both SSE and TSE, the residence time and specific mechanical energy (SME) input can be controlled, and high-efficiency production can be achieved. Other processing techniques such as film blowing and injection molding are often combined with the extrusion. More details about the specifics of the processing techniques for starch polymers as well as the recent advances in the understanding of starch processing can be found elsewhere (Liu et al. 2009a; Xie et al. 2014).

A schematic of twin-screw extrusion process for the production of TPS is shown below in Fig. 4 (Xie et al. 2012). The native starch granules are introduced, preferably by a powder gravimetric feeder, into the extruder in a hungry way (i.e., the feeding capacity is less than the conveying capacity of the screws at the feeding port). Liquids (typically plasticizer) could be introduced in a following location, preferably using a pressure-injection way to ensure uniform mixing between the solid(s) and the liquid(s). The granules undergo exposure to high temperatures and pressures in the extruder, resulting in the disruption, and gelatinization/melting, of starch granules (Liu et al. 2006). After gelatinization, the TPS will undergo further melting and compression, which may be increased with increased use of high mixing (kneading or reversing) elements in the screw. It is important to note that degradation of starch molecules also occurs with the thermal mechanical treatment in the extruder, with amylopectin molecules suffering more than amylose (Li et al. 2014; Liu et al. 2010b). And the mechanism for the scission of the polymer chains is believed to preferentially take place close to the center of the molecule, causing the size distribution to narrow

DOI 10.1007/978-3-319-03751-6_50-1

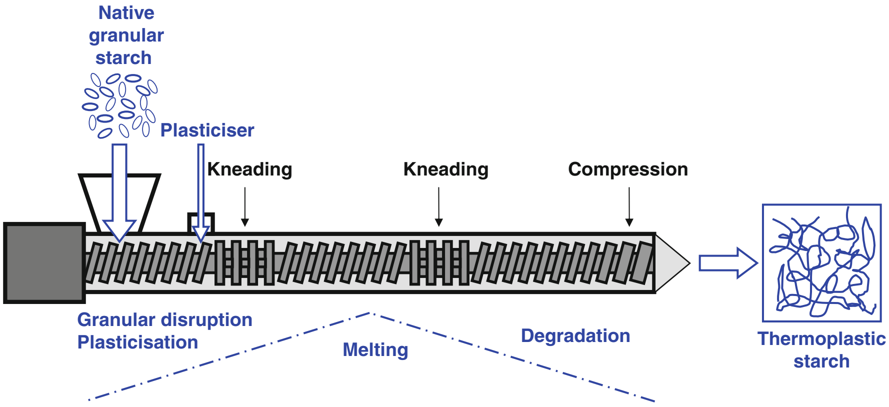

Fig. 4 Schematic representation of starch processing by extrusion (Reprinted from Xie et al. (2012), Copyright (2012), with permission from Elsevier)

and converge toward a maximum stable size (Liu et al. 2010b). The TPS is forced through the extrusion line and finally out of a die at the end of the extruder at a controlled rate (possibly with the aid of a melt pump to further control the flow rate).

3.2 Plasticizers

Water is indispensable for the thermal processing of starch. By reducing the moisture content, the melting temperature of starch would progressively increase, and that of dry starch is often larger than its degradation temperature as extrapolated by Flory Law (Liu et al. 2008; Russell 1987). Water functions by lowering the melting temperature and plasticizing the starch polymers. As a result, in practical processing, water acts as a volatile "plasticizer." Thus, unstable processing or undesirable foaming may be caused due to the evaporation of the water. Furthermore, the final products based on starch containing only water usually have poor mechanical properties especially due to the brittleness, because of its final temperature usually lower than its glass transition temperature (T_g) (Chaudhary et al. 2011b; Enrione et al. 2010; Forssell et al. 1997; Liu et al. 2011b, 2009b, 2010a; Lourdin et al. 1997) and/or resulting from the densification (happening below T_g) or retrogradation (also known as recrystallization, happening above T_g) (Atwell et al. 1988; Bulkin et al. 1987; Gudmundsson 1994; Liu and Thompson 1998). To overcome these issues, nonvolatile (at the processing temperature) plasticizers such as polyols (glycerol, sorbitol, glycol, etc.) (Da Róz et al. 2006; Enrione et al. 2010; Forssell et al. 1997; Gaudin et al. 1999; Kirby et al. 1993; Lin and Tung 2009; Liu et al. 2011d; Lourdin et al. 1997; Mathew and Dufresne 2002a; Nashed et al. 2003; Pushpadass and Hanna 2009; Pushpadass et al. 2009; Qiao et al. 2011; Rodriguez-Gonzalez et al. 2004; Shi et al. 2007a, b; Smits et al. 2003; Tan et al. 2004a, b; van Soest et al. 1994, 1996; Wang et al. 2009a; Yan et al. 2012; Zhang et al. 2008), nitrogen-based compounds (urea, ammonium derived, amines, etc.) (Dai et al. 2009b, 2010a, b; Ma and Yu 2004a, b, c; Ma et al. 2004, 2005, 2006; Shogren et al. 1992; Tung et al. 2011; Wang et al. 2009a; Yang et al. 2006a, b, c, 2007; Zhang et al. 2008; Zheng et al. 2009b), or citric acid (Shi et al. 2007b; Wang et al. 2007; Yu et al. 2005a) are utilized. In particular, citric acid has been regarded as an effective plasticizer for starch as the acidity of citric acid can promote the fragmentation and disruption of starch granules, as well as the effective interactions with the C–O groups of starch (more than glycerol) and thus the restriction of hydrogen bonds between the hydroxyl groups of starch. Therefore, citric acid can result in a greater degree of the amorphous state and a low degree of recrystallization (or "retrogradation," a term specifically for starch) (Yu et al. 2005a).

3.3 Chemical Modification

Chemical modification of starch by substituting ester or ether groups for the hydroxyls is an effective way to improve the processing and product properties. For example, hydroxypropylated starch displays improved processability (lower viscosity) and mechanical properties (Chaudhary et al. 2008; Lafargue et al. 2007; Vorwerg et al. 2004); and acetylated starches with a degree of substitution of 2–3 are water insoluble and have good mechanical properties (Fringant et al. 1996, 1998; Jarowenko 1986; Mbougueng et al. 2012; Volkert et al. 2010; Yan et al. 2012; Zamudio-Flores et al.2010). However, it should be noted that chemical modification often decreases the polysaccharide molar mass, potentially leading to materials with less mechanical strength, and also the toxic chemical residues may modify the biodegradability and negatively impact the life-cycle assessment (LCA) of the final products.

3.4 Starch-Based Blends and Composites

To improve the performance such as moisture resistibility, mechanical properties, and long-term stability, several starch-based multiphase systems have been developed during the last two decades, such as blends or composites. Starch is often blended with other polymers (mainly biodegradable) such as poly(lactic acid) (PLA), polycaprolactone (PCL), poly(butylene succinate adipate) (PBSA), poly(butylene adipate-*co*-terephthalate) (PBAT), poly(vinyl alcohol) (PVA), and many more, as extensively reviewed in several papers (Avérous 2004; Kalambur and Rizvi 2006a; Liu et al. 2009a; Tang and Alavi 2011; Wang et al. 2003; Yu et al. 2006a).

Starch biocomposites can be produced with the reinforcement by cellulose fibers (potato pulp, bleached leafwood fibers, fibers from bleached eucalyptus pulp, and flax and jute fibers) (Alvarez et al. 2004; Averous and Boquillon 2004; Avérous 2002, 2007; Avérous et al. 2001; Carvalho et al. 2003; Curvelo et al. 2001; Dufresne et al. 2000; Funke et al. 1998; Lawton et al. 2004; Matsui et al. 2004; Romhány et al. 2003; Wollerdorfer and Bader 1998) and lignin fillers (Baumberger et al. 1998a, b; Baumberger 2002). When the fillers are nanoscaled, nanocomposites are obtained. They exhibit drastic modification in the properties of the matrix, like improvement in the mechanical properties and barrier properties, and/or changes in the thermal and electrical conductivity (Alexandre and Dubois 2000). Various kinds of starch-based nano-biocomposites will be discussed in the following sections.

4 Nanofillers

There are a diversity of nanofillers that can be used for the preparation of nanocomposites. Regarding their shapes, three distinct types of nanofillers can be observed (cf. Fig. 5) (Kumar et al. 2009):

(a) Nanoparticles: When the three dimensions of particulates are in the order of nanometers, they are referred as equiaxed (isodimensional) nanoparticles.
(b) Nanotubes: When two dimensions are in the nanometer scale and the third is larger, forming an elongated structure, they are generally referred as nanotubes, also known as nanowhiskers/nanofibers/nanorods.
(c) Nanolayers: The particulates are characterized by only one dimension in nanometer scale and are present in the form of sheets of one to a few nanometers in thickness and hundred to thousand nanometers in length.

Polysaccharides
DOI 10.1007/978-3-319-03751-6_50-1

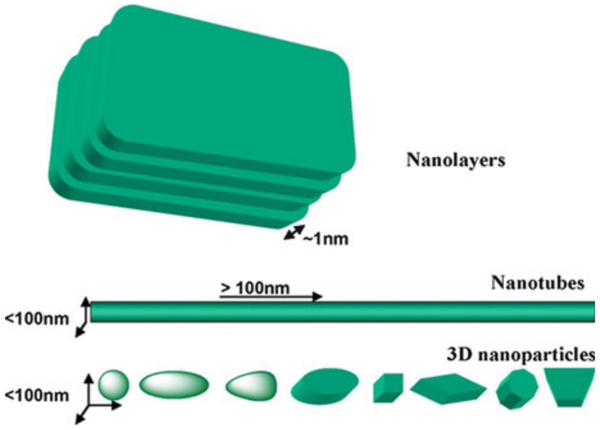

Fig. 5 Various types of nanofillers: nanolayers, nanotubes, and nanoparticles (Reprinted from Kumar et al. (2009), Copyright (2009), with permission from Elsevier)

Nevertheless, it should be noted that the term "nanoparticles" is also frequently used in broad sense in the literature to describe a nanofiller regardless of its shape.

The different nanofillers that have been examined for the use in starch-based nano-biocomposites are summarized in Table 1. They have different geometry (size and shape) and surface chemistry; therefore, different kinds of interactions between the nanofiller and the starch matrix and variation in the reinforcing capability are expected. Among them, phyllosilicates, especially montmorillonite (MMT), are most frequently utilized due to their appealing advantages such as wide availability, low cost, and low toxicity. In addition, polysaccharide nanofillers especially cellulose nanowhiskers and starch nanoparticles have also been widely used with one of the advantages in using them being the similar polysaccharide chemical structure of the nanofiller and the matrix, which could benefit the nanofiller–matrix interactions. The use of carbonaceous nanofillers (in particular carbon nanotubes (CNTs)) is also interesting to be incorporated into starch due to their superior reinforcing abilities as demonstrated in other polymer systems as well as their potentials for developing nanocomposites with new functionalities (e.g., electrical conductivity and electroactivity), although there have been a limited number of the related reports so far. CNT-reinforced nanocomposites have already shown great potentials in biomedical applications such as sensors, stimulators of bone cells, etc. (Harrison and Atala 2007; Lahiff et al. 2010; Tsai et al. 2007; Wang 2005; Wu and Liao 2007; Xiao and Li 2008), although the toxicity of CNTs appears still controversial (Famá et al. 2011; Valdés et al. 2009). Moreover, despite the long list of nanofillers in Table 1, some only appear in very recent reports, and their potential as nanofillers for reinforcing starch-based materials remains uncertain. For example, unfortunately synthetic nanolayers like LDH and brucite can hardly be intercalated by starch molecules (Wilhelm et al. 2003a), which greatly limited their usability.

Different kinds of starch-based nano-biocomposites could result from the use of a variety of nanofillers, which are discussed in the following sections separately.

5 Starch-Based Nano-biocomposites Reinforced by Phyllosilicates

5.1 Phyllosilicates

Phyllosilicates, or layered silicates, are an important group of minerals that includes the clay minerals, the micas, chlorite, serpentine, talc, etc. They possess some strong advantages such as wide availability, low cost, versatility, eco-friendliness, and low toxicity. They have different

DOI 10.1007/978-3-319-03751-6_50-1

Table 1 Overview of the nanofillers used for starch-based nanocomposites

Category/source	Nanofiller	Dimensional type	Remark
Phyllosilicates			
Clay minerals			
Kaolinite group	Kaolinite	Nanolayer	Non-expandable
	Halloysite	Nanolayer (actually in cylindrical shape)	Non-expandable
Smectite group	Montmorillonite	Nanolayer	Most expandable; most frequently used; natural sodium montmorillonite being a preferable choice due to the matching of polarity with starch
	Hectorite	Nanolayer	Expandable
Sepiolite group	Sepiolite	Nanolayer (actually in needle shape)	–
Synthetic clays	Somasif™ ME 100 fluorohectorite/ fluoromica	Nanolayer	Montmorillonite- or hectorite-type synthetic clay
	Laponite® B, Laponite® RD	Nanolayer	Hectorite-type synthetic clay
Mica group	Muscovite	Nanolayer	Non-expandable
	Paragonite	Nanolayer	Non-expandable
	Illite[a]	Nanolayer	Non-expandable
Polysaccharides			
Cellulose	Nanowhiskers/nanofibrils/ nanofibers from plant cellulose (flax, hemp, ramie, wood, pea hull, cassava bagasse, wheat straw) and microcrystalline cellulose (commercially available)	Nanotube/ nanoparticle	Tend to form aggregates; size, shape, and crystallinity largely dependent on the preparation method and conditions
	Nanorods from tunicin (animal cellulose)	Nanotube	
	Nanofibrils/nanofibers from bacterial cellulose	Nanotube	High crystallinity
Starch	Nanoparticles/nanocrystals from starch (waxy maize and regular maize)	Nanoparticle	Tend to form aggregates
Chitin	Nanoparticles from chitin	Nanoparticle	
Chitosan	Nanoparticles from chitosan	Nanoparticle	
Carbonaceous materials			
	Carbon nanotubes	Nanotube	–
	Graphite oxide	Nanolayer	–
	Carbon black	Nanoparticle	–
Metalloid oxides			
	Silicon dioxide (also silica) [SiO_2]	Nanoparticle	–
	Antimony trioxide [Sb_2O_3]	Nanoparticles	–

(*continued*)

DOI 10.1007/978-3-319-03751-6_50-1

Table 1 (continued)

Category/source	Nanofiller	Dimensional type	Remark
Metal oxides and chalcogenides			–
	Zinc oxide [ZnO]	Nanoparticle	
	Hydrous zirconium dioxide (also zirconia) [$ZrO_2 \cdot nH_2O$]	Nanoparticle	–
	Titanium dioxide (also titania) [TiO_2]	Nanoparticle	–
	Cadmium sulfide [CdS]	Nanoparticle	–
	Cadmium selenide [CdSe]	Nanoparticle	–
Metal phosphates			
	α-Zirconium phosphate [$Zr(HPO_4) \cdot H_2O$]	Nanolayer	–
Layered double hydroxides (LDH)			
	$[M^{II}_{1-x}M^{III}_{x}(OH)_2]_{intra}[A^{m-}_{x/m} \cdot nH_2O]_{inter}$[b]	Nanolayer	–
Nonsilicate minerals			
	Brucite [$Mg(OH)_2$]	Nanolayer	–
	Hydroxyapatite [$Ca_{10}(PO_4)_6(OH)_2$]	Nanoparticle	–

Somasif™ is a trademark of CBC Co., Ltd. Japan; Laponite® is a registered trademark of Laporte Ind. Ltd. (SCP)

[a] Hydrous mica, considered to belong to the clay–mica group, sometimes categorized to the clay minerals

[b] "M^{II}" and "M^{III}" are metal cations, "A" is the anion, and "intra-" and "inter-" denote the intralayer domain and the interlayer space, respectively

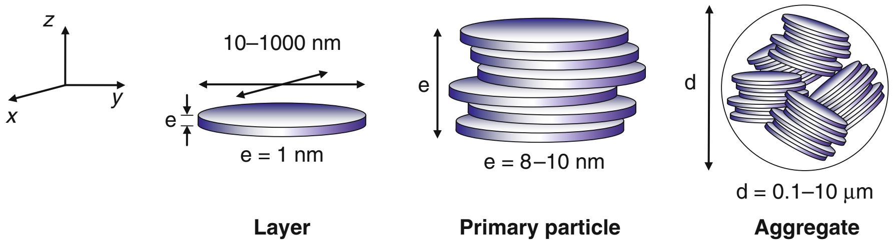

Fig. 6 Phyllosilicate multi-scale structure showing the individual clay platelet, a stack of a few platelets forming the primary particle, and the aggregate structure consisting of associated primary particles with their characteristic dimensions (thickness *e* and average diameter *d*) (Reprinted from Chivrac et al. (2009a), Copyright (2009), with permission from Elsevier)

structure, texture, and/or morphology. Due to the complexity of the structure, it is no surprise to find the classification of phyllosilicates to be different according to the literature source. Table 1 lists the most commonly used phyllosilicates for starch-based nano-biocomposites in the literature.

Phyllosilicates mainly present three organizational levels depending on the observational scale, i.e., (a) the layer, (b) the primary particle, and (c) the aggregate (cf. Fig. 6) (Chivrac et al. 2009a):

(a) The layer is equivalent to a disk or a platelet with the width varying from 10 nm to 1 μm and the thickness of 1 nm. These layers, especially the widest, are flexible and deformable.

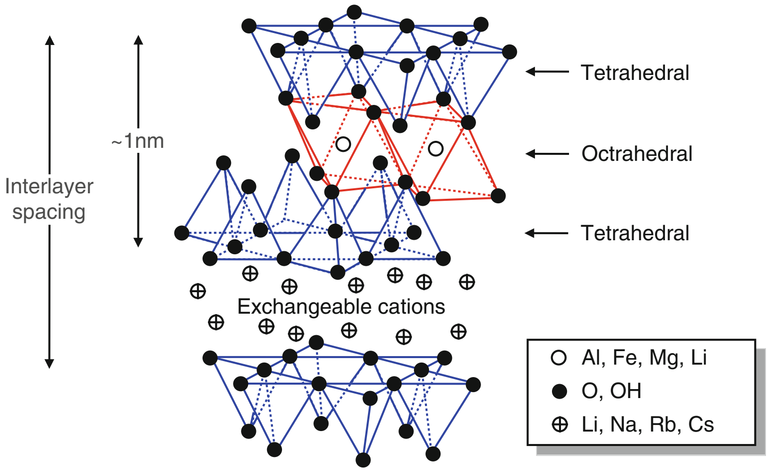

Fig. 7 Structure of 2:1 phyllosilicate (Adapted with permission from Sinha Ray et al. (2003). Copyright (2008) American Chemical Society)

(b) The primary particle is composed of five to ten stacked platelets. The cohesion of the structure is assured by van der Waals and electrostatic attraction forces between the cations and the platelets. The stacking of these particles is perpendicular to the *z* direction and is disordered in the plane (*x*, *y*). The structure thickness is around 10 nm.
(c) The aggregate is the association of primary particles orientated in all the directions. The size of the aggregates varies from 0.1 to 10 μm.

The layer is the result of the condensation of tetrahedral sheets (T) and octahedral sheets (O) (Bergaya et al. 2012). Phyllosilicates are often referred to as 1:1 or 2:1. A 1:1 phyllosilicate would consist of one tetrahedral sheet and one octahedral sheet (T–O), and examples would be kaolinite and serpentine. A 2:1 phyllosilicate consists of an octahedral sheet sandwiched between two tetrahedral sheets (T–O–T), such as the smectite, illite, and chlorite (although chlorite has an external octahedral sheet often referred to as “brucite”). For a 2:1 phyllosilicate, the crystal structure is based on the pyrophyllite structure $Si_4Al_2O_{10}(OH)_2$ and can be described as a crystalline 2:1 phyllosilicate with a central alumina octahedral sheet sandwiched between two silica tetrahedral sheets corresponding to seven atomic layers superposed (cf. Fig. 7) (Hendricks 1942). This structure becomes $(Si_8)(Al_{4-y}Mg_y)O_{20}(OH)_4$, M_y^+ for MMT or $(Si_8)(Al_{6-y}Li_y)O_{20}(OH)_4$, M_y^+ for hectorite. The differences are mainly due to the isomorphic substitutions that take place inside the aluminum oxide layer (Jozja et al. 2003). These substitutions induce a negative charge inside the silicate platelet, which is naturally counterbalanced by inorganic cations (Li^+, Na^+, Ca^{2+}, K^+, Mg^{2+}, etc.) located in the interlayer spacing. The global charge varies depending on the phyllosilicate. For the smectite and the mica families, this charge varies from 0.4 to 1.2 and from two to four per unit cell, respectively. The charge amount is characterized by the cationic exchange capacity (CEC) and corresponds to the amount of monovalent cations necessary to compensate the platelet negative charge, which is usually given in milliequivalent per 100 g (meq/100 g). For instance, the CEC of MMT varies from 70 to 120 meq/100 g depending on their extraction site (Thomas et al. 1999).

The distance observed between two platelets of the primary particle, named interlayer spacing or *d*-spacing (d_{001}), depends on the phyllosilicate type. This value does not entirely depend on the layer crystal structure but also on the type of the counter-cation and on the hydration state of the phyllosilicate. For instance, the d_{001} equals 1.2 nm in usual conditions, but the value becomes

DOI 10.1007/978-3-319-03751-6_50-1

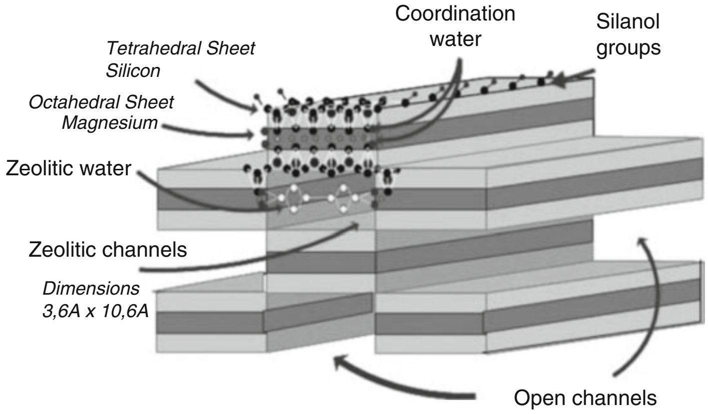

Fig. 8 Structure of sepiolite (Reprinted with permission from Duquesne et al. (2007). Copyright (2007) Wiley-VCH Verlag GmbH & Co. KGaA, Weinheim)

0.96 nm for anhydrous MMT with sodium as the counterion. This increase is linked to the adsorption of one layer of water molecules between the silicate platelets (Alexandre and Dubois 2000).

Particularly, some phyllosilicates do not display a normal layered structure. Sepiolite is also a phyllosilicate and displays a kind of fibrous structure. In opposition to all the other phyllosilicates mentioned above which have continuous tetrahedral and octahedral sheets, sepiolite has a discontinuous magnesium oxide–hydroxide octahedral sheet between two-dimensional silica tetrahedral sheets that are continuous but exhibit regular inversions of tetrahedron orientation along one crystallographic direction (*b*). In fact, the lath-like fragments of T–O–T structure extend along the *c* axis, being connected by siloxane bridges (Fig. 8) (Bergaya et al. 2012; Duquesne et al. 2007). Some isomorphic substitutions occur inside these central layers creating a negative charge naturally counterbalanced by the presence of inorganic cations (Na^+, Ca^{2+}, etc.). The sepiolite channels are filled both with coordinated water molecules, which are bonded to the Mg^{2+} ions located at the edges of the octahedral sheets, and with zeolitic water, which is associated to the structure by hydrogen bonding. The discontinuity of the silica sheets gives rise to the presence of silanol groups (Si–OH) at the edges of the external surfaces of sepiolite nanoparticles (Chivrac et al. 2010d). Another example is halloysite, which has a structure similar to kaolinite but has a single layer of water molecules existing between the T–O sheets. It has structural constraints in the layers which cause them to curl and forms spheroidal aggregates (Bergaya et al. 2012).

The phyllosilicate multi-scale structure has different porosity levels, which drive its swelling ability. The water absorption occurs, thanks to the intercalated cation hydration, which lowers the attractive forces between the silicate layers (Sposito and Grasso 1999), and also thanks to the water capillarity phenomenon, which takes place in the interparticle and inter-aggregate porosities (Luckham and Rossi 1999; Mering 1946). For a given pressure, this swelling is characterized by a d_{001} increase until an equilibrium distance (Cases et al. 1992). In general, the smaller the cation and the lower its charge, the higher is the phyllosilicate swelling. For MMT, the swelling decreases depending on the cation chemical type according to the trend $Li^+ > Na^+ > Ca^{2+} > Fe^{2+} > K^+$ (Powell et al. 1997, 1998; Tettenhorst 1962). The potassium cation is a specific case because its size is equal to the dimension of the platelet surface cavity. Thus, the potassium is trapped in these cavities, leading to the reduced hydration ability.

Swelling is typical enough of smectites to have provided their alternative name of “swelling clays” (Bergaya et al. 2012). In contrast, the other natural phyllosilicates lack the ability to swell in water, which greatly limits their application in the development of starch-based nano-biocomposites.

Polysaccharides
DOI 10.1007/978-3-319-03751-6_50-1

To enhance the intercalation/exfoliation process (which will be discussed in Sect. 5.2) in a polymer matrix, chemical modification of the phyllosilicate surface, with the aim to match the polymer polarity, is often carried out (Alexandre and Dubois 2000; Sinha Ray and Okamoto 2003). Cationic exchange is the most common technique, but other original techniques such as organosilane grafting (Dai and Huang 1999; Ke et al. 2000), the use of ionomers (Lagaly 1999; Shen et al. 2002), and block copolymers adsorption (Fischer et al. 1999) are also used.

The cationic exchange involves the substitution of inorganic cations by organic ones. These cations are often alkylammonium surfactants having at least one long alkyl chain. Phosphonium salts are also interesting silicate modifiers, thanks to their higher thermal stability, but they are not often used (Wilkie et al. 2001). The ionic substitution is performed in water because of the phyllosilicate swelling which facilitates the organic cation insertion between the platelets. Then, the solution is filtered, washed with distilled water (to remove the salt formed during the surfactant adsorption and the surfactant excess), and lyophilized to obtain the organomodified phyllosilicate. In addition to the modification of the phyllosilicate surface polarity, organomodification increases the d_{001}, which will also facilitate the polymer chain intercalation (Lagaly 1986). Using this technique, various organomodified MMTs (OMMTs) and hectorites used for the fabrication of starch-based nano-biocomposites (cf. Table 2) can be produced, which mainly differ in the counter-cation nature and the CEC. It is noteworthy that, in contrast to most synthetic polymers which are hydrophobic, starch possesses the nature of being highly hydrophilic as previously mentioned (cf. Sect. 2.1); however, most conventional organomodifiers increase the hydrophobicity of the phyllosilicate. Consequently, the compatibility with the starch matrix could be reduced using most of the commercial OMMT presented in Table 2. Thus, it is one of the key points to consider for the development of phyllosilicate-reinforced starch-based nano-biocomposites.

5.2 Nanocomposite Structures

Depending on the processing conditions and the matrix–nanolayer affinity, different structures can be obtained when a phyllosilicate (except sepiolite and halloysite) is associated with a polymer (cf. Fig. 9) (Alexandre and Dubois 2000; Avérous and Halley 2009; Kumar et al. 2009; Paul and Robeson 2008; Sinha Ray et al. 2003; Sinha Ray and Okamoto 2003; Sinha Ray and Bousmina 2005; Tang et al. 2008b; Vaia and Giannelis 1997):

(a) *Phase-separated composite (microcomposite)*: the polymer chains have not penetrated into the phyllosilicate interlayer spaces, and the silicate layers are mainly stacked and aggregated. The aggregates are micron sized, and the corresponding behavior is close to a conventional composite. (In this case, the nanocomposite designation is actually incorrect.)
(b) *Intercalated nanocomposite*: the polymer diffusion into the phyllosilicate interlayer spaces leads to an increase in the d_{001}. This structure shows regularly alternating silicate layers and polymer chains.
(c) *Exfoliated nanocomposite*: the silicate layers are individually delaminated and homogeneously and fully dispersed into the matrix. (In some papers, this category is further divided into oriented–exfoliated and unoriented–exfoliated systems.)

5.3 Preparation Techniques

Normally, the incorporation of phyllosilicate nanolayers into a polymer matrix can be carried out with one of the three main techniques, i.e., (a) solution intercalation, (b) in situ intercalative polymerization, or (c) melt intercalation (Alexandre and Dubois 2000; Giannelis 1996; Mallapragada and Narasimhan 2006; Sinha Ray and Okamoto 2003; Sinha Ray and Bousmina

Table 2 Unmodified and organomodified smectite group clays used for starch-based nanocomposites with the corresponding chemical structures of counterions and their commercial trade names (Reprinted from Xie et al. (2013), Copyright (2013), with permission from Elsevier)

Clay type	Counter-cation	Name
Montmorillonite (MMT)	Na$^+$	Natural sodium MMT; MMT–Na$^+$; Cloisite® Na$^+$; Dellite® LVF; Dellite® HPS; Nanofil® 757; BH Natural
	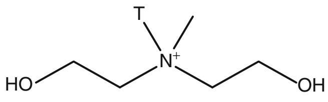 Methyl-tallow-bis-2-hydroxyethyl ammonium	Cloisite® 30B
	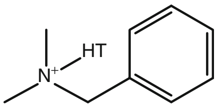 Dimethyl-benzyl-hydrogenated tallow ammonium	Cloisite® 10A; Bentone® 111; Dellite® 43B
	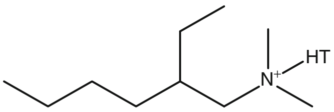 Dimethyl-hydrogenated tallow-2-ethylhexyl ammonium	Cloisite® 25A
	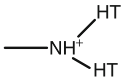 Methyl-dihydrogenated tallow ammonium	Cloisite® 93A
	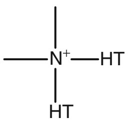 Dimethyl-dihydrogenated-tallow ammonium	Cloisite® 20A; Cloisite® 15A; Cloisite® 6A; Dellite® 67G; Dellite® 72 T
	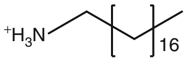 Octadecyl ammonium	Nanomer® I.30E
	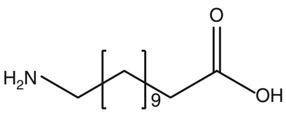 Aminododecanoic acid	Nanofil® 784
	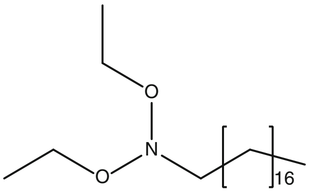 Stearyl dihydroxyethyl ammonium	Nanofil® 804

(*continued*)

Table 2 (continued)

Clay type	Counter-cation	Name
	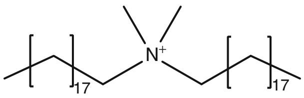 Distearyl dimethyl ammonium chloride	Nanofil® 948
	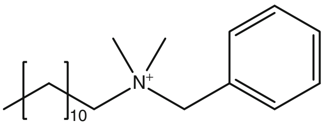 Dodecyl benzyl dimethyl ammonium bromide	–
	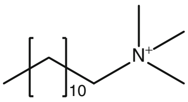 Dodecyl trimethyl ammonium	–
	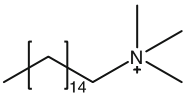 Hexadecyl trimethyl ammonium	–
	Cationic starch	–
	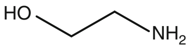 Ethanolamine	–
	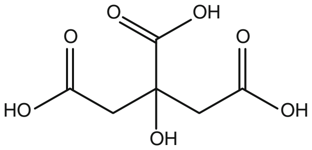 Citric acid	–
Hectorite	Ca^{2+}	Natural calcium hectorite; Bentone EA-163
	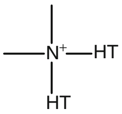 Dimethyl-dihydrogenated-tallow ammonium	Bentone 109

Cloisite® is a trademark of South Clay Products, Inc. (USA); Nanomer® is a trademark of Nanocor, Inc.; Dellite® is a trademark of Laviosa Chimica Mineraria, S.p.A. (Italy); Nanofil® is a trademark of Süd Chemie AG (Germany); BH Natural is a product from Black Hills Bentonite LLC (USA); Bentone® is a trademark of Elementis Specialties (USA); Nanomer® is a trademark of Nanocor, Inc. (USA)
The surface hydrophobicity of Cloisite clays: $Na^+ < 30B < 10A < 25A < 93A < 20A < 15A$
T tallow (≈65 % C18, ≈30 % C16, ≈5 % C14), *HT* hydrogenated tallow

2005). It should be noted that these techniques might not be fully applicable to sepiolite and halloysite due to special structures as previously mentioned.

Solution intercalation process is based on a solvent system in which the polymer is soluble and the phyllosilicate is swellable and dispersible. The swelling of phyllosilicates is crucial for

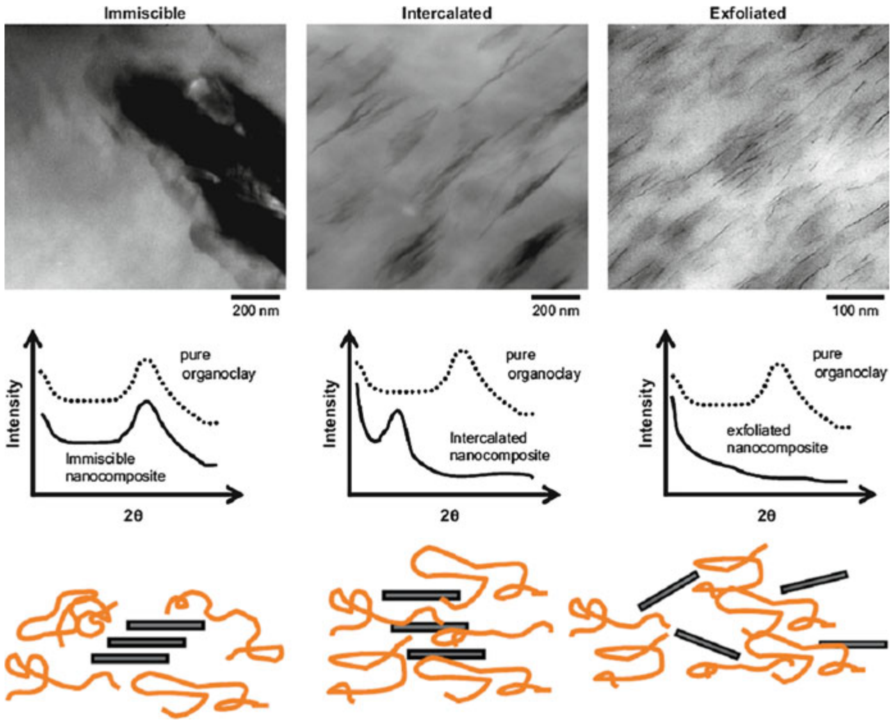

Fig. 9 Illustration of different states of dispersion of phyllosilicate in polymers with the corresponding typical results of XRD and TEM. (In this copyrighted material, the word "organoclay" could be appropriately replaced by "phyllosilicate" in the context of the current chapter) (Reprinted from Paul and Robeson (2008), Copyright (2008), with permission from Elsevier)

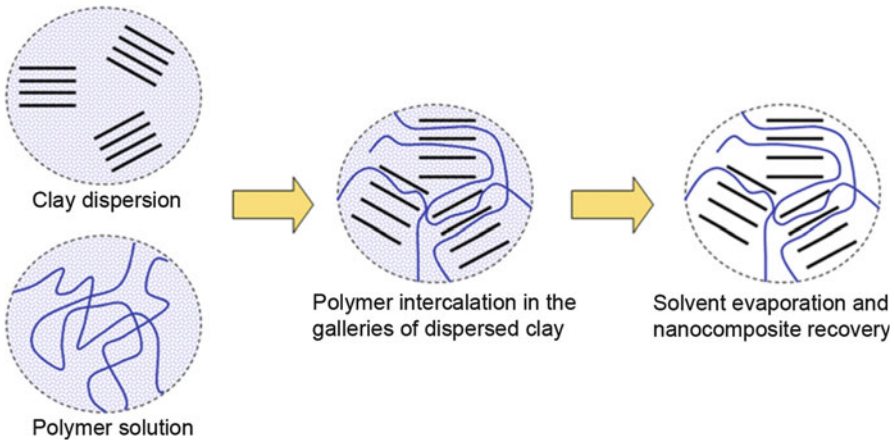

Fig. 10 Schematic representation of polymer–phyllosilicate nanocomposites obtained by intercalation from solution (Reprinted from Pavlidou and Papaspyrides (2008), Copyright (2008), with permission from Elsevier)

nanocomposite structure development, and thus swellable phyllosilicates (mainly smectite group clays) are preferably used (cf. Table 1). Starch, as the matrix, is first dissolved in an appropriate solvent. Water is often used since starch is usually gelatinized in water. In parallel, the phyllosilicate is swollen in the same or another solvent such as water, chloroform, or toluene to obtain a miscible solution. Sonication may be employed to assist the swelling and dispersion process. When the solution of starch and that of swollen phyllosilicate are mixed, the polymer chains intercalate and may replace the solvent molecules within the interlayer spaces of the aggregated phyllosilicate

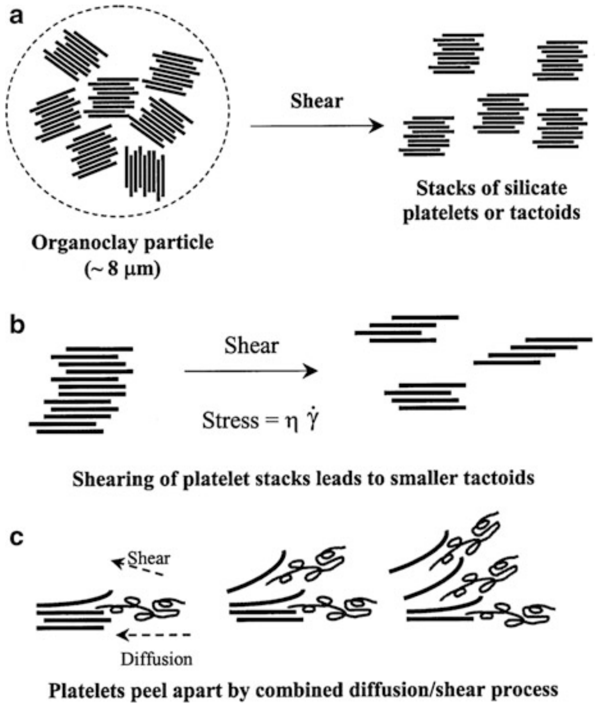

Fig. 11 Stepwise mechanism of phyllosilicate platelet exfoliation in the melt compounding of nanocomposites: (**a**) organoclay particle breakup, (**b**) clay tactoid breakup, and **c** platelet exfoliation. (In this copyrighted material, the word "organoclay" could be more appropriately replaced by "phyllosilicate" in accordance with the context of the current paper) (Reprinted from Fornes et al. (2001), Copyright (2001), with permission from Elsevier)

nanoparticles. Upon solvent removal, the intercalated structure remains, resulting in nanocomposite formation. Figure 10 is a schematic representation of solution intercalation for fabricating polymer–phyllosilicate nanocomposites (Pavlidou and Papaspyrides 2008).

For the preparation of starch–phyllosilicate nano-biocomposites, it is important to minimize the intercalation of the plasticizer (glycerol) in the phyllosilicates (which will be detailed in Sect. 5.6). Regarding this, the mixing order of different ingredients (starch, nanofiller, and plasticizer) in solution processing could have some effect on the intercalation/exfoliation of silicate layers and thus the properties of the resulting nano-biocomposites (Pandey and Singh 2005). For this sample reason, Chung et al. (2010) introduced a new way to prepare well-dispersed starch–phyllosilicate nano-biocomposites by adding a dilute phyllosilicate dispersion to a solution of starch followed by coprecipitation in ethanol.

In situ polymerization is often used to make conventional nanocomposites. In this case, a phyllosilicate is swollen in a monomer solution, and then the monomer polymerization takes place, leading to a d_{001} increase, till in some cases a fully exfoliated morphology (Sinha Ray and Okamoto 2003). Since starch molecular chains are synthesized during plant growth and then extracted from the vegetal, in situ polymerization is limited to nano-biocomposites with chemically modified starch such as starch graft copolymer, which is synthesized in situ with a phyllosilicate (Al et al. 2008; Luo et al. 2005; Namazi et al. 2009; Wu et al. 2000; Zhou et al. 2011).

Compared with solution intercalation, melt intercalation has strong advantages such as the absence of solvents and the compatibility with current industrial polymer processing techniques, such as extrusion and injection molding. As a result, melt intercalation has often been used and described in the literature to produce starch–phyllosilicate nano-biocomposites.

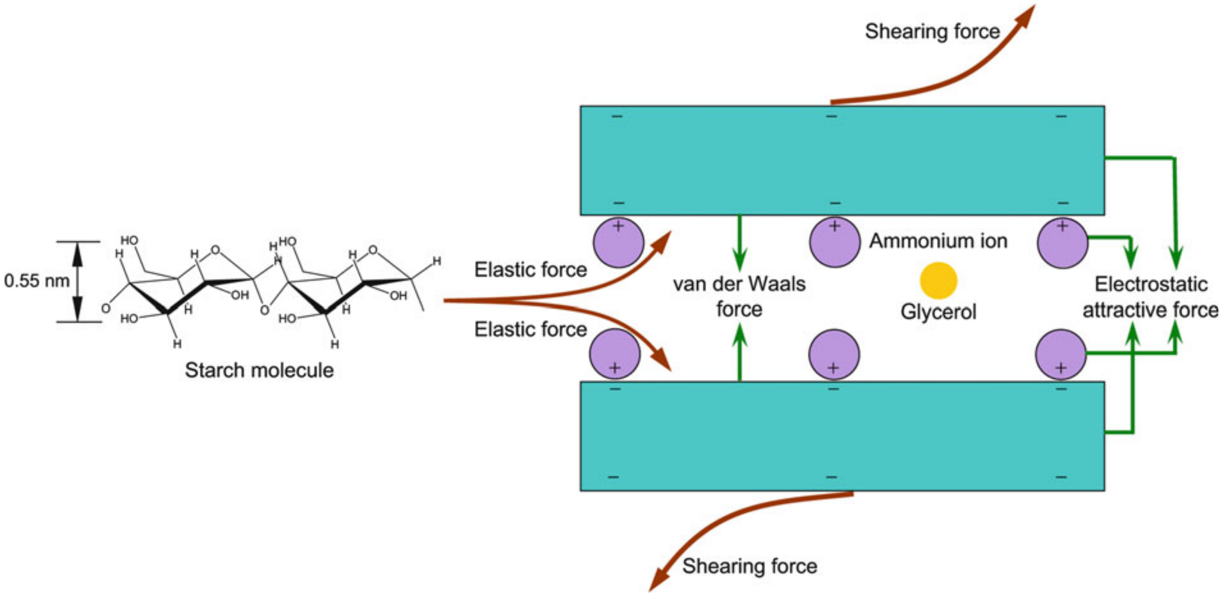

Fig. 12 Schematic representation of the intercalation process between starch and organomodified phyllosilicate (Reprinted from Zhang et al. (2007), Copyright (2007), with permission from Elsevier)

Melt intercalation involves processing a mixture of a polymer with a phyllosilicate in a melt processing unit (e.g., extruder or internal mixer). During processing, the chains diffuse between the aggregated silicate layers to produce a (nano)structured system that is controlled by the processing conditions such as temperature, shearing, and residence time in the processing equipment. Shearing is necessary to induce platelet delamination from the phyllosilicate tactoids, and extended residence time is needed to allow the polymer chains to diffuse into the interlayer spaces and then to obtain exfoliated morphology (Dennis et al. 2001). Fornes et al. (2001) proposed a stepwise mechanism for describing the phyllosilicate dispersion and exfoliation under shear stress during melt processing (cf. Fig. 11). However, it should be noted that the strong shear and long residence time would also contribute to the degradation of the starch matrix. Therefore, it is necessary to balance the processing parameters to minimize the polymer chain degradation and to obtain a kind of well-exfoliated morphology.

More related to starch–phyllosilicate nano-biocomposites, Zhang et al. (2007) proposed a schematic depicting the main force components operating on a pair of adjacent silicate layers in melt processing (Fig. 12). The van der Waals force and the electrostatic attractive force act against silicate layer exfoliation, while the shearing force and the elastic force arising with starch molecular intercalation favor silicate layer exfoliation (Zhang et al. 2007). Both the molar mass of the polymer and the polar interactions between the phyllosilicate and the polymer could influence the polymer intercalation (Vaia and Giannelis 1997).

5.4 Effect of Phyllosilicate Addition

Starch-based systems reinforced by phyllosilicates normally exhibit increases in tensile strength (Chivrac et al. 2008b, 2010d; Chung et al. 2010; Cyras et al. 2008; Dai et al. 2009a; de Carvalho et al. 2001; Gao et al. 2012; Hassan Nejad et al. 2011; He et al. 2012; Huang et al. 2004, 2005a, b, 2006; Huang and Yu 2006; Ibrahim 2011; Kvien et al. 2007; Lilichenko et al. 2008; Ma et al. 2007b; Majdzadeh-Ardakani et al. 2010; Maksimov et al. 2009; Mondragón et al. 2008; Müller et al. 2011; Park et al. 2002, 2003; Qiao et al. 2005; Ren et al. 2009; Tang et al. 2008b, 2008c; Wang et al. 2009b,

DOI 10.1007/978-3-319-03751-6_50-1

2010b; Xie et al. 2011), Young's modulus (Chaudhary 2008; Chen and Evans 2005; Chivrac et al. 2009b, 2010c, d; Chung et al. 2010; Cyras et al. 2008; de Carvalho et al. 2001; Hassan Nejad et al. 2011; He et al. 2012; Huang et al. 2004, 2005a, b; Huang and Yu 2006; Lilichenko et al. 2008; Ma et al. 2007b; Majdzadeh-Ardakani et al. 2010; Maksimov et al. 2009; Mondragón et al. 2008; Müller et al. 2011; Nejad et al. 2010; Pandey and Singh 2005; Ren et al. 2009; Wang et al. 2010b; Wilhelm et al. 2003b), storage modulus (measured by dynamic mechanical analysis [DMA]) (Kvien et al. 2007; Park et al. 2003; Wilhelm et al. 2003a, b), T_g (Chivrac et al. 2010a, c; Huang et al. 2006; Kvien et al. 2007; Nejad et al. 2010; Park et al. 2003; Wang et al. 2009d; Wilhelm et al. 2003b; Xiong et al. 2008; Xu et al. 2005), thermal stability (Chiou et al. 2007; Chivrac et al. 2010d; Cyras et al. 2008; Dai et al. 2009a; Huang et al. 2004, 2005a, b; Huang and Yu 2006; Ma et al. 2007b; Namazi et al. 2009; Pandey and Singh 2005; Park et al. 2002, 2003; Wang et al. 2009d; Wilhelm et al. 2003a, b; Xu et al. 2005; Zhou et al. 2011), moisture resistance (i.e., moisture uptake, water vapor permeability [WVP], etc.) (Chiou et al. 2006, 2007; Chivrac et al. 2010a; Cyras et al. 2008; Dai et al. 2009a; de Carvalho et al. 2001; Gao et al. 2012; Huang et al. 2004, 2005a; Huang and Yu 2006; Ibrahim 2011; Lilichenko et al. 2008; Maksimov et al. 2009; Müller et al. 2011; Pandey and Singh 2005; Park et al. 2002, 2003; Tang et al. 2008b, c; Wang et al. 2009b, 2010b), oxygen barrier property (Zeppa et al. 2009), and biodegradation rate (Magalhães and Andrade 2009), generally meaning improved performance, even though the elongation at break was observed to be reduced in most studies (Chivrac et al. 2008b, 2010c; Chung et al. 2010; Cyras et al. 2008; Dai et al. 2009a; de Carvalho et al. 2001; Hassan Nejad et al. 2011; Huang et al. 2004, 2005a, b; Ibrahim 2011; Ma et al. 2007b; Majdzadeh-Ardakani et al. 2010; Maksimov et al. 2009; Pandey and Singh 2005; Park et al. 2002, 2003; Qiao et al. 2005; Ren et al. 2009; Tang et al. 2008b, c; Wang et al. 2009b; Wilhelm et al. 2003b). While these changes could usually be ascribed to the structural reasons such as (a) the homogeneous dispersion of silicate layers in the starch matrix (Chivrac et al. 2010d; Chung et al. 2010; de Carvalho et al. 2001; Huang et al. 2005a, 2006 Huang and Yu 2006; Ibrahim 2011; Kampeerapappun et al. 2007; Kvien et al. 2007; Ma et al. 2007b; Majdzadeh-Ardakani et al. 2010; Nejad et al. 2010; Wang et al. 2009b, 2010b; Zhang et al. 2007), (b) the strong interactions (typically by hydrogen bonding) between the silicate nanofiller and the starch matrix (Chivrac et al. 2008b, 2010d; Cyras et al. 2008; Dai et al. 2009a; Huang et al. 2004; Ma et al. 2007b; Majdzadeh-Ardakani et al. 2010; Park et al. 2003; Ren et al. 2009; Tang et al. 2008c; Wang et al. 2009b, 2010b), and (c) the high aspect (width-to-thickness) ratio and thus the vast exposed surface of the silicate layers (Cyras et al. 2008; Huang and Yu 2006; Ibrahim 2011), the detailed mechanisms regarding the changes in different properties are summarized below from the literature:

- Glass transition: an increase in the T_g can be a result of the restriction of chain mobility due to nanofiller–polysaccharide interactions (Kvien et al. 2007; Xu et al. 2005).
- Mechanical properties: increases in Young's modulus, storage modulus (DMA), and tensile strength can be ascribed to (a) the facilitation of stress transfer from the starch matrix to the nanofiller as a result of the strong nanofiller–matrix interactions (Chivrac et al. 2008a; Chung et al. 2010; Tang et al. 2008c); (b) the formation of a physical cross-linking network as a result of the high nanofiller–matrix interactions, which strengthens the material through mechanical percolation (Park et al. 2003; Ren et al. 2009); and (c) the stretching resistance of the oriented backbones of the chains in the interlayer spaces (Cyras et al. 2008). Besides, a decrease in the elongation at break can be attributed to the decreased flexibility of the starch molecules in the presence of the nanofiller (Cyras et al. 2008; Ren et al. 2009; Tang et al. 2008c).

Polysaccharides
DOI 10.1007/978-3-319-03751-6_50-1

- Moisture resistance: the homogeneous dispersion of high-aspect-ratio silicate layers (a) introduces tortuous and thus longer pathways through the starch polymer matrix for the diffusion of water molecules (Cyras et al. 2008; Dai et al. 2009a; Ibrahim 2011; Lilichenko et al. 2008; Maksimov et al. 2009; Mondragón et al. 2008; Park et al. 2003; Tang et al. 2008c; Wang et al. 2009b, 2010b) and also (b) causes the shielding of the exposed water-sensitive hydroxyl groups of the starch (Müller et al. 2011; Wang et al. 2009b, 2010b), both of which contribute to a reduction in the moisture sensitivity.
- Oxygen barrier property: a higher oxygen barrier can be ascribed to the silicate layers inducing a higher tortuosity and longer diffusion pathways for oxygen molecules (Lilichenko et al. 2008; Maksimov et al. 2009; Zeppa et al. 2009).
- Thermal stability: improvement in the thermal stability can be due to several concomitant phenomena such as (a) the higher thermal stability of the inorganic phase (phyllosilicate) compared to the organic one (starch), (b) the phyllosilicate acting as a heat barrier which enhances the overall stability (Cyras et al. 2008; Ibrahim 2011), (c) the increase in the tortuosity of the diffusion pathways for oxygen and the combustion (pyrolysis) gas (Alexandre and Dubois 2000; Chiou et al. 2007; Chivrac et al. 2010d; Cyras et al. 2008; Namazi et al. 2009; Xu et al. 2005), and (d) the reorganization of the starch structure with less exposed hydroxyl groups and thus less susceptibility to degradation (Pandey and Singh 2005; Wang et al. 2010b; Wilhelm et al. 2003b).

In spite of the changes in the properties mentioned above, increased elongation at break (Chivrac et al. 2010d; Chung et al. 2010; Huang and Yu 2006; Huang et al. 2006; Kvien et al. 2007; Pandey and Singh 2005), decreased thermal stability (Magalhães and Andrade 2010), unchanged thermal stability (Qiao et al. 2005), decreased T_g (de Carvalho et al. 2001; Gao et al. 2012), and unchanged moisture resistance (Chivrac et al. 2010c) have also been observed in certain cases. Majdzadeh-Ardakani et al. (2010) found that the elongation at break first decreased with the phyllosilicate addition level of up to 6 %, while further increasing the nanofiller content causes an increase in the elongation at break. Some authors reported that the phyllosilicate addition reduced the melting temperature of glycerol-plasticized starch-based nano-biocomposites (Liu et al. 2011c), but increased that of sorbitol-plasticized starch-based nano-biocomposites (Chaudhary et al. 2011a; Kvien et al. 2007). Furthermore, breaking energy could either be increased (Huang et al. 2004, 2005a, b; Huang and Yu 2006; Ma et al. 2007b; Wang et al. 2010b) or decreased (Chivrac et al. 2010c; Huang et al. 2004) with the addition of a phyllosilicate. To address these discrepancies, it is useful to consider the crystalline structures in the materials as influenced by the nanofillers. Crystallinity and/or crystal size could affect the biodegradation (Magalhães and Andrade 2009), mechanical properties (Chivrac et al. 2010c, d; Chung et al. 2010; Majdzadeh-Ardakani et al. 2010), and moisture resistance (Cyras et al. 2008). Most typically, a higher crystallinity could embrittle nanocomposite materials with lower elongation at break values (Chivrac et al. 2010c, 2010d; Majdzadeh-Ardakani et al. 2010). Nevertheless, the literature shows that the recrystallization of a starch-based material could either be restrained (Chung et al. 2010; Huang et al. 2004, 2005a; Liu et al. 2011c; Magalhães and Andrade 2009, 2010; Ren et al. 2009; Wang et al. 2009b; Zhang et al. 2007), unchanged (Zeppa et al. 2009), or enhanced (Chaudhary 2008; Müller et al. 2011) with the addition of a phyllosilicate.

5.5 Effects of Phyllosilicate Type and Content

Table 2 highlights various natural and organomodified MMT nanofillers that have been utilized in starch-based nano-biocomposite systems. It is important to note that the surface hydrophobicity of Cloisite MMT nanofillers follows the order $Na^+ < 30B < 10A < 25A < 93A < 20A < 15A < 6A$.

Although OMMT could provide much greater d_{001} than natural sodium MMT (MMT–Na$^+$ or Cloisite Na$^+$) to possibly facilitate starch molecular intercalation, it has been demonstrated that the structure of the resulting composites more highly depends on the hydrophilicity of MMT (Zhang et al. 2007). It has been shown that the incorporation of hydrophobic OMMT nanofillers such as Cloisite 15A, Cloisite 6A, Cloisite 10A, Nanomer I.30E, etc. (cf. Table 2 for designations and corresponding chemical structures) led to the formation of microcomposites (Chiou et al. 2005; Park et al. 2002; Tang et al. 2008c), as evidenced by the unchanged values of the d_{001}. When Cloisite 30B, a more hydrophilic OMMT, was utilized, higher d_{001} values were obtained, with a slight d_{001} shift and a strong decrease in the diffraction peak intensity, corresponding to higher dispersion (Chen and Evans 2005; Chiou et al. 2005, 2006; Park et al. 2003). Exfoliated nanocomposites have also been produced with MMT–Na$^+$ due to the more hydrophilic character of the Na$^+$-based nanofiller, which makes it more compatible with plasticized starch (Chen and Evans 2005; Chen et al. 2005; Chiou et al. 2005, 2006, 2007; Cyras et al. 2008; Huang et al. 2004; Pandey and Singh 2005; Park et al. 2002, 2003; Tang et al. 2008c; Zeppa et al. 2009; Zhang et al. 2007). Uniform dispersion of the MMT in the plasticized starch can be achieved in this case due to the polar interactions, especially hydrogen bonds formed between the hydroxyl groups of the MMT and the hydroxyl groups of the starch molecules (Huang et al. 2004; Park et al. 2002, 2003; Tang et al. 2008c).

Chiou et al. (2005) investigated the rheology during the solution processing of starch biocomposites filled by different MMT nanofillers. They demonstrated that the paste with Cloisite Na$^+$ displayed a larger increase in the rheological elastic modulus (G') at the temperature reaching 95 °C due to an intercalation process during the starch gelatinization, while the samples with the more hydrophobic MMT nanofillers had comparable modulus values to the neat starch sample (Chiou et al. 2005). More importantly, the high compatibility of MMT–Na$^+$ with a starch matrix and corresponding good dispersion could result in improved properties (as previously mentioned in Sect. 5.4) compared with those of other starch–OMMT hybrids (Park et al. 2002, 2003). In addition, these last authors also showed that MMT–Na$^+$ could shift the T_g of the starch-rich phase and the β-transition of the glycerol-rich phase of the starch matrix to higher temperatures (from 7 °C to 12 °C and from -64 to -53 °C, respectively), whereas the two relaxation temperatures were decreased for the other starch–OMMT hybrids (Park et al. 2002, 2003). These results were clearly attributed to the matching of the surface polarity of and the interactions between the Cloisite Na$^+$ and the starch (Park et al. 2002). Moreover, Zhang et al. (2007) showed that while a starch-based biocomposite reinforced by MMT–Na$^+$ has a higher thermal decomposition temperature, that reinforced by Cloisite 93A displayed a reduced thermal stability, which was ascribed to the earlier decomposition of the organic alkylammonium on the clay. However, Magalhães et al. (Magalhães and Andrade 2010) proposed that the catalytic effect of acidic sites of MMT may also reduce the thermal stability of starch.

Though OMMT is normally less capable than natural MMT–Na$^+$ to bring about the nanostructure of starch-based biocomposites, some other reasons may account for the desired property improvement of starch–OMMT hybrids. For example, by water absorbance tests, Chiou et al. (2006) found that, while a MMT–Na$^+$ sample containing the most dispersed (exfoliated) nanoclays had the lowest water uptake, a Cloisite 30B sample also absorbed less water than the MMT–Na$^+$ sample containing intercalated clay. This might be due to Cloisite 30B being more hydrophobic than MMT–Na$^+$ (Chiou et al. 2006). Actually, for understanding the moisture sensitivity of a nanocomposite, it could be better to consider the water uptake capacity of each component (nanofiller, matrix, and plasticizer), especially when a hydrophilic nanofiller like MMT–Na$^+$ is used (Mondragón et al. 2008; Zeppa et al. 2009). However, proper organomodification of MMT may display even better reinforcing ability than natural MMT–Na$^+$. As reported by Qiao et al. (2005), the use of OMMT based on trimethyl dodecyl ammonium with acetylated starch matrix could result in a nano-biocomposite with higher tensile strength and storage modulus than the sample reinforced by MMT–Na^+. This was attributed to the higher dispersion and d_{001} of the OMMT in the acetylated starch matrix (Qiao et al. 2005). Remarkably, Chivrac et al. (2008b, 2009b, 2010a, b, c; de Carvalho et al. 2001) used cationic starch as a new phyllosilicate organomodifier to better match the polarity of a starch matrix and thus to facilitate phyllosilicate exfoliation process. The morphological analyses (X-ray diffraction [XRD] and transmission electron microscopy [TEM]) showed that MMT organomodified by cationic starch (OMMT–CS) (which can be prepared either in solution with ultrasonication or in a mixer with strong shear treatment, with the latter resulting in greater delamination of the clay platelets) allowed the preparation of well-exfoliated nano-biocomposites, compared to natural MMT–Na^+, which only led to the formation of intercalated nano-biocomposites (Chivrac et al. 2008b). As a result, the OMMT–CS could lead to greater stiffness without affecting the elongation at break. Such a behavior is not observed for most other starch-based nano-biocomposites reinforced by MMT–Na^+ (Chivrac et al. 2008b, 2009b).

Although Tang et al. (2008c) reported that the MMT content did not have any significant effect on the occurrence of intercalation or exfoliation as observed by XRD, it is worth noting that there can be an optimized level of MMT addition for the greatest improvement in properties such as mechanical properties (Huang and Yu 2006; Huang et al. 2006; Kampeerapappun et al. 2007; Mondragón et al. 2008; Park et al. 2003; Tang et al. 2008c), moisture barrier property (Chiou et al. 2007; Mondragón et al. 2008), and thermal stabilities (Park et al. 2003). A higher content of MMT might contribute to aggregates and stacks of MMT in a starch matrix (Chung et al. 2010; Huang et al. 2004; Kampeerapappun et al. 2007; Majdzadeh-Ardakani et al. 2010; Park et al. 2003) and also to lower plasticization of the starch phase (Wang et al. 2009b).

Other clays (natural or synthetic) such as hectorite (Chen and Evans 2005; Kvien et al. 2007; Wilhelm et al. 2003a, b) and kaolinite (Chen and Evans 2005; de Carvalho et al. 2001; Wilhelm et al. 2003a) have also been incorporated into starch. As a non-swelling clay, kaolinite can hardly generate intercalation/exfoliation, and thus increases in the tensile strength and Young's modulus and a decrease in the WVP could be, though observed, limited (de Carvalho et al. 2001). A recent study reported that kaolinite could be intercalated by dimethyl sulfoxide (DMSO) which is an aprotic polar molecule, and thus the dispersion of kaolinite could be enhanced (Mbey et al. 2012). However, DMSO as a toxic solvent may cause health and environmental problems. Although natural hectorite might perform better than kaolinite for the formation of a nanocomposite structure (as shown by the increasing d_{001}) (Chen and Evans 2005; Wilhelm et al. 2003a), organomodified hectorite (Bentone 109) could only result in conventional composite like kaolinite (Chen and Evans 2005). Again, this can be explained by the dominant role of the hydrophilicity of a phyllosilicate in determining the structure of the resulting biocomposite. In addition, the CEC of nanofillers may also account for the alteration of some properties (Dean et al. 2007). For example, the CEC of MMT–Na^+ is 92 meq/100 g, whereas the CEC of fluoromica (FHT–Na^+) is only 70–80 meq/100 g. A larger CEC could contribute to a stronger water retention property which could influence the mechanical properties (Dean et al. 2007).

Chivrac et al. (2010d) initiated the use of sepiolite to reinforce starch-based materials and found the reinforcing effect of sepiolite was even better than that of MMT, as evidenced by the higher Young's modulus, elongation at break, and breaking tensile strength values, which was ascribed to the stronger interactions established between the sepiolite nanofiller and the polysaccharide chains. Nevertheless, when sepiolite was modified by cationic starch for better interactions with starch, the thermal stability of the nano-biocomposites could be deteriorated, due to the fast thermal decomposition of cationic starch (Chivrac et al. 2010d).

DOI 10.1007/978-3-319-03751-6_50-1

Halloysite, a hydrated kaolinite, has recently been tried to be incorporated into starch, but the mechanical strength of the resulting materials was not high enough to apply for packaging (Xie et al. 2011). This is because halloysite nanotubes are easily aggregated owing to its large specific areas and polar functional groups, and this causes halloysite nanotubes poorly dispersed in a polymer matrix. It was reported that this problem could be solved by ball-milling treatment together with polyethylene glycol (PEG) as the dispersing agent and water–ethanol mixture as the medium. PEG also improved the compatibility between the nanofiller and the starch phase, resulting improved tensile strength and Young's modulus (He et al. 2012).

5.6 Effect of Plasticizers/Additives

Glycerol has been a widely used plasticizer in the preparation of starch–phyllosilicate nano-biocomposites (Bagdi et al. 2006; Chen and Evans 2005; Chiou et al. 2007; Chivrac et al. 2008a, b, 2009b, 2010a, b, c, d; Chung et al. 2010; Cyras et al. 2008; de Carvalho et al. 2001; Huang et al. 2004; Ibrahim 2011; Kampeerapappun et al. 2007; Lilichenko et al. 2008; Liu et al. 2011c; Magalhães and Andrade 2009, 2010; Majdzadeh-Ardakani et al. 2010; Maksimov et al. 2009; Mondragón et al. 2008; Müller et al. 2011; Pandey and Singh 2005; Park et al. 2002, 2003; Tang et al. 2008b, c; Wang et al. 2009b, d; Wilhelm et al. 2003b; Zeppa et al. 2009; Zhang et al. 2007). It has been demonstrated in the previous studies (Cyras et al. 2008; Park et al. 2002) that, because of the strong polar interactions between the hydroxyl groups from the starch polymer chains, from the glycerol, and from the silicate layers, glycerol and/or starch chains can enter into silicate interlayers to form intercalated starch–MMT nano-biocomposites. However, it was highlighted by Wilhelm et al. (2003a, b) that, for high glycerol-to-clay ratio, an intercalated structure could be formed in such systems with the d_{001} increasing to about 18.5 Å, a very well-known value which was attributed to the intercalation of glycerol instead of starch molecules, whereas a total exfoliation could be obtained in the absence of the plasticizer. Such a similar phenomenon has also been reported elsewhere with glycerol (Chivrac et al. 2010c; Zhang et al. 2007) and also with sorbitol (Chivrac et al. 2010c; Ma et al. 2007b). Such materials, with a very limited polymer chain intercalation, must rather be considered as conventional microcomposites (Chivrac et al. 2010c). Furthermore, the trapping of the plasticizer in the interlayer spaces could also induce a lower plasticization effect on the starch phase (Chivrac et al. 2010c; Müller et al. 2011).

Pandey and Singh (2005) examined the effect of mixing order on the intercalation of MMT–Na^+ in samples containing maize starch, water, and glycerol. They found that the nanofiller dispersion became highly heterogeneous and the product became more brittle when the starch was plasticized with the glycerol before filling with the clay due to the formation of a bulky structure resulting from electrostatic interactions between the starch and the plasticizer. However, if the glycerol was added after mixing the clay into the starch matrix, best dispersion and thus best mechanical properties could be obtained. This study demonstrated that glycerol and starch both have the tendency to penetrate into silicate interlayers, with glycerol being favored by its smaller size (Pandey and Singh 2005). The effect of glycerol content on the nanostructure of starch–MMT biocomposites has also been reported. In a study on MMT–Na^+-reinforced wheat starch–based biocomposites prepared by twin-screw extrusion, Chiou et al. (2007) showed that the addition of 5 wt % glycerol produced the mostly exfoliated nanoclay, whereas adding 10 or 15 wt % glycerol produced the intercalated nanoclay. Similarly, Tang et al. (2008b) reported that the degree of clay exfoliation increased as the glycerol decreased from 20 % to 5 %. As a result, the film with 5 % glycerol exhibited the lowest WVP (0.41 g mm/kPa h m^2), highest T_g (53.8 °C), and highest tensile strength (35 MPa), but a low elongation at break value (2.15 %). From these studies, it was proposed that samples containing higher glycerol concentrations had an increase in the starch–glycerol interactions, which competed

DOI 10.1007/978-3-319-03751-6_50-1

with the interactions with the nanoclay surfaces (Chiou et al. 2007; Majdzadeh-Ardakani et al. 2010; Tang et al. 2008b). To address this issue, Chung et al. (2010) introduced a novel method to prevent the intercalation of glycerol into silicate interlayer spaces: starch and clay were first well dispersed in a water solution at very low concentrations, which was then coprecipitated by ethanol, followed by hot-pressing with glycerol. This method was reported to lead to good dispersion of the clay in the starch matrix (Chung et al. 2010).

Chiou et al. (2007) proposed that the hydrophilic nature of glycerol could negate the improved water resistance of starch-based nano-biocomposites containing exfoliated MMT. This issue has been extensively addressed by Chivrac et al. (2010a), who investigated the effect of plasticizer (glycerol) content on the structure of starch-based nano-biocomposite materials and on their moisture barrier properties (permeability, water sorption, and diffusivity). It was shown that the relatively high plasticizer content (23 wt % glycerol) could induce a phase separation, with plasticizer-rich and starch-rich phases, resulting in the nanoclay being preferentially located in the starch-rich domains (Chivrac et al. 2010a). As a result, a preferential pathway for water transfer was more likely to be created in the very hydrophilic glycerol-rich domains where the nanoclay platelets were almost totally absent. Thus, even if exfoliated morphology was achieved, the heterogeneous clay distribution and phase separation phenomenon explained the lack of improvement and even the decline in the moisture barrier property for these glycerol-plasticized starch-based nano-biocomposites (Chivrac et al. 2010a).

Other plasticizers such as sorbitol (Chivrac et al. 2010c; Kvien et al. 2007; Ma et al. 2007b), citric acid (Wang et al. 2009b), urea (Chen et al. 2005; Huang and Yu 2006; Huang et al. 2006; Ren et al. 2009; Tang et al. 2008b; Wang et al. 2010b; Zeppa et al. 2009), formamide (Huang et al. 2004, 2005a, b, 2006; Ma et al. 2007b; Tang et al. 2008b; Wang et al. 2010b), *N*-(2-hydroxyethyl) formamide (Dai et al. 2009a), ethanolamine (Huang et al. 2005a, b; Huang and Yu 2006; Ren et al. 2009; Zeppa et al. 2009), or their combinations have been used in the preparation of starch–phyllosilicate nano-biocomposites and have been proved to be effective in enhancing the dispersion and exfoliation of silicate layers. Also, 1-allyl-3-methylimidazolium chloride, a hydrophilic ionic liquid (IL), which can be considered as a plasticizer, has been experimented for the preparation of starch-based nano-biocomposites with promising results (Wang et al. 2009c). Nevertheless, some systems mentioned above are highly eco-toxic and cannot be used to develop safe “green” materials. However, the use of these latter plasticizers may avoid the disturbance of small polyols in the intercalation/exfoliation of silicate layers, as mentioned before. As a result, the starch-based nano-biocomposites plasticized by these plasticizers usually have improved properties. For example, Tang et al. (Tang et al. 2008b, c) demonstrated that a formamide- or urea-plasticized starch–MMT nano-biocomposite film exhibited a lower WVP, higher T_g, and higher tensile strength than a glycerol-plasticized nano-biocomposite film. Particularly, Chen et al. (2005) reported that the use of urea as the plasticizer enhanced the dispersion of ammonium-treated MMT in a starch matrix, making exfoliated starch–clay nano-biocomposites possible. This is due to the $-NH_2$ groups from urea, which could develop strong interactions with the quaternary ammonium from the organoclay, providing better dispersion of the organoclay in the matrix (Chen et al. 2005).

Nevertheless, the strong plasticizer–nanoclay interactions might play a negative effect on the exfoliation in nanohybrid materials. In a study on wheat starch–based nano-biocomposites reinforced by OMMT–CS, Chivrac et al. (2010c) reported that a kind of exfoliated morphology was obtained with glycerol as the plasticizer, while an intercalated/exfoliated structure could be formed with Polysorb®, a glycerol and sorbitol mixture, or with only sorbitol. The sorbitol-plasticized starch-based nano-biocomposite displayed a slight decrease in the mechanical properties corresponding to a more aggregated structure compared with the glycerol-plasticized sample (Chivrac et al. 2010c).

For producing more desirable starch-based nano-biocomposites, phyllosilicates can be pretreated with glycerol (Wang et al. 2009b, d), ethanolamine (Huang et al. 2005a, b; Huang and Yu 2006), citric acid (Huang et al. 2006; Majdzadeh-Ardakani et al. 2010), urea (Wang et al. 2010b), 1-allyl-3-methylimidazolium chloride (Wang et al. 2009c), etc. before the compounding step. This pretreatment can increase the *d*-spacing and destruct the stacked layered structure of a phyllosilicate during a preprocessing procedure. As reported by Huang et al. (2005a, b, 2006; Huang and Yu 2006), when MMT–Na^+ was treated with citric acid or ethanolamine, the XRD peak of the MMT–Na^+ (001) crystal plane moved to a lower value, which indicates that the distances between the layers of the MMT–Na^+ widened, and the citric acid or ethanolamine had intercalated into the layers of the MMT–Na^+. This made it easy for the MMT–Na^+ to interact with plasticized starch to achieve total dispersion and exfoliation, as indicated by the disappearance of the diffraction peak d_{001} (Huang et al. 2005a, b, 2006; Huang and Yu 2006). A two-step processing method was recently utilized for the preparation of starch-based nano-biocomposites reinforced by plasticizer-modified MMT–Na^+ (Ma et al. 2007b; Wang et al. 2009b, d, 2010b; Zhang et al. 2007). In the first modification step, the plasticizer enlarged the *d*-spacing and destructed the stacked multilayer structure of the MMT–Na^+ effectively either by using high-speed emulsifying machine (Wang et al. 2009b, d) or by using a SSE (Ma et al. 2007b; Wang et al. 2010b; Zhang et al. 2007), and the resulting MMTs were propitious to form an intercalated or exfoliated nano-biocomposite in the melt extrusion processing in a second step. Nonetheless, the possible competition between the starch and the plasticizer for the intercalation might decrease the plasticization of starch, because the intense interactions (the hydrogen bonding and the ion–dipole) existed in these multiphase nano-biocomposites (Wang et al. 2009b, 2010b).

Alternatively, chitosan, an abundant polysaccharide, has been focused as a new eco-friendly compatibilizer to promote MMT platelet exfoliation in solution (Chung et al. 2010; Kampeerapappun et al. 2007). Unfortunately, the intercalation of chitosan was not observed since the molar mass of chitosan was too high (Kampeerapappun et al. 2007). However, it was assumed that this polycation can act as a compatibilizing agent leading to fewer clay aggregates and improved mechanical properties (Kampeerapappun et al. 2007).

5.7 Effects of Starch Type, Amylose Content, and Chemical Modification

The amylose content of starch or starch type was also reported to have a structural impact on starch-based biocomposites, even though the results were not consistent (Mondragón et al. 2008; Tang et al. 2008c). Mondragón et al. (2008) compared regular maize starch, high-amylose maize starch (maize starch with 70 % amylose), and waxy maize starch (almost pure amylopectin) and concluded that the plasticized waxy starch molecules were the easiest of them all to form an intercalated/exfoliated structure. The structural features corresponded with the mechanical properties as the tensile strength and Young's modulus of the nano-biocomposites tended to increase with the MMT content and experienced an incremental improvement following the order high-amylose $<$ normal $<$ waxy maize starch (Mondragón et al. 2008). In contrast, Tang et al. (2008c) reported that a regular maize starch–based film presented better barrier and mechanical properties than either a waxy starch– or high-amylose starch–based nano-biocomposite film. Besides, the WVP, tensile strength, and elongation at break of the films did not change significantly as the amylose content increased to >50 %. These results should be ascribed to complicated reasons including the degree of gelatinization and the starch crystallinity. Moreover, Chiou et al. (2005) reported that amylose, leached from the granules during the gelatinization when the temperature was

DOI 10.1007/978-3-319-03751-6_50-1

higher than 95 °C, was intercalated into the MMT–Na^+ interlayer spaces, resulting in a large increase in the elastic modulus during rheological measurement. In addition, MMT–Na^+ samples containing wheat and normal maize starch had comparable elastic modulus values during the gelatinization, while both potato and waxy maize starch samples had elastic modulus values that decreased rapidly at higher temperatures. The results of the potato starch sample could be explained in part by a higher swelling capacity, while the waxy maize starch results could be explained by the lack of amylose resulting in fewer physical cross-links between the leached amylose, the starch granule, and the nanoclay (Chiou et al. 2005).

To seek better performance, various chemically modified starches have also been experimented to develop nano-biocomposites (Gao et al. 2012; Hassan Nejad et al. 2011; Kvien et al. 2007; Namazi et al. 2009; Nejad et al. 2010; Qiao et al. 2005; Wilhelm et al. 2003a; Xu et al. 2005). Chemical modification can result in starch derivatives with varied properties such as the molecular chain length and hydrophilicity, which could affect the interactions with a phyllosilicate. For example, Wilhelm et al. (2003a) showed that the substitution of an unmodified starch matrix by an oxidized starch gave rise to the d_{001} value of the nano-biocomposite, indicating that the short oxidized starch chains were easier to intercalate into the silicate interlayer spaces. They also found that the glycerol (the plasticizer) intercalation was minimized in the oxidized starch film where the intercalation of the oxidized starch chains was preferred (Wilhelm et al. 2003a). On the other hand, by replacing some hydroxyl groups of starch with less hydrophilic functional groups such as acetate groups, the polarity matching between the starch and a specific phyllosilicate can differ (Gao et al. 2012; Hassan Nejad et al. 2011; Namazi et al. 2009; Nejad et al. 2010). For instance, Nejad et al. (2011, 2010) reported that OMMT (Dellite 67G or Dellite 43B), compared with MMT–Na^+ (Dellite LVF), matched better with hydrophobic starch derivatives (starch acetate, starch propionate, and starch propionate acetate laurate) as the matrices. As a result, very good dispersion and partially exfoliated structures were achieved.

5.8 Effects of Preparation Techniques and Processing Conditions

Namazi et al. (2009) compared solution intercalation and in situ polymerization methods for preparing starch-*g*-PCL nano-biocomposites reinforced by Cloisite 15A. Their result showed that, even though the d_{001} could be varied by the clay addition level and swelling/process time, the diffusion and intercalation of copolymer into the interlayer spaces were generally better by solution intercalation than by in situ intercalative method (Namazi et al. 2009).

Chiou et al. (2006) examined the effects of moisture content, temperature, and screw speed in a twin-screw extrusion process of wheat starch–based biocomposites reinforced by MMT–Na^+ and Cloisite 30B. They found that the moisture content was the major factor affecting the MMT–Na^+ dispersion; an increase in the water content led to intercalation and eventual exfoliation (for the sample with 47 wt % moisture) of the nanoclay. The results were explained by the greater degree of gelatinization at a higher moisture content, which allowed more leaching of hydrophilic amylose and amylopectin molecules from the granules to penetrate into the MMT–Na^+ interlayer spaces (Chiou et al. 2006). However, the other processing parameters like temperature and screw speed had little effect on the MMT–Na^+ dispersion (Chiou et al. 2006). For the samples based on Cloisite 30B, only an increase in the temperature produced slight intercalation of the nanoclay, while changes in the moisture content and screw speed did not produce intercalation. This was ascribed to the incompatibility of starch with the rather hydrophobic Cloisite 30B (Chiou et al. 2006). For both Cloisite Na^+ and 30B samples, intercalation did not depend on the SME (Chiou et al. 2006).

Dean et al. (2007) investigated the effects of the levels of phyllosilicates (1–3.2 %) and plasticizer (13–20 %), types of phyllosilicates (MMT–Na^+ and sodium fluorohectorite), dispersion

DOI 10.1007/978-3-319-03751-6_50-1

methodologies, and processing conditions on the degree of intercalation/exfoliation of the starch-based nano-biocomposites. Three different mixing regimes were studied, i.e., (a) dry blending of the components prior to extrusion, (b) conventional mixing of the phyllosilicate in solution prior to high-speed mixing with starch and extrusion, and (c) ultrasonic treatment of the phyllosilicate in solution prior to high-speed mixing with starch and extrusion. It was shown that the use of ultrasonics was only advantageous in terms of phyllosilicate dispersion at medium nanofiller concentrations for the MMT–Na^+ samples and at higher nanofiller concentrations for the sodium fluorohectorite samples due to the difference in the cationic exchange capacity. When the levels of the phyllosilicate, water, and starch were optimized, an exfoliated structure could be produced via conventional standard mixing (Dean et al. 2007). This seems in contrast with a recent study (Majdzadeh-Ardakani et al. 2010) where starch-based nano-biocomposites were reinforced by either MMT–Na^+, Cloisite 30B, or citric acid–modified MMT–Na^+ and were prepared via a solution casting method. The authors of this publication (Majdzadeh-Ardakani et al. 2010) reported that a combined mechanical and ultrasonic mixing mode led to the most dispersion of the silicate layers in the nano-biocomposites and thus the highest Young modulus, irrespective of the clay type, compared to a process involving only one mixing mode, either mechanical or ultrasonic. This is due to the contribution of both dispersive (the breakup of the silicate agglomerates to individual silicate layers, provided by the ultrasonic device) and distributive (a spatial uniformity of all the components in system, provided by the mechanical mixer) mixing mechanisms (Majdzadeh-Ardakani et al. 2010).

5.9 Effect of Blending with Other Polymers

In order to produce starch-based nano-biocomposites with better properties, starch has been blended with different biodegradable and nonbiodegradable polymers, including PLA (Arroyo et al. 2010; Lee and Hanna 2008, 2009; Lee et al. 2007b, 2008a, b), PCL (Ikeo et al. 2006; Kalambur and Rizvi 2005, 2006b, 2004; Perez et al. 2008, 2007, 2008a, b; Vertuccio et al. 2009), PVA (Dean et al. 2008, 2011; Majdzadeh-Ardakani and Nazari 2010), PBAT (Nayak 2010; Raquez et al. 2011), PBSA (Bocchini et al. 2010), and some trademarked polyesters (Ikeo et al. 2006; McGlashan and Halley 2003; Park et al. 2007). In addition, starch–natural rubber nano-biocomposites have also been studied (Mondragón et al. 2009). Some of these studies (Nayak 2010; Perez et al. 2008, 2007; Pérez et al. 2008a, b; Raquez et al. 2011), though also quite interesting, will less be discussed in the present paper since they involved nano-biocomposites of which the matrix contained starch as a minor component (e.g., Mater-Bi® Z, containing 18 % starch, 75 % PCL, and 7 % additives).

McGlashan and Halley (2003) successfully prepared starch–polyester nanocomposite films by melt extrusion and film blowing. They found that the addition of MMT to the matrix could make the processing more stable: the die and die lip temperature could be lowered without detrimentally affecting the film blowing process (McGlashan and Halley 2003). The reason could be the exfoliated MMT acting as a barrier for plasticizer migration and evaporation. This also contributed to the products with greater stability with storing time (McGlashan and Halley 2003). Ikeo et al. (Vertuccio et al. 2009) suggested that the addition of MMT–Na^+ could improve the compatibility between starch and PCL. Besides, Dean et al. (2011) suggested there was a “nanostabilization” effect of MMT–Na^+ in starch–PVA blends, meaning the starch recrystallization could be disrupted by the nanofiller, which reduced the rate of embrittlement over time, in agreement with a previous study (McGlashan and Halley 2003).

In some studies (Arroyo et al. 2010; Avella et al. 2005; Bocchini et al. 2010; Dean et al. 2008; Majdzadeh-Ardakani and Nazari 2010; McGlashan and Halley 2003), systematic investigations were carried out to find out the effects of the second polymer content, the nanofiller type and content, and some other parameters on the properties of the nanocomposites and also to find out the optimized applicable products. Nanocomposites based on starch blends are also expected to show improved characteristics such as mechanical properties (increases in the storage modulus (Bocchini et al. 2010; Vertuccio et al. 2009), Young's modulus (Arroyo et al. 2010; Avella et al. 2005; Dean et al. 2008, 2011; Ikeo et al. 2006; McGlashan and Halley 2003; Mondragón et al. 2009; Pérez et al. 2007), and tensile strength (Arroyo et al. 2010; Avella et al. 2005; Dean et al. 2008, 2011; Ikeo et al. 2006; McGlashan and Halley 2003; Mondragón et al. 2009; Pérez et al. 2007)). However, it is quite significant to note that the incorporation of another polymer (usually being relatively hydrophobic) would modify the hydrophilic/hydrophobic balance of the material. As a result, MMT–Na^+ would probably not match anymore the polarity of the blend. In the study by McGlashan and Halley (2003), it was proposed that the organic constituents of the OMMT consisted of alcohols and hydrogenated tallow could be more thermodynamically compatible with the polyester in the matrix. Lee and co-workers (Lee and Hanna 2008, 2009; Lee et al. 2007b, 2008a, b) carried out a series of studies on nanocomposite foams based on tapioca starch and PLA by melt intercalation using different MMTs. Their results showed that Cloisite 30B, instead of MMT–Na^+, could result in the greatest extent of intercalation (Lee et al. 2007b). The greatest enlargement in the d_{001} of the Cloisite 30B in the nanocomposite was caused by the strong hydrogen bonding between the hydroxyl groups of the matrix and the hydroxyl groups of the Cloisite 30B organomodifier (Lee et al. 2007b). Therefore, the functional properties of the nanocomposite filled with Cloisite 30B were generally better than those of the Cloisite Na^+ counterpart at a nanoclay addition level of 3 wt % (Lee et al. 2007b). Similarly, in another study by Bocchini et al. (2010) who experimented with systems based on starch and PBSA with different ratios and filled with either MMT–Na^+ or Cloisite 30B as the nanofiller, only Cloisite 30B could result in an exfoliated structure because of the high affinity between the Cloisite 30B and the PBSA. Majdzadeh-Ardakani and Nazari (2010) compared starch–PVA nanocomposites reinforced by either MMT–Na^+, Cloisite 30B, or citric acid–modified MMT. The results showed that the citric acid–modified MMT led to better mechanical properties in comparison with the MMT–Na^+ and Cloisite 30B because of the strong interactions between the citric acid and the starch–PVA polymer chains (Majdzadeh-Ardakani and Nazari 2010).

Despite of the above discussion, the properties can be not only dependent on the degree of intercalation/exfoliation. Dean et al. (2008) prepared a series of plasticized starch–PVA nanocomposites reinforced by MMT–Na^+ which exhibited intercalated and highly exfoliated structures and investigated the key interactions in these products. Their results showed that the relative concentration of the PVA and MMT–Na^+ could be directly correlated to the change in the d_{001} (Dean et al. 2008). Although good dispersion of the nanoclay platelets was important in improving the mechanical properties in these nanocomposites, the interfacial interactions between the nanofiller and the matrix played also a key role. The more agglomerated biocomposites containing both the MMT–Na^+ and PVA showed significant increases in the tensile strength (up to 67 % increase) and Young's modulus (up to 85 % increase) as compared to the better dispersed biocomposites without PVA. The improvement in the properties could be attributed to both the interfacial interactions and the disruption of the starch retrogradation (recrystallization process) (Dean et al. 2008).

Starch is known to often show problems of compatibility with other polymers, which can also be an issue in materials based on nano-biocomposites. In a study on starch–PLA nano-biocomposites, Arroyo et al. (2010) found that the MMT–Na^+ was preferentially located in the starch phase or at the blend interface, which could reduce the interactions between the plasticized starch and PLA phases in the compatibilized blends resulting in lower stress transfer from the PLA matrix to the plasticized starch dispersed phase. In another study on starch–natural rubber nano-biocomposites, Mondragón

DOI 10.1007/978-3-319-03751-6_50-1

et al. (2009) revealed that the MMT–Na^+ nanolayers were mainly dispersed in the natural rubber domains forming a well-ordered intercalated structure. This could be ascribed to the reasons related to the high molar mass and the matching polarity of the natural rubber (Mondragón et al. 2009). Of course, some studies have addressed the compatibility issue, and methods such as high-energy ball milling (for starch–PCL nano-biocomposites (Vertuccio et al. 2009)) and reactive processing (for starch–PCL nano-biocomposites (Ikeo et al. 2006; Kalambur and Rizvi 2005, 2006b, 2004) and starch–PBAT nano-biocomposites (Nayak 2010; Raquez et al. 2011)) have been employed, which showed to be quite effective.

5.10 Toward Some Applications

There have been some studies on starch graft copolymer–phyllosilicate superabsorbent nano-biocomposites with excellent water absorbency and retention properties (Al et al. 2008; Luo et al. 2005; Wu et al. 2000; Zhou et al. 2011), which can be applied in industrial, agricultural, and horticultural applications. The graft copolymer could either be starch-*graft*-polyacrylamide (Wu et al. 2000), starch-*graft*-acrylic acid (Al et al. 2008), or starch-*graft*-poly[acrylamide-*co*-(acrylic acid)] (Luo et al. 2005; Zhou et al. 2011). The addition of a low-cost phyllosilicate which is abundant of –OH groups into the starch matrix is expected to improve the morphological homogeneity, water absorbing property, and gel strength because the cross-linking network can be improved with homogeneous dispersion of MMT (Luo et al. 2005). Wu et al. (2000) compared the water absorbency values of starch-*g*-polyacrylamide nano-biocomposites filled with either bentonite (MMT), kaolinite, or sericite (mica) and found that the best result was obtained with kaolinite which had the right hydration and distension to form the most suitable cross-linking density. On the other hand, several studies (Al et al. 2008; Luo et al. 2005; Zhou et al. 2011) indicated that increasing the phyllosilicate content or phyllosilicate-to-monomer ratio would first increase and then decrease the water absorbency of the nano-biocomposites, which was also ascribed to the reasons related to cross-linking density. When the cross-linking density was high, the space in the network would become small with an adverse effect to absorb water (Al et al. 2008; Luo et al. 2005; Wu et al. 2000; Zhou et al. 2011). Furthermore, Al et al. (2008) showed that this kind of materials could also be useful in the removal of a dye (safranine T) from an aqueous solution.

Xu et al. (2005) prepared starch acetate–based nano-biocomposite foams reinforced by different OMMTs by melt extrusion and found the nano-biocomposite foams showed a decrease in the cell size. The incorporation of OMMT also significantly decreased the compressibility of the nano-biocomposite foams but did not substantially affect their spring index (Xu et al. 2005). Chen et al. (2005) prepared novel starch-based nano-biocomposite foams with ammonium-treated MMT as the nanofiller and urea as the plasticizer. Spontaneously formed regular foam structure with 84 % porosity was obtained due to the ammonium surfactant of the clay which produces ammonia gas acting as an internal blowing agent (Chen et al. 2005).

Wang et al. (2009c) prepared starch-based nano-biocomposites filled with MMT, with the use of IL both as the plasticizer for the starch and the modifier for the MMT. They found that the MMT and water contents exerted an important influence on the conductance of the nano-biocomposite films, with the maximum conductance being $10^{-0.3}$ S/cm with the MMT content of 9 wt % and the moisture content of 23 wt % (Wang et al. 2009c), which was higher than alkali metal–doped plasticized starch (Ma et al. 2007a). This makes IL-plasticized starch-based nano-biocomposites to be a promising alternative for the development of new solid electrolytes, which had a wide variety of potential applications such as antistatic plastics, electronic shielding, biosensor, environmentally sensitive membranes, etc. (Wang et al. 2009c). Studies (Wang and Zhao 2006; Zhao et al. 2008) have been carried out to investigate the electrorheological activity of a novel ternary kaolinite–dimethyl

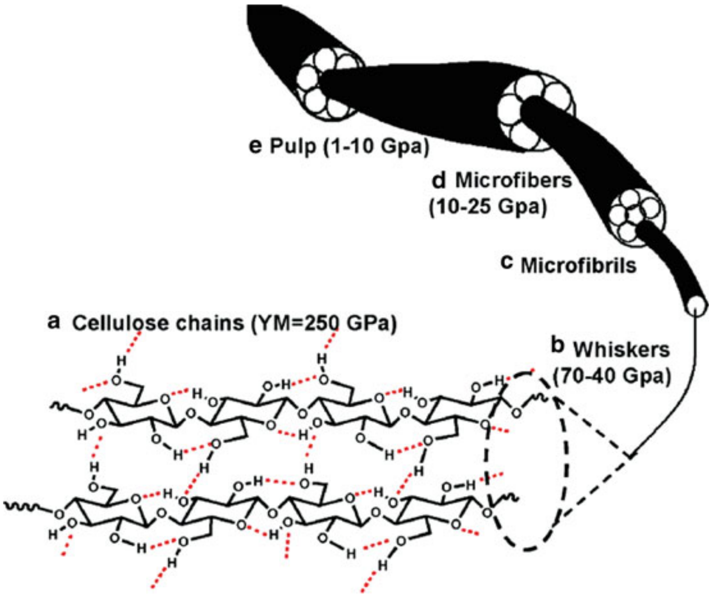

Fig. 13 Schematic representation of cellulose chemical structure and fibrillar organization (Reprinted from Kumar et al. (2009), Copyright (2009), with permission from Elsevier)

sulfoxide–carboxymethyl starch (CMS) nano-biocomposite as an electrorheological fluid (which could produce an instantaneous, reversible change in rheological properties when exposed to an electric filed in the flow direction), which was influenced by the degrees of intercalation and substitution.

6 Starch-Based Nano-biocomposites Reinforced by Cellulose Nanowhiskers/Nanoparticles

6.1 Cellulose Nanowhiskers

Cellulose, which is the most abundant biopolymer on earth and can be obtained from various sources such as plants, animals, and bacteria, is a linearly condensed polymer consisting of β-1,4-linked D-anhydroglucopyranose units (cf. Fig. 13). Depending on the source, the DP ranges from 2,500 to 15,000 (Kumar et al. 2009). Often associated with hemicellulose and lignin, cellulose is the main constituent of wood, flax, ramie, hemp, or cotton (Chivrac et al. 2009a).

Since polysaccharides such as cellulose normally have a semicrystalline structure, the most common method to prepare polysaccharide nanofillers is by acid hydrolysis, which can remove the amorphous regions and leave the highly crystalline parts of the material. The resulting nanocrystals occur as rodlike particles or whiskers, whose dimensions depend on the nature of the polysaccharide (Dufresne 2008).

CNWs (also cellulose nanofibers, which are typically cellulose nanocrystals; cf. Fig. 13) can be isolated from biomass like flax (Cao et al. 2008a), hemp (Cao et al. 2008b), ramie (Lu et al. 2006), peal hull (Chen et al. 2009a, b), cassava bagasse (Teixeira et al. 2009), and tunicate (a sea animal) (Angles and Dufresne 2000, 2001; Mathew and Dufresne 2002b; Mathew et al. 2008), or from microcrystalline cellulose (Chang et al. 2010c; Kvien et al. 2007), through acid hydrolysis with a concentrated mineral acid (typically sulfuric acid) under strictly controlled conditions of time and temperature (Angles and Dufresne 2000; Azizi Samir et al. 2004, 2005; Bondeson et al. 2006; Cao et al. 2008a, b; Chen et al. 2009a, b; Dong et al. 1996; Lu et al. 2006; Mathew and Dufresne 2002b; Teixeira et al. 2009). Acid action results in a decrease of the amorphous parts by removing the polysaccharide material closely bonded to the crystallite surface and breaking down portions of glucose chains in most accessible, nanocrystalline regions and by acid hydrolysis of cellulosic materials. Generally, the final geometrical characteristics depend on the cellulose origin and the acid hydrolysis process conditions such as time, temperature, and purity of the materials (Kumar et al. 2009). Tunicin (animal cellulose) nanowhiskers have a comparatively high aspect ratio (*L*/*D*: 50–200), which could enhance the interfacial phenomena between this nanofiller and a polymer matrix (Xie et al. 2013).

Chen et al. (2009b) investigated the effect of the hydrolysis time on the length (*L*), diameter (*D*), and *L*/*D* of the resulting CNWs from pea hull fiber. The authors showed that the chemical removal of hemicellulose and lignin from the original pea hull fiber was mostly complete in the first 4 h of acid hydrolysis and that 8 h of hydrolysis was long enough to remove most of the amorphous regions in the pea hull fiber, when the CNWs showed the highest *L*/*D* value (36). However, if the hydrolysis time was too long (particularly 24 h), the crystalline regions could be destroyed (Chen et al. 2009b).

Though direct acid hydrolysis is frequently used to prepare CNWs, other methods have been employed to produce this kind of nanofiller as well, as some examples listed below:

- The precipitation of a NaOH/urea/H_2O solution of microcrystalline cellulose by dropwise addition of an ethanol/HCl aqueous solution; particularly, the resulting material is in the form of particles (Cai and Zhang 2005; Chang et al. 2010c).
- The disintegration of the plant fiber cell wall by mild enzymatic hydrolysis combined with mechanical shearing and high-pressure homogenization (Mohanty et al. 2005; Paakko et al. 2007; Svagan et al. 2009).
- The extraction from wheat straw using steam explosion, acidic treatment, and high shear mechanical treatment (Kaushik et al. 2010).
- The production by *Acetobacter* bacteria; enzyme hydrolysis may be applied further (Grande et al. 2008, 2009; Wan et al. 2009; Woehl et al. 2010).

It is worth noting that, regardless of the preparation method, a high crystallinity of the nanofiller is generally encouraging because the higher the crystallinity, the higher the Young modulus of the nanofiller (Kumar et al. 2009) (cf. Fig. 13), which is beneficial to mechanical property improvement in the resulting nano-biocomposites. Complementary treatments in addition to the traditional hydrolysis may further decrease the contents of hemicellulose and lignin, disintegrate the bundles, and increase the crystallinity of CNWs. In a study by Kaushik et al. (2010), for example, the crystallinity increased from 54 % for untreated wheat straw to 67 % for the chemically treated sample and to 80 % for the CNWs treated both chemically and mechanically. Nevertheless, nanoparticles or nanowhiskers were not fully crystalline in some studies (Cai and Zhang 2005; Chang et al. 2010c).

Though much less frequently, commercially available CNWs (e.g., Celish, Daicel Chemical Industries Co. Ltd., Japan) have also been used in some studies to develop starch-based nano-biocomposites (Sreekala et al. 2008).

6.2 Preparation Techniques

A solution casting method has been mostly used to prepare starch-based nano-biocomposite films, which were then conditioned at specific temperature and relative humidity conditions. For the predominant use of the solution casting method, two reasons might account:

- Cellulose nanowhiskers/nanoparticles tend to aggregate due to the association by strong hydrogen bonding in the presence of high density of the –OH groups (Cao et al. 2008a, b; Kaushik et al. 2010).
- The nanofiller is prepared in aqueous condition, with the resulting dispersion (without either sedimentation or flocculation, as a consequence of charge repulsion due to the surface sulfate groups created during the sulfuric acid treatment) easy to be incorporated into a starch solution (Angles and Dufresne 2000; Cao et al. 2008a, b; Chen et al. 2009a, b; Kvien et al. 2007; Lu et al. 2006; Mathew and Dufresne 2002b).

In a solution for preparing starch-based nano-biocomposites, the key point is to fully gelatinize starch and to break nanofiller aggregates and create a homogeneous dispersion state. For the dispersion of nanowhiskers/nanoparticles in a starch matrix, some additional treatments such as ultrasonication and homogenization might be helpful (Chang et al. 2010c; Kaushik et al. 2010).

As far as bacterial cellulose nanowhiskers (BCNWs) are concerned, some special preparation methods were practiced when this kind of nanofiller is used as reinforcement. In a study by Wan et al. (2009), pellicles of BCNWs were incorporated into glycerol-plasticized starch via a solution impregnation method (Wan et al. 2009). Grande et al. (2008, 2009) developed a bioinspired bottom-up technique to produce self-assembled nano-biocomposites of cellulose synthesized by *Acetobacter* bacteria and native starch. As a final step, in order to produce starch–BCNW nano-biocomposite sheets, the BCNW–starch gels were hot-pressed and the starch phase underwent a “second gelatinization” (Grande et al. 2008, 2009). This technique took advantages of the way some bacteria “extrude” cellulose nanofibers and of the transport process that occurs during gelatinization of starch. The interesting solution preparation method could result in nano-biocomposites with a coherent morphology (Grande et al. 2008, 2009).

Contrary to most studies where the preparation processes were carried out in solution conditions, Teixeira et al. (2009) used a batch mixer equipped with roller rotors to hot melt (140 °C) a mixture of starch, the plasticizer, stearic acid, and the nanofiller with low moisture content (previously adjusted to 20 %), which was then hot-pressed at 140 °C into sheets. This preparation technique is promising since it is close to the way that the thermal processing of plasticized starch-based materials is normally carried out.

6.3 Effect of Cellulose Nanowhisker Addition

With homogeneous dispersion of CNWs within a starch matrix, property enhancement could often be observed. According to the different reports, the mechanical properties (tensile strength and Young’s modulus), thermal property (T_g), and moisture resistance generally show improvement (Angles and Dufresne 2000, 2001; Cao et al. 2008a, b; Chang et al. 2010c; Chen et al. 2009a, b; Grande et al. 2009; Kaushik et al. 2010; Kvien et al. 2007; Lu et al. 2006; Mathew and Dufresne 2002b; Mathew et al. 2008; Svagan et al. 2009; Teixeira et al. 2009; Wan et al. 2009; Woehl et al. 2010). The improvement in different properties can be linked to the morphology of nano-biocomposites which showed not only good dispersion of nanofillers in the matrix but also good adhesion between the nanofiller and the matrix. This can be explained by the chemical similarity between starch and cellulose and the hydrogen-bonding interactions existing at the nanofiller–matrix interface (Cao et al. 2008a; Chen et al. 2009b; Lu et al. 2006). Specifically, the main reasons for such improvements are summarized below:

- Mechanical properties: improvement in the mechanical properties (but usually at the expense of the elongation at break) can be benefited by (a) the formation of a rigid network of the CNWs connected by hydrogen bonds, the mutual entanglement between the nanofiller and the matrix, and the good bonding and thus the efficient stress transfer from the matrix to the nanofiller (Kaushik et al. 2010; Siqueira et al. 2008) and by (b) the increase in the overall crystallinity of the system resulting from the nucleating effect of the CNWs (Mathew and Dufresne 2002b; Mathew et al. 2008). (The latter point (b) has been in dispute since the hindrance, by the CNW dispersion and CNW–matrix interfacial adhesion, of the lateral rearrangement of the starch polymer chains, and hence the hindrance of the recrystallization, was observed in some studies (Kaushik et al. 2010).)

– Glass transition: an increase in the T_g of the starch-rich domains can be ascribed to (a) the occurrence of intermolecular interactions between the starch and the stiff CNWs, which restricted the mobility of the amorphous starch polymer chains in contact with the CNW surface (Cao et al. 2008b; Chen et al. 2009a; Lu et al. 2006); to (b) the increased crystallinity upon the CNW addition, which also restricted the mobility of the amorphous starch polymer chains (Mathew and Dufresne 2002b; Mathew et al. 2008); and to (c) the relocation of the plasticizer(s) (including water) from the starch matrix to the CNW surfaces (detailed in Sect. 6.5), which decreases the plasticization effect on the amorphous regions of the bulk starch matrix (Angles and Dufresne 2000, 2001).
– Moisture resistance: the reasons for the improvement include (a) the less hydrophilic nature of cellulose and the geometrical impedance created by the CNWs, (b) the constraint of the starch swelling due to the presence of the CNW network (initial moisture absorption may also contribute to the establishment of strong hydrogen bonds), (c) the resistance of the diffusion of water molecules along the nanofiller–matrix interface due to the strong adhesion between them (Angles and Dufresne 2000; Luo et al. 2006; Mathew and Dufresne 2002b; Sreekala et al. 2008; Svagan et al. 2009; Wan et al. 2009), and (d) the decrease in the mobility of the amylopectin chains, resulting from an increase in the T_g or the crystallinity (Angles and Dufresne 2000).

It is noteworthy that a high level of nanofiller addition is not necessarily good because of the aggregation which results in the reduction in the matrix homogeneity and cohesion. This could affect the properties in an inverse trend (Chen et al. 2009a). Moreover, one controlling factor which needs to be emphasized here is the moisture content (usually related to the relative humidity during post-processing conditioning). The moisture plays a key role in controlling the abovementioned properties of the nano-biocomposites by assisting in the formation of the hydrogen bonding between the CNWs and by (together with the other plasticizers) increasing the mobility of the starch chains which is favorable either for its recrystallization during the conditioning process or for the decrease in its T_g (Angles and Dufresne 2000, 2001; Mathew and Dufresne 2002b; Mathew et al. 2008).

In addition to the properties mentioned above, Chen et al. (2009a, b) reported that nano-biocomposites filled with CNWs showed transparency (tested by light transmittance in the wavelength range of 200–800 nm) very close to or even slightly higher than that of the pure starch matrix, which was attributed to the nanosize and the homogeneous dispersion of the nanofiller.

In the meantime, the addition of CNWs to a starch matrix could probably result in a decrease in the thermal stability (as observed by the thermal decomposition temperature) of the nano-biocomposites (Chen et al. 2009a, b; Kaushik et al. 2010). The reason might be that, for the CNWs prepared by sulfuric acid treatment, the presence of acid sulfate groups decreased the thermal stability of the cellulose by dehydration; thus, the decrease in the thermal decomposition temperature of the CNWs also decreased the thermal stability of the starch matrix by the incorporation of this nanofiller (Chen et al. 2009a, b; Roman and Winter 2004; Teixeira et al. 2009). Interestingly, such a phenomenon also occurred when hydrochloric acid was used for the acid hydrolysis of cellulose; however, this point was not reasonably explained by the authors (Kaushik et al. 2010). In contrast in another study (Chang et al. 2010c), when a non–acid hydrolysis method was used, the nano-biocomposites showed improved thermal stability.

6.4 Effect of Nanofiller Preparation

Compared to microcomposites based on plasticized starch and common cellulose fibers, the global behaviors of CNW-reinforced materials are primarily driven by the nanofiller–matrix interface. Chen et al. (2009a, b) systematically investigated the effect of the acid hydrolysis time (t) during the CNW preparation on the structure and performance of pea starch–based nano-biocomposites reinforced by pea hull fiber–derived nanowhiskers. Firstly, they found that the starch–CNW nano-biocomposites ($t = 4$–24 h) generally exhibited much better properties, i.e., the higher tensile strength, elongation at break, Young's modulus, T_g, transparency, and moisture resistance except for the thermal stability (the lower thermal decomposition temperature, due to the reason already discussed before), than the microcomposites obtained with the native pea hull fibers (without acid hydrolysis) (Chen et al. 2009a). These were related to the smooth and compact morphology of the starch–pea hull fiber nanowhisker films, while the starch–pea hull fiber composite film showed cracks, holes, and fiber-like aggregates (even though the CNWs could also show aggregates at high content) (Chen et al. 2009a). Secondly, they discovered that, though there were no apparent differences in the results of Fourier transform infrared spectroscopy (FTIR) and XRD of the nano-biocomposites filled with CNWs obtained at different hydrolysis times ($t = 4$–24 h), the morphological results revealed the smoother cross section of the 8 h hydrolyzed CNW nano-biocomposite sample than those of the other nano-biocomposite films (Chen et al. 2009b). The more homogeneous dispersion of the CNWs within the starch matrix and the fewer outstanding particle-like CNWs on the cross section of the sample indicated that, in this nano-biocomposite sample, the CNWs (obtained after 8 h of acid hydrolysis) were wrapped more tightly by the starch matrix (Chen et al. 2009b). It was suggested that this stronger adhesion between the CNWs and the starch matrix resulted from the highest aspect ratio of the CNWs after 8 h hydrolysis and contributed to the superior properties of the nano-biocomposite such as transparency, tensile strength, and elongation at break (Chen et al. 2009b).

Woehl et al. (2010) studied the effect of enzyme hydrolysis of bacterial cellulose (to prepare CNWs) on the structure and mechanical properties of the resulting starch-based nano-biocomposites. Their results showed that hydrolysis for 60 min decreased the DP of the cellulose without changing its crystallinity index or promoting a significant mass loss. However, the nano-biocomposites reinforced by such CNWs displayed the most improved mechanical properties than those with CNWs hydrolyzed for either shorter or longer time (Woehl et al. 2010). The authors proposed two mechanisms for the enzyme-treated CNWs, i.e., (a) the elimination of less organized regions between the fibers that entangled them to each other in the original material, thus allowing much better dispersion of the reinforcing agent into the starch matrix, and (b) the reduction of defects in the surface of the fibers that could act as crack propagators (Woehl et al. 2010). However, they also mentioned that longer hydrolysis time could lead to gradual hydrolysis and weakening of the crystalline regions of the CNWs, resulting in worsening mechanical properties (Woehl et al. 2010), which is in agreement with the study by Chen et al. (2009b).

A noteworthy fact is that the preparation of CNWs may also result in non-cellulose components, which could be, together with the CNWs, incorporated into a starch matrix and affect the properties of the resulting nano-biocomposites. Teixeira et al. (2009) prepared CNWs from cassava bagasse (mainly composed of water (70–80 wt %), residual starch, and cellulose fibers) by acid hydrolysis

DOI 10.1007/978-3-319-03751-6_50-1

and found that sugars (mainly glucose and sucrose) could be originated from starch hydrolysis during the acid extraction. For glycerol-plasticized nano-biocomposites, these sugars caused considerable reduction in the T_g of the starch-rich domains and inhibited the formation of V_H-type crystalline structure, as agreed by the increased elongation at break (Teixeira et al. 2009). This is because the chemical similarity between the starch and the sugars (such as glucose) could favor the interactions between them, reducing the specific interactions between the starch matrix and the CNWs, which resulted in very high mobility of the starch chains (Teixeira et al. 2009).

6.5 Plasticizer Relocation and Transcrystallization Phenomena

Dufresne and co-workers (Angles and Dufresne 2000, 2001) have undertaken a series of studies on plasticized waxy maize starch–based nano-biocomposites reinforced by tunicin nanowhiskers. The results indicated that, though the strong interactions between CNWs such as hydrogen bonding (which could be affected by the moisture content) could lead to a rigid network, which was responsible for the improved mechanical performance, some effects could tamper the reinforcement induced by the CNWs (Angles and Dufresne 2000, 2001):

- The accumulation of the plasticizer in the vicinity of the cellulose/amylopectin interfacial zone (because of the stronger interactions of either the water or glycerol with the cellulose than with the starch, as demonstrated by the contact angle measurements), enhanced in moist conditions.
- The coating of the CNWs by a soft plasticizer-rich interphase as a result of the previous effect.
- Especially in highly moist conditions, the abovementioned plasticizer accumulation, and the presence of the CNWs as a nucleating agent, could improve the ability of the amylopectin chains to crystallize, leading to the formation of a highly oriented layer, i.e., transcrystalline zone, around the CNWs.

These effects could then interfere with the inter-CNW hydrogen-bonding forces and hinder the stress transfer at the nanofiller–matrix interface and thus compromise the mechanical properties of the ensuing nano-biocomposites (Angles and Dufresne 2000, 2001).

However, by the substitution of sorbitol for glycerol as the plasticizer, no evidence of the preferential migration of the plasticizer toward the cellulose and the transcrystallization phenomenon of the amylopectin on the CNW surfaces could be observed; instead, only a single glass transition was observed for the nano-biocomposites (Mathew and Dufresne 2002b; Mathew et al. 2008). In this case, strong interactions among the CNWs, starch matrix, sorbitol, and water and a rigid three-dimensional network of the CNWs were formed, benefiting the mechanical enhancement (Mathew and Dufresne 2002b; Mathew et al. 2008).

While Dufresne and co-workers (Angles and Dufresne 2000, 2001) used waxy maize starch as the matrix and tunicin nanowhiskers as the nanofiller in their systems, it would be probable that the plasticizer relocation and transcrystallization phenomena also happen in other CNW-reinforced systems, as one example demonstrated by Teixeira et al. (2009).

7 Starch-Based Nano-biocomposites Reinforced by Starch Nanoparticles

7.1 Starch Nanoparticles

As previously presented in Sect. 2.1, starch has multilevel structures. A review by Le Corre et al. (2010) has summarized starch SNPs prepared by different methods, mainly (a) starch

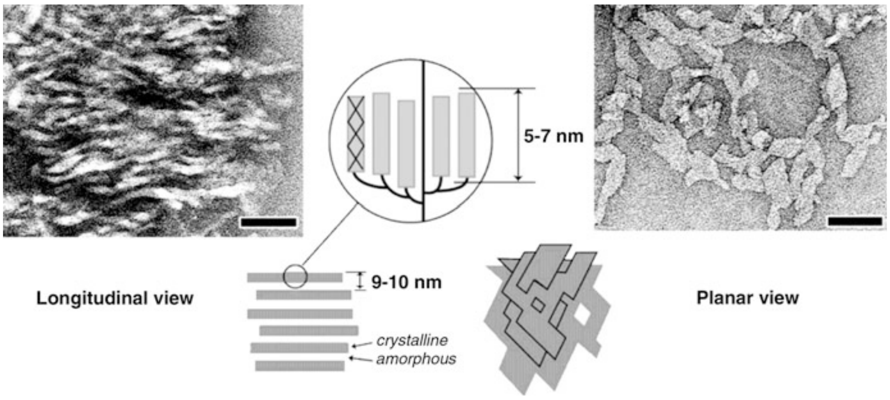

Fig. 14 TEM images of starch nanocrystals: longitudinal and planar views (Reprinted with permission from Putaux et al. (2003). Copyright 2003 American Chemical Society)

nanocrystals resulting from the disruption of amorphous domains from semicrystalline granules by acid hydrolysis and (b) starch nanoparticles produced from gelatinized starch.

Starch nanocrystals can be obtained by acid (normally sulfuric acid) hydrolysis of native starch granules by strictly controlling the temperature, acid concentration, starch concentrations, hydrolysis duration, and stirring speed (Angellier et al. 2004; García et al. 2009; Putaux et al. 2003; Viguié et al. 2007; Zeng et al. 2011). Figure 14 shows one of the first observations of starch nanocrystals by TEM with longitudinal and planar views. The starch nanocrystals prepared by acid hydrolysis have a strong drawback since they gelatinize in hot water which could be a problem when preparing plasticized starch nano-biocomposites.

In the second method, SNPs were prepared by dropwise delivering ethanol as the precipitant into a gelatinized starch solution with constant stirring, followed by centrifugation, washing with ethanol, and oven-drying. The resulting SNPs free from water were further modified by citric acid in a dry preparation technique. The so-formed amorphous citric acid–modified SNPs could not be swelled or gelatinized in hot water because of the cross-linking induced by the citric acid (Ma et al. 2008c). The reaction between the SNPs and the citric acid decreased the aggregation of the SNPs, and the size of the SNPs was reduced (Ma et al. 2008c).

7.2 Preparation Techniques

Similarly as for those reinforced with cellulose nanowhiskers/nanoparticles, solution casting is most commonly used to prepare starch-based nano-biocomposite films reinforced with SNP, which were then conditioned at specific temperature and relative humidity conditions. The reasons for this could be:

- SNPs tend to aggregate due to the association by strong hydrogen bonding in the presence of high density of the –OH groups (Angellier et al. 2006; García et al. 2009, 2011; Viguié et al. 2007).
- The structure of SNPs may be destroyed (gelatinized) at high temperature (e.g., during extrusion), which tampers the reinforcing ability (Angellier et al. 2006; Viguié et al. 2007).
- The nanofiller is prepared in aqueous condition, with the resulting dispersion (without either sedimentation or flocculation, as a consequence of charge repulsion due to the surface sulfate groups created during the sulfuric acid treatment) easy to be incorporated into a starch solution (Angellier et al. 2006; García et al. 2009, 2011; Viguié et al. 2007).

DOI 10.1007/978-3-319-03751-6_50-1

In a solution for preparing starch-based nano-biocomposites, the key point is to fully gelatinize starch and to break SNP aggregates and create a homogeneous dispersion state. SNPs may be added to a gelatinized starch solution at reduced temperature to avoid gelatinization (Angellier et al. 2006; Viguié et al. 2007).

7.3 Effect of Starch Nanoparticle Addition

The nano-biocomposites generally showed increased values of the strength at break, Young's modulus (Angellier et al. 2006; Ma et al. 2008c; Viguié et al. 2007), and T_g (of the starch-rich domains) (Angellier et al. 2006; Ma et al. 2008c; Viguié et al. 2007) and decreased values of the WVP (García et al. 2009; Ma et al. 2008c), indicating improved performance. However, some unfavorable property changes were also observed, e.g., higher water uptake percentage (García et al. 2009) and lower thermal decomposition temperature (García et al. 2009, 2011).

Compared with CNWs, SNPs should have strong affinity with a starch matrix due to the same chemical structure. As a result, good interfacial interactions (nanofiller–nanofiller and nanofiller–matrix) by hydrogen bonding and hence a strong reinforcing effect of SNPs could be expected (Angellier et al. 2006; Ma et al. 2008c; Viguié et al. 2007). Besides, SNPs, acting as a nucleating agent, could facilitate the recrystallization process of the starch polymer chains at the interface, as demonstrated by the increases in the melting temperature and in the melting enthalpy, indicating the increase in the size of the crystalline domains and in the global crystallinity, respectively. However, at high nanofiller content, SNPs seem to hinder the formation of crystalline domains possibly because of an increase in the viscosity in the nano-biocomposite (Viguié et al. 2007). Starting from these points, the mechanisms accounting for all the property changes are summarized below:

- Mechanical properties: increases in Young's modulus and strength at break and a decrease in the elongation at break result from (a) the good interfacial interactions and the strong reinforcing effect of the SNPs (Angellier et al. 2006; Ma et al. 2008c; Viguié et al. 2007) and (b) the increased crystallinity in the starch matrix (Angellier et al. 2006; Viguié et al. 2007).
- Glass transition: an increase in the T_g (of the starch-rich domains), indicating the restraint of the starch polymer chain mobility and the reduction in the free volume, was due to the presence of the SNPs (a) which function as physical joints, bringing the adjacent starch polymer chains closer and strengthening the intermolecular interactions (Angellier et al. 2006; Ma et al. 2008c; Viguié et al. 2007), and (b) which increase the crystallinity in the starch matrix (Angellier et al. 2006; Viguié et al. 2007).
- Moisture resistance: a reduction in the WVP is ascribed to (a) the less hydrophilic nature of the SNPs (especially citric acid–modified SNPs, of which the hydrophilic –OH groups were substituted by hydrophobic ester groups (Ma et al. 2008c)) and to (b) the tortuous pathways introduced by the SNPs for water molecules to pass through (García et al. 2009; Ma et al. 2008c).
- Thermal stability: a decrease in the thermal decomposition temperature is attributed to (a) the sulfate groups on the acid-hydrolyzed SNPs (García et al. 2009, 2011; Roman and Winter 2004), the reason similar to that for the nano-biocomposites reinforced by CNWs as discussed before; another reason might be (b) the strong interactions between the SNPs and the glycerol (García et al. 2009, 2011), which will be discussed in detail hereafter.

DOI 10.1007/978-3-319-03751-6_50-1

7.4 Effect of Plasticizer

Regarding some property deterioration and result discrepancy in the literature, it is believed that a starch–SNP nano-biocomposite is a complex system governed by more than the nanofiller. One major factor affecting the structure and properties of the nano-biocomposites could be the plasticizer.

By comparing the data of starch–CNW nano-biocomposites and those of starch–SNP nano-biocomposites reported in the literature, it would be interesting to note that the reinforcing effect of waxy maize SNPs in plasticized starch generally is higher than that of tunicin nanowhiskers (Angellier et al. 2006; Angles and Dufresne 2001), even though tunicin nanowhiskers have a higher aspect ratio than SNPs. Nevertheless, this should not be surprising by understanding that starch–tunicin nanowhisker nano-biocomposites have the problems of the plasticizer relocation and transcrystallization (cf. Sect. 6.5), which undermine the interactions between the tunicin nanowhiskers and the starch matrix. It should be reasonable to think that these phenomena are quite limited for starch–SNP nano-biocomposites because of the same chemical nature of the filler and matrix and thus the same affinity of plasticizers such as glycerol and water for both components (Angellier et al. 2006). As a result, Angellier et al. (2006) suggested that strong interactions between the SNPs and between the nanofiller and matrix could be established. The same study (Angellier et al. 2006) also proposed that the same chemical nature of the nanofiller and matrix possibly results in "crystallization" (co-crystallization?) occurring at the nanofiller–matrix interface, which was favorable for mechanical property improvement. These could possibly explain the results from this group of people (Angellier et al. 2006; Viguié et al. 2007) showing that, for waxy maize starch–waxy maize SNP nano-biocomposites, the relative reinforcing effect of the SNPs was more significant when the plasticizer content (glycerol or sorbitol) was high. Nonetheless, Viguié et al. (2007) from the same research group had to admit a possible "transcrystallization" phenomenon occurring for starch–SNP nano-biocomposites plasticized by sorbitol regarding their DMA results. Anyway, the authors also suggested that there was an increase in the crystallinity (double helices) during aging, which enhanced the mechanical stiffness (though intramolecular crystallites could result in a reduction of intermolecular interactions and in the cohesion of the matrix and thereby result in cracks) (Angellier et al. 2006; Viguié et al. 2007).

Despite the same chemical nature of plasticized starch and SNPs, García et al. (2009) suggested that the large number of –OH groups on the surfaces of SNPs, which were mainly the crystalline zones of hydrolyzed waxy starch, led to more association of the SNPs with glycerol molecules through hydrogen bonding than with the cassava starch matrix. This contributed to the cassava starch matrix having more –OH groups available to interact with moisture, as compared to the unfilled film. As a result, an increase in the water uptake with the SNP addition was observed (García et al. 2009). In another study where waxy maize starch was used as the matrix, García et al. (2011) suggested that the SNPs were mainly located in the glycerol-rich domains of the matrix. They compared a nano-biocomposite without glycerol plasticization and the plasticized one and found the former displayed a rather smooth and homogeneous surface associated with a brittle fracture, while the latter showed a nanometric fibrillar structure, as shown in the images of scanning electron microscopy (SEM). The peculiar structure was referred as "nanothreads" which resulted from the association of the aggregated SNPs through the glycerol. They proposed that the nanothreads were formed by the SNPs, glycerol, and transcrystallized amylopectin. The nanothreads which have high concentration of –OH groups become a preferential path for water vapor diffusion, resulting in an increase in the WVP (García et al. 2011).

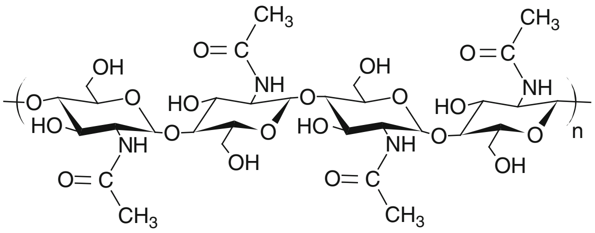

Chitin

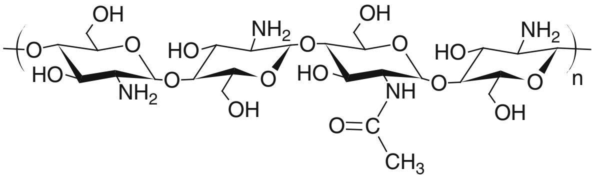

Chitosan

Fig. 15 Chemical structures of chitin and chitosan

8 Starch-Based Nano-biocomposites Reinforced by Chitin/Chitosan Nanoparticles

8.1 Chitin/Chitosan Nanowhiskers/Nanoparticles

Chitin is the second most abundant polysaccharide produced in nature after cellulose, appearing as ordered crystalline microfibrils forming structural components in the exoskeleton of arthropods or in the cell walls of fungi and yeast, but also being produced by a number of other living organisms in the lower plant and animal kingdoms, serving in many functions where reinforcement and strength are required (Rinaudo 2006). It is an acetylated polysaccharide composed of *N*-acetyl-D-glucosamine units linked by β(1→4) linkages (cf. Fig. 15). Chitosan is obtained from chitin by deacetylation. Interestingly, chitosan shows antibacterial activity (Dutta et al. 2009).

Chitin nanowhiskers of slender parallelepiped rods can be made from different chitin sources such as crab shells (Gopalan Nair et al. 2003), shrimp shells (Sriupayo et al. 2005), squid pens (Paillet and Dufresne 2001), and tubes of *Tevnia jerichonana* (Saito et al. 1997) and *Riftia pachyptila* tube worms (Morin and Dufresne 2002). They are obtained by deproteinization in a boiling alkaline (KOH) solution and then hydrolyzing the sample with a boiling HCl solution with vigorous stirring. Besides, Chang et al. (2010b) introduced a modified method to prepare chitin nanoparticles, in which two identical acidic treatments were applied followed by repeated disruption/dispersion processes with sonication. The chitin nanoparticles obtained had a low crystallinity because acid hydrolysis converted some of the crystalline regions into amorphous parts (Chang et al. 2010b). The use of chitin nanoparticles has been reported in starch-based nano-biocomposites, whereas chitin nanowhiskers have hardly been used in this case so far.

Besides, for transforming chitosan into a nanofiller, a very simple and mild method based on ionotropic gelation between chitosan and sodium tripolyphosphate was used: chitosan was dissolved into an acetic acid solution, followed by the dropwise addition of sodium tripolyphosphate into the solution with vigorous stirring and sonication (Chang et al. 2010a; Shu and Zhu 2000; Tsai et al. 2008). This method involves physical cross-linking by electrostatic interactions (instead of chemical cross-linking), which avoids possible toxicity of reagents and other undesirable effects (Shu and Zhu 2000).

DOI 10.1007/978-3-319-03751-6_50-1

8.2 Nanocomposites Reinforced by Chitin/Chitosan Nanoparticles

The use of chitin and chitosan nanoparticles in starch-based nano-biocomposites has been recently described. Chang et al. (2010b) investigated chitin nanoparticle–reinforced starch-based nano-biocomposites and found that the chitin nanoparticles could be uniformly dispersed in the starch matrix at low loading levels (e.g., 2 wt %), while, at a higher level (5 wt %), conglomeration of the chitin nanoparticles occurred. However, the tensile strength, storage modulus (DMA), T_g, and WVP of the starch–chitin nanoparticle nano-biocomposites showed improvement with the addition of the nanofiller at loading levels up to 5 wt %, due to the good interfacial interactions between the nanofiller and the starch matrix (Chang et al. 2010b). The same group of people (Chang et al. 2010a) carried out another similar study, whereas chitosan nanoparticles instead were used as the nanofiller. Similarly, the nanofiller addition resulted in increases in the tensile strength, storage modulus (DMA), T_g, WVP, and thermal decomposition temperature. The mechanisms of the property improvement in both studies are similar to those for starch–SNP nano-biocomposites. It should be noted that the aggregation of the nanoparticles at high content could deteriorate the reinforcing effect of the nanofiller, as demonstrated by the decrease in the tensile strength when the content of chitosan nanoparticles was higher than 6 wt % (Chang et al. 2010a).

9 Starch-Based Nano-biocomposites Reinforced by Carbon Nanotubes

9.1 Carbon Nanotubes

CNTs are tubular derivatives of fullerenes but exhibit properties quite different from those of the closed cage fullerenes such as C_{60}, C_{70}, C_{76}, etc. CNTs can be visualized as a sheet of graphite that has been rolled into a tube. Unlike diamond, where a three-dimensional diamond cubic crystal structure is formed with each carbon atom having four nearest neighbors arranged in a tetrahedron, graphite is formed as a two-dimensional sheet of carbon atoms arranged in a hexagonal array. In this case, each carbon is covalently bonded to three neighboring carbon atoms through sp^2 hybridization in such a way to form a seamless shell. “Rolling” sheets of graphite into cylinders forms CNTs (Falvo et al. 1997; Kumar et al. 2009; Nicole 2007; Schadler 2003; Wilder et al. 1998). The properties of nanotubes depend on the atomic arrangement (how the sheets of graphite are “rolled”), the diameter and length of the tubes, and the morphology or nanostructure. This rolling can be from one (single-wall carbon nanotubes (SWCNTs)) or more (multiwall carbon nanotubes (MWCNTs)) cylindrical shells of graphitic sheets, with the latter being simply composed of concentric SWCNTs held together with relatively weak van der Waals forces (Kis and Zettl 2008; Kumar et al. 2009; Thostenson et al. 2001). The special topologies are responsible for the unique and interesting properties of CNTs. Due to their high mechanical strength, capillary properties, and remarkable electronic structures, a wide range of potential uses have been reported within the field of materials science research (Kumar et al. 2009).

Though CNTs have already been widely used for other polymer nanocomposite systems (Kumar et al. 2009; Spitalsky et al. 2010), the use of CNTs as the nanofiller to develop starch-based nano-biocomposites has just been initiated, and mostly MWCNTs were involved (Cao et al. 2007; Famá et al. 2011; Liu et al. 2011e; Ma et al. 2008d) (with the only exception that Bonnet et al. (2007) used SWCNTs in their initial study). This may be due to the lower price and more abundance of MWCNTs than SWCNTs. Besides, MWCNTs also exhibit high aspect ratio (as high as 1,000) and excellent mechanical (with Young’s modulus as high as 1 TPa), thermal, and electrical properties (Ajayan 1999; Curran et al. 1998; Qi et al. 2003).

DOI 10.1007/978-3-319-03751-6_50-1

The effectiveness of utilizing CNTs for nanocomposites strongly depends on two main factors: (a) homogeneous dispersion of nanotubes throughout the matrix without destroying the integrity of them and (b) adequate interfacial adhesion between the phases (Kumar et al. 2009; Ruan et al. 2003). These are difficult to achieve especially in the fabrication of starch-based nano-biocomposites regarding the highly hydrophilic nature of starch. For these purposes, chemical modifications such as surface modification with the aid of surfactants, functionalization of endcaps, and functionalization of sidewalls can be helpful (Cao et al. 2007; Kumar et al. 2009). However, care must be taken since these types of procedures might destroy the extended networks on the CNT surfaces, diminishing their mechanical and electronic properties (Famá et al. 2011). The modification methods for CNTs to be incorporated into a starch matrix mainly include:

– The treatment by a surfactant (e.g., sodium dodecyl sulfate (Ma et al. 2008d) and sodium dodecyl benzene sulfonate (Bonnet et al. 2007))
– The carboxylation by strong acids (e.g., sulfuric acid and nitric acid) (Cao et al. 2007; Liu et al. 2011e)
– The wrapping by an aqueous solution of a starch–iodine complex (Famá et al. 2011)

The last method is especially interesting regarding starch-based nanocomposites. This method was initiated by Star et al. (2002), in which the helical conformation of amylose was initially formed by complexation with iodine (or bromide (Casey et al. 2005)), and then a subsequent treatment with SWCNTs displaced the iodine molecules inside the helix. The other methods for the wrapping of CNTs with starch (either amylose or amylopectin) have also been reported (Fu et al. 2007; Kim et al. 2003; Lii et al. 2003; Stobinski et al. 2003; Yang et al. 2008). While the original purpose of these studies was just to improve the dispersion stability of CNTs in aqueous solutions, the described methods may be of great interest for the preparation of starch–CNT nanocomposites since it could be a very smart solution to address the two main issues mentioned earlier, namely, the homogeneous dispersion of nanotubes and a good interfacial adhesion between the phases.

While it is relatively easy to prepare modified CNTs in a non-covalent way (e.g., the wrapping with starch and the modification by a surfactant), the covalent modification of CNT surfaces seems more promising since strong interactions between the CNTs and the starch are expected for the dispersion of the CNTs into a starch matrix and the enhancement of the nanofiller–matrix interface. The successful grafting of different polysaccharides such as chitosan (Wu et al. 2007), cellulose acetate (Ke 2010), and starch (Yan et al. 2011) onto the CNT surfaces has already been reported, although these kinds of modified CNTs have never been tried into starch-based nano-biocomposites. Starch-grafted MWCNTs, prepared by covalently grafting starch onto carboxylated MWCNTs (Yan et al. 2011), are especially interesting in regard to the same chemical nature of the grafts and the starch matrix. Nevertheless, one should bear in mind that covalent sidewall functionalization usually destroys the extended networks on the CNT surfaces, diminishing their mechanical and electronic properties (Famá et al. 2011).

9.2 Preparation Techniques

Starch–CNT nano-biocomposites were mostly prepared by a convenient solution process assisted by sonication and strong stirring, which are necessary to achieve dispersion of CNTs in a solvent. However, care should be taken since the sequence of adding ingredients might affect the nanofiller dispersion, the gelatinization/plasticization, and thus the final structure of the nano-biocomposite. Summarized from the literature, three ways of solution preparation process were practiced:

DOI 10.1007/978-3-319-03751-6_50-1

(a) The nanofiller was first dispersed in a water solution (with surfactant or starch–iodine complex) and treated with sonication, and then starch and glycerol were added to the same solution with strong stirring and increased temperature for gelatinization, followed by casting (Bonnet et al. 2007; Famá et al. 2012, 2011; Liu et al. 2011e; Ma et al. 2008d).

(b) The nanofiller was dispersed in water with sonication; in parallel, starch and glycerol were dispersed in water with increased temperature and strong stirring for gelatinization. After that, the two dispersions were mixed with stirring, followed by casting (Cao et al. 2007).

By the first method, there might be an anti-gelatinization/plasticization effect of the nanofiller, which deteriorates the cohesion of the starch matrix and thus the final properties (Liu et al. 2011e). For better gelatinization of starch, the second method could be better.

9.3 Effect of Carbon Nanotube Addition

The incorporation of MWCNTs generally increased the ultimate tensile strength (Cao et al. 2007; Famá et al. 2011; Ma et al. 2008d), Young's modulus (Cao et al. 2007; Famá et al. 2011; Ma et al. 2008d), T_g (Cao et al. 2007; Famá et al. 2012, 2011), and thermal decomposition temperature (Liu et al. 2011e) and decreased water sensitivity (Cao et al. 2007; Famá et al. 2012), showing improved performance. Homogeneous dispersion of the nanofiller in the matrix and strong interactions between the nanofiller and the matrix can account for the property enhancement (Cao et al. 2007; Famá et al. 2012, 2011; Liu et al. 2011e; Ma et al. 2008d), which relies on the proper MWCNT modification. Specially, the reasons for the variation in the different properties by the incorporation of MWCNTs are summarized below:

- Glass transition: a shift in the T_g (of the starch-rich phase) to higher temperature can be attributed to the occurrence of interactions between the starch and the stiff MWCNTs, which reduced the flexibility of the starch molecular chains in contact with the MWCNT surfaces (Cao et al. 2007). Moreover, a depression in the loss tangent (tan δ) in DMA indicates the reduction in the number of the mobile chains during the relaxation process (Famá et al. 2012; Rao and Pochan 2006).
- Thermal melting: a reduction in the melting enthalpy could reflect the restraint of the starch recrystallization, with the reason being the good dispersion of the MWCNTs and the formation of MWCNT–starch interactions spatially preventing the starch molecules from moving, interacting, and crystallizing again (Cao et al. 2007; Ma et al. 2008d).
- Mechanical properties: higher values of the tensile strength and Young's modulus can be ascribed to (a) the formation of an isotropic, three-dimensional nanotube network by the MWCNT interactions, which inhibits the crack propagation (Ma et al. 2008d); (b) the interfacial adhesion between the MWCNTs and the starch matrix, which allows the effective stress transfer from the matrix to the nanofiller (Ma et al. 2008d); and (c) the increase in the T_g, which contributes to the increase in the stiffness (Famá et al. 2012, 2011).
- Thermal stability: there are several reasons for an increase in the thermal decomposition temperature: (a) MWCNTs are more stable than starch, and (b) a barrier effect of the nanotubes and their formed aggregates hinders the diffusion of the degradation products from the bulk of the polymer into the gas phase (Chatterjee and Deopura 2006; Liu et al. 2011e; Yang et al. 2005).
- Moisture sensitivity: a reduction in moisture sensitivity can be associated with (a) the nanofiller–matrix interactions which suppress the swelling of the starch matrix when submitted to a highly moist atmosphere (Cao et al. 2007), (b) the relatively low water sensitivity of MWCNTs which reduces the moisture sensitivity of the whole nano-biocomposite system (Cao

et al. 2007), and (c) the increase in the T_g (for the starch-rich phase) which significantly decreases the free volume where the water diffusion occurs (Famá et al. 2012; Pinnavaia and Beall 2000).

While a small amount of MWCNT addition can result in significant improvement in the properties, a high loading level of MWCNTs may have some counter-effect. For example, for starch-based nano-biocomposites reinforced with MWCNTs treated by a surfactant, Ma et al. (Ma et al. 2008d) found that the maximum value of the tensile strength occurred at the 3.8 % level of MWCNT addition, while, in another study by Liu et al. (2011e), the optimized addition level of carboxylated MWCNTs was 1.5 %. Noting that starch was added to the MWCNT solution during the preparation of nano-biocomposites, it was suggested that high content of the MWCNTs could not only deteriorate the plasticization of starch which destructed the efficient load transfer from the starch matrix to the ultra-strong MWCNTs (as demonstrated by SEM and FTIR) but also destructed the continuity of the starch matrix (Liu et al. 2011e).

It is worth noting that there have been discrepancies over the trends of the property changes with the MWCNT addition. For example, while it is no surprise to observe a decrease in the toughness or elongation at break with the loading of a nanofiller like MWCNTs into a starch matrix, which was attributed to the spatial restraint of the slippage movement of the starch molecules with good dispersion of the MWCNTs, yielding the increasingly brittle samples (Ma et al. 2008d), there have also been some exciting reports showing that MWCNTs could enhance the toughness (Famá et al. 2011) or elongation at break (Cao et al. 2007; Famá et al. 2011; Liu et al. 2011e) in addition to the tensile strength and Young’s modulus. Again, this is a consequence of the homogeneous dispersion of the MWCNTs in the starch matrix and the really strong interfacial adhesion, resulting from the proper nanofiller modification, which will be further detailed.

9.4 Effect of Nanofiller Modification

The effects of two kinds of modification of MWCNTs, namely, carboxylation and starch–iodine complex wrapping, are discussed here regarding their effect on the nanofiller dispersion and interface adhesion and thus the property changes.

For the carboxylated MWCNTs, the acid-treatment process can incorporate various polar groups (carboxylic, carbonyl, and hydroxyl groups), which can improve the hydrophilicity and reduce the agglomeration of the MWCNTs (Cao et al. 2007; Liu et al. 2011e). Interestingly, Liu et al. (2011e) showed that, compared with water, glycerol containing much hydroxyl groups could dramatically increase the dispersion of these MWCNTs in a solution and restrain their agglomeration (Liu et al. 2011e). As a result, the hydrogen-bonding interactions and thus the compatibility between the acid-treated MWCNTs and a starch matrix could be enhanced, resulting in improvement in the mechanical performance of starch–MWCNT nano-biocomposite films (Cao et al. 2007). It was shown that the tensile strength and Young’s modulus did not come at the expense of the elongation at break (which usually exists in conventional filled polymer systems), which increased from 30 % to 42 % with the MWCNT addition level up to 1 % and then slightly decreased with higher MWCNT content (which might be due to some degree of aggregation of the MWCNTs) (Cao et al. 2007). Furthermore, the carboxyl groups on the surface of the MWCNTs could increase the interfacial interactions between the MWCNTs and the starch matrix, which improved the degradation activation energy (Liu et al. 2011e).

Very recently, Famá et al. (2012, 2011) experimented with starch-based nano-biocomposites reinforced by MWCNTs wrapped with starch–iodine complex, where the starch used to wrap the MWCNTs was the same as the one used as the matrix. The SEM results showed that, because of the wrapping, the failure around an MWCNT agglomerate occurred within the matrix rather than

DOI 10.1007/978-3-319-03751-6_50-1

between the MWCNTs and their starch coating, indicating strong MWCNT–starch adhesion (Famá et al. 2011). As a consequence, the efficient load transfer from the matrix to the nanofiller was attained, and the high tensile strength and elongation at break of the MWCNTs were transferred to the biocomposites (Famá et al. 2011). Therefore, the good interfacial adhesion obtained avoided the formation of holes and kept a high deformation, resulting in an increase in the toughness (defined as the work done to break a sample which is determined by integrating the stress–strain curve) with the nanofiller loading (Famá et al. 2011). This work is remarkable since very small content of MWCNTs, i.e., 0.055 %, could result in great changes in the material performance as a result of the exceptionally well-dispersed MWCNT and optimized interfacial adhesion (Famá et al. 2011).

9.5 Electrical Conductivity

Besides the properties discussed above, the addition of CNTs into a starch matrix gives the resulting nano-biocomposite electrical conductivity (Liu et al. 2011e; Ma et al. 2008d). For this purpose, an amorphous state of the starch matrix should be advantageous because the recrystallization of starch could reduce the good dispersion of the MWCNTs in the matrix (Ma et al. 2008d). On the other hand, the electrical conductivity can be influenced by the water content and the MWCNT content of the nano-biocomposites (Liu et al. 2011e; Ma et al. 2008d). As demonstrated in a study by Ma et al. (2008d), higher water content would result in an increase in the electrical conductivity in a very sensitive way, with the conductivity (y) versus water content (x) relationship being described with a second-order polynomial ($y = B_2x^2 + B_1x + B_0$); an increase in the MWCNT content decreased the sensitivity of conductivity of the nano-biocomposites to water (both the monomial coefficient B_1 and the binomial coefficient B_2 approached more to zero), until an electrical percolation threshold was reached when the effect of water content was eliminated. If the water content was fixed at 0 %, the electrical conductivity firstly observed a gradual increase with increasing the MWCNT content and then a stepwise increase when a specific level (3.8 wt %) of MWCNT content was reached (Liu et al. 2011e; Ma et al. 2008d). The reasons accounting for these phenomena are:

(a) Although water is advantageous to improve the conductivity of a starch matrix (Meyer 1998) by improving the movement of the starch polymer chains (Van Soest and Knooren 1997), the introduction of MWCNTs and good dispersion of the MWCNTs in the matrix spatially restrained the movement of the starch polymer chains even at high water content (Ma et al. 2008d).
(b) While the gradual increase in the conductivity with the increase in the MWCNT content at a low MWCNT addition level (<2.85 wt %) was due to the formation of a conductive network through hopping and tunneling processes (Lee et al. 2007a), the creation of an interconnected structure of the MWCNTs allows a very high percentage of electrons to flow through the sample at an applied electric field at the MWCNT content higher than a specific value (Ma et al. 2008d).

10 Starch-Based Nano-biocomposites Reinforced by Graphite/Graphite Oxide

10.1 Graphite and Graphite Oxide

Graphite is composed of layers of graphene which has a structure of one-atom-thick two-dimensional individual sheet composed of sp^2-hybridized carbon (Geim and Novoselov 2007). It combines the lower price and the layered structure of phyllosilicates with the superior thermal and electrical properties of CNTs. As a result, graphite can also be used to produce nanocomposites with competitive multifunctional properties (Jiang et al. 2010; Kim and Macosko

DOI 10.1007/978-3-319-03751-6_50-1

2009; Wei et al. 2009). While as-prepared graphite cannot be dispersed in water or organic solvent, which makes the fabrication of nanocomposites difficult, graphite oxide (GO) is hydrophilic and can form strong physical interactions with a polymer like starch due to its various oxygen functional groups including hydroxyls, epoxides, carbonyls, and carboxyls (Li et al. 2011b). Therefore, GO can be regarded as a promising nanofiller for the development of high-performance starch-based nano-biocomposites. On the other hand, because of the layered structure of GO just like that of a phyllosilicate, a GO-reinforced polymer nanocomposite is expected to have an intercalated or exfoliated structure, and the mechanisms for discussing phyllosilicate-reinforced polymer nanocomposites might also be useful to explain the property variation of GO-reinforced nanocomposites.

10.2 Nanocomposites Reinforced by Graphite Oxide

Li et al. (2011b) pioneered the work on starch-based nano-biocomposites reinforced by GO, of which the content was up to 2 wt %. GO was first dispersed in a water solution and treated with sonication, and then starch and glycerol were added to the same solution with strong stirring and increased temperature for gelatinization, followed by casting (Li et al. 2011b). They found that hydrogen bonding formed between the GO and the starch matrix, as revealed by FTIR, and that the nanofiller was well dispersed (exfoliated) when the GO loading was low, whereas aggregation occurred when the GO loading was high, as demonstrated by XRD and atomic force microscopy (AFM) (Li et al. 2011b). With increasing the GO loading level, the tensile strength, Young' modulus, and thermal decomposition temperature were continuously increased, the ultraviolet (UV) transmittance and elongation at break were decreased, and the moisture uptake percentage first decreased to a lowest value and then slightly increased (Li et al. 2011b). For the improvement in the mechanical properties, the good dispersion of the GO within the starch matrix and the strong interfacial interactions between the GO and the matrix were responsible for the stress transfer from the matrix to the nanofiller, although they also restrained the slippage movement of the starch molecules, which resulted in the decrease in the elongation at break (Li et al. 2011b). For the variation in water resistance, the layered structure of the nanofiller provided tortuous pathways, and the strong nanofiller–matrix interactions reduced the diffusion of water molecules in the materials (Li et al. 2011b).

11 Starch-Based Nano-biocomposites Reinforced by Carbon Black

11.1 Carbon Black

CB is a very fine powdered form of amorphous elemental carbon with a high surface area-to-volume ratio. It plays an important role in the improvement in the mechanical and/or electrical properties of high-performance polymeric materials (typically rubber), due to the formation of a physically bonded flexible filler network and strong polymer–filler couplings, which refer to a high surface activity and specific surface of the filler particles (Donnet et al. 1993; Kluüppel et al. 2007; Kraus 1965; Payne 1962, 1963, 1964, 1965a, b). As the most widely used conductive filler for polymers, a high-structural CB (original millimeter-sized CB particles) consists of many primary nanoparticles fused together in a grapelike aggregate (Norman 1970). Due to the high surface tension, flocculation in a quiescent melt can be formed by dispersing the CB aggregates during processing, which promotes the formation of a conductive network (Böhm and Nguyen 1995). As demonstrated in other polymer systems, this process depends on the compatibility between CB and the matrix, which is related to the similarity of the surface tension of them (Miyasaka et al. 1982; Sumita et al. 1991),

DOI 10.1007/978-3-319-03751-6_50-1

and the flocculation process, which relies on the viscosity of the matrix (Breuer et al. 1997; Tchoudakov et al. 1996; Yu et al. 2005b). In Sect. 11.2, the development of novel starch–CB nano-biocomposites by different processing techniques will be discussed.

11.2 Nanocomposites Reinforced by Carbon Black

Ma et al. (2008a) compared two preparation methods, i.e., melt extrusion and solution casting with microwave radiation, on the properties of starch-based nano-biocomposites reinforced by CB. It was revealed that the samples prepared by solution method contained the CB in good dispersion, whereas isolated agglomerates of the CB particles existed in those prepared by melt extrusion. As a consequence, the former approach shows better tensile strength, WVP, and electrical conductivity. It was suggested that the CB particles could act as physical cross-linking points of the starch molecules, which resulted in the increased tensile strength, although the dispersion of the CB particles in the matrix also spatially restrains the slippage movement of the starch molecules, resulting in a decrease in the elongation at break (Ma et al. 2008a). A decrease in the WVP arises from the longer and tortuous diffusive pathways with the dispersion of the CB in the matrix (Ma et al. 2008a). Moreover, the CB could form an electrical conductance network in the matrix (Ma et al. 2008a). The same research group (Ma et al. 2008b) also investigated the effect of the glycerol content on the samples prepared by solution casting with microwave irradiation and found that lower glycerol content (and thus lower viscosity) facilitated the flocculation of the CB during the solution process and thus a better electrical conductive network in the biocomposite.

12 Nanocomposites Reinforced by Metalloid Oxides, Metal Oxides, and Metal Chalcogenides

Metalloid oxides (e.g., silicon dioxide [SiO_2] and antimony trioxide [Sb_2O_3]), metal oxides (e.g., zinc oxide [ZnO], titanium dioxide [TiO_2], and hydrous zirconium dioxide [$ZrO_2 \cdot nH_2O$]), and metal chalcogenides (e.g., cadmium sulfide [CdS] and cadmium selenide [CdSe]) are grouped together in this section because of their similar chemical categories, preparation methods, and nanofiller reinforcement mechanisms. Novel applications are expected for starch-based nano-biocomposites reinforced by this type of nanofillers. Particularly, metal oxides and chalcogenides are normally semiconductor materials. The incorporation of such a filler into a polymer matrix can result in nanocomposites to be used as components for photovoltaic solar cells, light-emitting diodes, photodiodes, and gas sensors (Godovsky 2000). In addition, Sb_2O_3 is an excellent UV filter (Tigau et al. 2005). Thus, nanocomposites filled with Sb_2O_3 might find applications in UV light-emitting devices and solar cell technology (Chang et al. 2009; Zheng et al. 2009a). Furthermore, TiO_2, particularly in the anatase form, shows a photocatalytic activity under UV light and is suitable for developing nanocomposites for environmental purification (Yun et al. 2011).

The paragraphs below will firstly provide general discussion on starch-based nano-biocomposites reinforced by different metalloid oxides, metal oxides, and metal chalcogenides. Then, nano-biocomposites based on starch blended with PVA, and reinforced by SiO_2, will be separately discussed regarding the particular intermolecular interaction and network structure in such a multiphase system.

12.1 Nanofillers and Preparation Techniques

In order to fabricate a starch-based nano-biocomposite reinforced by a metalloid oxide, metal oxide, or metal chalcogenide, only solution methods have been used, which are listed below:

DOI 10.1007/978-3-319-03751-6_50-1

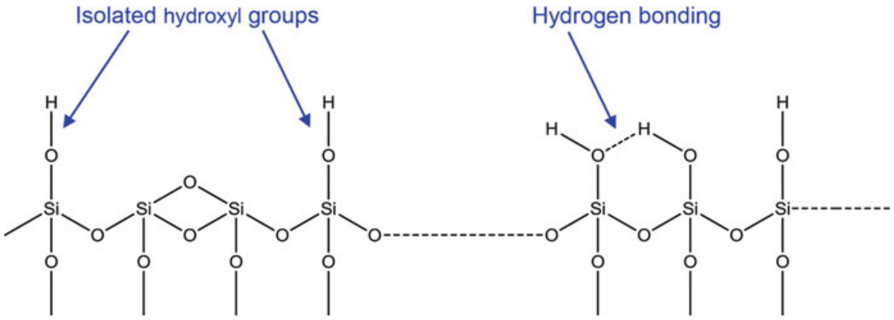

Fig. 16 Structure of nano-SiO_2

(a) The nanoparticles (SiO_2 (Wu et al. 2009b; Xiong et al. 2008) and TiO_2 (Yun et al. 2011)) are directly added into a starch matrix dispersion.
(b) The nanoparticles (ZnO (Ma et al. 2009; Yu et al. 2009) and Sb_2O_3 (Chang et al. 2009; Zheng et al. 2009a)) are firstly synthesized with a stabilizing template, and then the resulting encapsulated nanoparticles are incorporated into a starch dispersion.
(c) The nanoparticles (SiO_2 (Tang et al. 2008a; Yao et al. 2011), TiO_2 (Liao and Wu 2008), CdS (Radhakrishnan et al. 2007), and CdSe (Zhao et al. 2008)) are directly synthesized in a starch dispersion, which acts not only as the stabilizer but also as the matrix of the resulting nano-biocomposite (sol–gel method).

The first method has only been applied to nano-SiO_2, which is a kind of amorphous powder with a molecular structure that is a three-dimensional net, the structure of which is shown in Fig. 16. Nano-SiO_2 deviates from a stable silicon–oxygen structure for the lack of oxygen in its surface. Its molecular formula is SiO_{2-x}, in which x ranges from 0.4 to 0.8 (Tang et al. 2009; Xiong et al. 2008). Because of its small size (30–60 nm), large specific surface area (>400 m^2/g), high surface energy, as well as a lot of unsaturated chemical bonds and hydroxyl groups on the surface, nano-SiO_2 is easy to disperse into a polymer matrix (Tang et al. 2009; Wu et al. 2009b; Xiong et al. 2008). However, the direct addition of nano-SiO_2 into a starch slurry normally requires intensive sonication and/or shearing; otherwise, large aggregates of the nanoparticles will remain, resulting in less improved or even deteriorated properties (Frost et al. 2011; Wu et al. 2009b). A better solution to achieve good dispersion of SiO_2 nanoparticles in a starch matrix is by using the third method (Tang et al. 2008a; Yao et al. 2011). It is worth noting that the sol–gel method has recently been extended to a reactive extrusion (REX) process for producing starch–PVA nano-biocomposites (Frost et al. 2011), which will be detailed in Sect. 12.3.

The nanoparticles of metal oxides and chalcogenides are mainly prepared by the second and third methods. For the nanoparticle synthesis in the second method, polysaccharides such as native starch (Rodriguez et al. 2008), soluble starch (Chairam et al. 2009; Li et al. 2007; Ma et al. 2009; Radhakrishnan et al. 2007; Vigneshwaran et al. 2006; Wei et al. 2004), and CMC (Chang et al. 2009; Liu et al. 2011a; Yu et al. 2009; Zheng et al. 2009a) have been shown to be good stabilizers. Polysaccharides can form complexes with divalent metal ions due to their high number of coordinating functional groups (hydroxyl and glucoside groups) (Taubert and Wegner 2002) and present dynamic supramolecular associations facilitated by inter- and intramolecular hydrogen bonding, which can act as templates for metal nanoparticle growth (Raveendran et al. 2003). As a result, metal ions can preferentially be associated with a polysaccharide, of which the nucleating effect can promote the initial crystal growth of the metal oxide, improve the stability of the nanoparticles in water, and prevent the aggregation of the nanoparticles (Chang et al. 2009; Ma

DOI 10.1007/978-3-319-03751-6_50-1

et al. 2009; Yu et al. 2009; Zheng et al. 2009a). After synthesis, there is normally strong binding in the ZnO nanoparticles, although no obvious formation of covalent bonds occurs between the stabilizer (soluble starch or CMC) and the ZnO (Ma et al. 2009; Yu et al. 2009). In contrast, for the CMC-stabilized $ZrO_2 \cdot nH_2O$, interaction exists between the ZrO_2 and the C–O groups of the CMC (Liu et al. 2011a; Pawlak and Mucha 2003). On the other hand, by using the third method, the average size (3.6–5 nm) of CdS nanoparticles can be dependent on the initial concentration of cadmium acetate during the sample preparation (Radhakrishnan et al. 2007).

12.2 Effects of the Addition of Metalloid Oxides, Metal Oxides, and Chalcogenides

As reported in the literature, uniform dispersion of a nanofiller in a starch matrix and strong interfacial adhesion through hydrogen bonding between the nanoparticles and the matrix could normally be achieved, especially for polysaccharide-encapsulated metal nanoparticles due to the similar chemical structures of the stabilizer and the matrix (Chang et al. 2009; Liu et al. 2011a; Ma et al. 2009; Yu et al. 2009; Zheng et al. 2009a). As a result, improvement in the performance could be normally observed, even though some aspects of property deterioration have also been reported. The details are summarized below:

- Mechanical properties: increases in the tensile strength (Chang et al. 2009; Liu et al. 2011a; Ma et al. 2009; Wu et al. 2009b; Yu et al. 2009; Yun et al. 2011; Zheng et al. 2009a), Young's modulus (Ma et al. 2009; Yu et al. 2009), and the storage modulus (DMA) (Ma et al. 2009; Yu et al. 2009) and a decrease in the elongation at break (Chang et al. 2009; Liu et al. 2011a; Zheng et al. 2009a) have been reported. These could be ascribed to the decreased mobility of the polymer chains in the presence of the nanofiller, which has strong interactions with the matrix (ZnO (Ma et al. 2009; Yu et al. 2009), $ZrO_2 \cdot nH_2O$ (Liu et al. 2011a)).
- Glass transition: an increase in the T_g (Ma et al. 2009; Yu et al. 2009) could result from the reduced free volume with the presence of the nanoparticles which act as physical joints (ZnO (Ma et al. 2009; Yu et al. 2009)).
- Water resistance: a decrease in the WVP with the addition of ZnO (Ma et al. 2009; Yu et al. 2009), ZrO_2 (Liu et al. 2011a), or Sb_2O_3 (Chang et al. 2009) nanoparticles was reported, which was ascribed to the introduction of the nanoparticles providing fewer and more tortuous pathways for water molecules to diffuse. However, Radhakrishnan et al. (2007) observed an increase in the water uptake of starch–CdS nano-biocomposites at specific relative humidity and attributed this phenomenon to the higher exposed hydroxyl groups in the presence of the nanoparticles which broke the intermolecular interactions of the starch matrix.
- Melting/crystallinity: lower melting temperature but higher melting enthalpy was observed for starch–CdS nano-biocomposites by Radhakrishnan et al. (2007), who proposed that, though the CdS nanoparticles have a nucleating effect for the starch chain recrystallization (facilitated by the water diffusion), smaller crystals and broader melting crystal size distribution were also generated.
- Thermal stability: a decrease in the thermal decomposition temperature but an increase in the residual weight at the end of thermal decomposition was observed for nano-biocomposites reinforced by $ZrO_2 \cdot nH_2O$ (Liu et al. 2011a), CdS (Radhakrishnan et al. 2007), CdSe (Božanić et al. 2009), and Sb_2O_3 (Chang et al. 2009). While Liu et al. (2011a) and Chang et al. (2009) ascribed this to the poor thermal stability of the CMC in the nanoparticles, Radhakrishnan et al. (2007) and Božanić et al. (2009) explained that the increased hydroxyl groups (due to the presence of the nanoparticles which broke the intermolecular interactions of the starch matrix)

DOI 10.1007/978-3-319-03751-6_50-1

could result in thermal condensation between them, which could consequently direct the reaction toward carbonization instead of the formation of volatile components (Zhang et al. 2002),

- UV–visible light absorbance/transmittance: compared to the pure starch matrix, nano-biocomposites reinforced by ZnO (Ma et al. 2009; Yu et al. 2009) and Sb_2O_3 (Chang et al. 2009) displayed increased UV–Vis absorbance due to the quantum confinement effect of the nanofiller, and both the starch–CdS (Radhakrishnan et al. 2007) and starch–CdSe (Božanić et al. 2009) nano-biocomposite films showed improved light transparency.

A higher addition level of nanofiller may result in the agglomeration of nanoparticles (Chang et al. 2009; Liu et al. 2011a; Ma et al. 2009; Yu et al. 2009; Zheng et al. 2009a), which is unfavorable for the performance improvement of the nano-biocomposites. In a study on the starch–SiO_2 nano-biocomposites for textile applications, for example, Wu et al. (2009b) found that the best tensile strength and wear resistance could be achieved when the nano-SiO_2 addition level was 4 % and 3 %, respectively, with the reasons being the even distribution of the nanoparticles and the strong nanofiller–matrix interactions at these levels, while the lubricating effect of the rigid nanofiller could also contribute to improved abrasion resistance.

12.3 Starch–Poly(vinyl Alcohol)–Silicon Dioxide Nanocomposites

There have been a series of studies (Frost et al. 2011; Tang et al. 2009, 2008a; Xiong et al. 2008; Yao et al. 2011) on SiO_2-reinforced nanocomposites in which starch and PVA were the matrix. This may improve the mechanical properties and water resistance of starch–PVA films which are still lower than those of conventional polymers (Tang and Alavi 2011).

Xiong et al. (2008) utilized a solution casting method to prepare this kind of nanocomposites. It was found that the addition of nano-SiO_2 resulted in the formation of hydrogen bonds in the hybrid materials, whereas the intermolecular hydrogen bonding of the starch was decreased. Meanwhile, chemical bonds of C–O–Si were also formed in the nanocomposites. These contributed to the increased miscibility and compatibility between the starch and the PVA. In addition, the addition of the nano-SiO_2 had no influence on the crystalline type of the films, but decreased the crystallinity because of the disturbance of the parallel arrangement of the starch–PVA chains. As a result of the structural changes, the nanofiller played a key role as cross-linking points and restricted the movement of the chains. Therefore, the tensile strength, elongation at break, and light transmittance were increased and the water absorption was decreased. Nevertheless, biodegradation as a whole was not affected though there was a lower degradation rate at the early stage. Following this study, Tang et al. (2009) further investigated the effect of the nano-SiO_2 content (1–5 wt %, on the basis of starch and PVA) on the changes in the properties of the nanocomposites. They found that 3 wt % was the optimized level of the nano-SiO_2 for the best tensile strength and the lowest water absorption. The reduced tensile strength with the higher nano-SiO_2 content was due to the intensification of the elastic collision of the nanoparticles which showed aggregation and had phase separation with the matrix. In addition, the high surface energy and plenty of free hydroxyl groups of the nano-SiO_2, which is beneficial to interact with water, might have a counter-effect on moisture resistance when the nanofiller content was high (Tang et al. 2009).

Tang et al. (2008a) and Yao et al. (2011) used a sol–gel method to fabricate starch–PVA–SiO_2 composites, in which tetraethyl orthosilicate (TEOS) was used as the precursor to obtain SiO_2 in situ in the polymer solution. A network structure in the composites was formed by combining the SiO_2 with the starch–PVA with hydrogen and C–O–Si bonding (Tang et al. 2008a; Yao et al. 2011). The trends of changes in the properties (mechanical properties, water sensitivity, light transmittance, and biodegradation) with the SiO_2 content (Tang et al. 2008a; Yao et al. 2011) were similar to those in the previous studies (Tang et al. 2009; Xiong et al. 2008). Using the same principle, Frost et al. (2011) made the first trial of using a continuous REX process to produce films of such composites, where the TEOS-to-SiO_2 conversion efficiency was up to 41.3 % and the actual SiO_2 content was up to 1.24 wt %. The resulting films had spherical SiO_2 agglomerates of size ranging from 20 to <1 μm, which were responsible for the increased tensile strength, Young's modulus, and storage modulus (DMA).

In addition to product property improvement, it is noteworthy that SiO_2 can also be used to adjust the viscosity of a polymer and thus to improve the miscibility of this polymer with starch in a melt blending process (Bélard et al. 2009). More details are given in a recent review paper (Xie et al. 2012).

13 Nanocomposites Reinforced by Layered Double Hydroxides

The LDH structure is referred to as the natural hydrotalcite and described by the ideal formula $[M^{II}_{1-x}M^{III}_{x}(OH)]_{intra}[A^{m-}_{x/m} \cdot nH_2O]_{inter}$, where "$M^{II}$" and "$M^{III}$" are metal cations, "A" is the anion, and "intra" and "inter" denote the intralayer domain and the interlayer space, respectively (Leroux and Besse 2001). The structure consists of brucite-like layers constituted of edge-sharing $M(OH)_6$ octahedra (cf. Fig. 17) (Hofmeister and Platen 1992; Leroux and Besse 2001). Partial "M^{II}" and "M^{III}" substitution induces a positive charge for the layers, balanced with the presence of the interlayered anions (Leroux and Besse 2001).

Chung and Lai (2010) compared an LDH synthesized in a starch matrix (unmodified maize starch or acid-modified maize starch), which involved fast LDH nuclei precipitation followed by a hydrothermal treatment that simultaneously leached the starch molecules from the granules and aged the LDH nuclei, with one synthesized without the starch matrix. They found that the presence of starch during the synthesis effectively inhibited the stacking of the clay sheets, with the crystal size corresponding to approximately seven brucite-like layers (Chung and Lai 2010). However, no intercalated structure in the starch–LDH biocomposites was indicated, with the reason being ascribed to the rigid structure of the polysaccharide chains (Chung and Lai 2010). The LDH tended to present aggregated morphology in the unmodified maize starch, whereas almost individual dispersion of the LDH was observed in the acid-modified starch. This is due to the lower viscosity of the acid-modified starch. Unfortunately, even the acid-modified starch–LDH biocomposites only showed an increase in Young's modulus, whereas the crystallinity, tensile strength, moisture

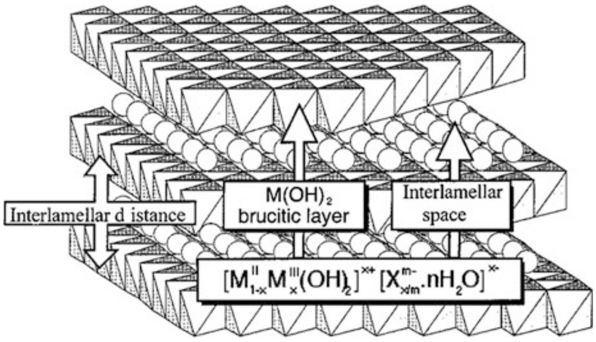

Fig. 17 Scheme of the typical LDH structure (Reprinted with permission from Leroux and Besse (2001). Copyright 2001 American Chemical Society)

DOI 10.1007/978-3-319-03751-6_50-1

sensitivity, and transparency were hardly affected. These results could be possibly attributed to the poor interaction between the LDH and the matrix (Chung and Lai 2010).

Alternatively, Wu et al. (2011) used carboxymethyl cellulose sodium (CMC) as a stabilizer to synthesize an LDH, of which the size and number of the stacked sheets were similar to that in the study by Chung and Lai (2010). However, starch-based biocomposites reinforced by this LDH at a low loading level (6 wt %) were reported to show obviously improved mechanical properties (increased tensile strength) and water resistance (decreased WVP) (Wu et al. 2011). There are two reasons for the improvement: (a) because polysaccharides could form complexes with metal ions due to the high number of coordinating functional groups (hydroxyl and glucoside groups) (Taubert and Wegner 2002), strong associations between the metal ions and the CMC occurred for the nucleation and initial crystal growth of the LDH, and thus the LDH was successfully encapsulated by the CMC and (b) the hydrophilic CMC component and the smaller size of each LDH stack allowed the LDH to be well dispersed in the starch matrix and good interactions between the nanofiller and the matrix were formed because of the CMC component (Wu et al. 2011). However, the biocomposites displayed a decrease in the thermal decomposition temperature because the weak thermal stability of the CMC could weaken the interactions between the LDH filler and the starch matrix and facilitate the decomposition of the starch (Wu et al. 2011). Furthermore, high LDH content (8 wt %) could result in the agglomeration of the nanofiller in the matrix and thus reduce the mechanical properties and WVP (Wu et al. 2011).

14 Nanocomposites Reinforced by α-Zirconium Phosphate

Synthetic α-ZrP (i.e., $Zr(HPO_4)_2 \cdot H_2O$) exhibits similar structural characteristics to natural MMT clay but has advantages such as high purity and ion exchange capacity and ease of intercalation and exfoliation (Clearfield et al. 1972; Clearfield and Berman 1981; Sun et al. 2005; Wu et al. 2009a). In addition, the particle size and aspect ratio can be manipulated by varying the reaction conditions (Wu et al. 2009a). Wu et al. (2009a) investigated starch-based nano-biocomposite films reinforced by α-ZrP at different loading levels. The results from XRD and SEM indicated that the plasticized starch and the α-ZrP interacted and formed strong hydrogen bonds, resulting in improved compatibility. Compared with the neat plasticized starch, the nano-biocomposite films showed increases in the tensile strength and elongation at break, decreases in the crystallinity and moisture uptake, and a slight decrease in the transparency. The improvement in the mechanical properties was due to the much enhanced nanofiller–matrix interaction since α-ZrP has huge surface area The decrease in the moisture sensitivity was attributed to the decreased number of –OH groups available for the interaction with migrating water molecules. Nevertheless, higher content of the nanofiller could contribute to an adverse effect on the improvement in the properties due to the phase separation and the aggregation of the nanofiller, but not as much to reach back the values of the pure starch film. Besides, the maximum thermal decomposition temperatures of the nano-biocomposite films decreased with an increase in the α-ZrP content, which could be ascribed to the increase in the acidity of the α-ZrP with the increase in the temperature, which induces the decomposition of the glycoside bonds (Wu et al. 2009a).

DOI 10.1007/978-3-319-03751-6_50-1

15 Nanocomposites Reinforced by Hydroxyapatite

The use of HA is mainly for making biomaterials for biomedical applications such as clinical orthopedics because HA has the chemical and crystallographic similarity to the inorganic component of natural bone and has excellent biocompatibility, bioactivity, and osteoconductivity (Murugan and Ramakrishna 2004). The successful use of injection molding to produce HA-reinforced starch–EVA nanocomposites with high mechanical performance for temporary tissue replacement applications has been demonstrated (Reis et al. 1997). Besides, like metalloid oxides, metal oxides, and metal chalcogenides, rodlike nano-HA crystals can be synthesized with controlled shape and size using soluble starch as a template (via an in situ biomimetic process) (Meskinfam et al. 2011; Sadjadi et al. 2010). The bioactivity and biocompatibility of the resulting biocomposites were verified (Meskinfam et al. 2011; Sadjadi et al. 2010). Sundaram et al. (2008) reported the fabrication of a porous scaffold biomaterial made from nano-HA, gelatin, and starch displaying the appropriate enhanced mechanical properties for bone repair and regeneration.

16 Conclusion

Starch-based nano-biocomposites are novel multiphase systems that can be tuneable via the type, geometry (size and shape), and surface chemistry of the nanofiller, the type/amylose content and chemical modification of the starch, the type and content of the plasticizer(s) and additive(s), and the processing steps and conditions.

A wide variety of nanofillers have been examined with starch matrix. Phyllosilicates have been mostly utilized to develop starch-based nano-biocomposites due to their advantages such as wide availability, low cost, and high aspect ratio and thus vast exposed surface area. In this group of nanofiller, smectite group clays especially MMT are most popular due to their swelling nature and large availability. In addition, polysaccharide nanofillers (typically CNWs and SNPs) represent the second most popular group of nanofillers to realize starch-based nano-biocomposites because of their abundance in nature, the biological sources, and the chemical similarity to starch. Unfortunately, the preparation of these biobased nanoparticles is time consuming and involves acid hydrolysis in multiple steps which is not eco-friendly. Furthermore, studies have also been carried out for incorporating many other nanofillers such as carbonaceous nanofillers (typically CNTs), metalloid oxides (e.g., SiO_2 and Sb_2O_3), metal oxides (e.g., ZnO, TiO_2, and $ZrO_2 \cdot nH_2O$), and metal chalcogenides (e.g., CdS, CdSe). One of the advantages in utilizing such nanofillers is that they can provide new functionalities to starch-based materials in addition to the general reinforcement. Unfortunately, some of these last nanoparticles (e.g., the CNTs) may have a detrimental impact on the human health and the environment (Helland et al. 2007; Klaine et al. 2008; Lam et al. 2006; Oberdörster et al. 2007). Finally, some much less frequently employed nanofillers are LDH, α-ZrP, and HA.

With the incorporation of the nanofiller, starch-based materials generally show improvement in some of their properties such as mechanical properties (typically tensile strength, Young's modulus, and storage modulus), T_g (of the starch-rich domains), thermal stability, moisture resistance, gas/solvent barrier property, and biodegradation rate. The improvement can be fundamentally ascribed to the homogeneous dispersion of the nanofiller in the matrix and the strong interface adhesion, which can contribute to the formation of a rigid nanofiller network and influence the molecular and crystalline structures in the matrix. Regarding the dispersion, intercalation or even exfoliation is desired for the nano-biocomposites reinforced by layered nanofillers, which can be assisted by some pretreatment/activation methods. To achieve good nanofiller dispersion and strong interface adhesion, the compatibility between the nanofiller and the matrix is the key point to address, although intensive processing means such as shearing, stirring, and sonication could also help. When phyllosilicates are used, the best nanofiller could be those containing Na^+ or cationic starch as the counter-cation due to better polarity matching with the starch matrix. Besides, while polysaccharide nanofillers normally do not have starch compatibility issues, some modifications have to be used for many other types of nanofillers to increase the compatibility with starch which has a hydrophilic nature. In all these systems, the interactions between the nanofiller and the matrix are usually achieved by hydrogen bonding. However, the nanofiller–matrix interactions can be affected by more factors such as the plasticizer(s)/additive(s), the starch chemical modification, the presence of other polymer(s) in the matrix, and the processing conditions. In spite of the discussion above, some property changes could not be exclusively attributed to the dispersion of the nanofiller in the matrix and the nanofiller–matrix interactions. Typical examples are the moisture resistance, which could be counter-affected by the hydrophilicity of the plasticizer(s) and the nanofiller, and the thermal stability, which could be counter-affected by the functional groups or the modifying/stabilizing polymer of the nanofiller. Furthermore, the nanofiller plays an important role in determining the properties of the nano-biocomposite. The extent of improvement can be related to the aspect ratio/surface area, chemistry, and mechanical properties of the nanofiller, which may have a relationship with its mixing preparation and modification of final structure and properties. A typical example is that the geometry (size and shape) and the crystallinity of cellulose nanowhiskers are highly dependent on the preparation method and conditions, influencing the final performance properties of the nano-biocomposites.

Nevertheless, how the nanofiller affected the crystalline structure and crystallinity of the starch matrix has not been unambiguously elucidated across the literature. Several reasons might account for this: (a) the crystalline structure and crystallinity of starch-based materials can be highly affected by the formulation (e.g., the amylose content of the starch and the type and content of the plasticizer), the processing conditions (e.g., temperature, pressure, shearing, and orientation), and the storing conditions (e.g., time, temperature, and relative humidity); (b) phase separation of the plasticizer, the starch, and/or the nanofiller may exist in the system, with the different domains showing different recrystallization/anti-crystallization behaviors; and (c) effective means are lacking in the accurate thermal and structural characterization of starch. It is significant to note that some of these reasons may also account for the discrepancies in some of the other results such as T_g and moisture resistance.

With improved properties that are comparable to those of traditional petroleum-based polymers such as polyethylene and polypropylene, starch-based nano-biocomposites can be designed into various products such as blown/casting films, extruded sheets, expanded foams, and thermoformed shapes. These can greatly enhance and widen the current applications of starch-based materials. In addition to the general reinforcement, some nanofillers have been reported to provide new functionalities to starch-based materials, such as superabsorption, electroactivity, electroconductivity, electrorheological behavior, UV shielding, drug releasing, scaffolding (in tissue engineering), and environmental purification. Consequently, starch-based nano-biocomposites have been or are expected to be applied in a wide range of fields such as packaging, agriculture, medicine, and electronics. Furthermore, the renewable resource and inherent environmental friendliness of such materials can justify its wide use for a sustainable future.

In the future research, it is still very important to test new nanofillers to be incorporated into starch for developing promising nano-biocomposites with excellent performance and new functionalities to be competitive in the materials world. Specifically, maintaining homogeneous dispersion of the nanofiller in the matrix and having strong interface adhesion are the key prerequisites. Good dispersion of the nanofiller results in a greater contact area; otherwise, the filler is not a nanofiller (but micron-sized aggregates) and the composite can only be regarded as microcomposite instead of nanocomposite. As pointed out by Schaefer and Justice (Schaefer and Justice 2007), the current nanocomposites are often not “nano enough,” resulting in the elusive realization of anticipated properties. They discovered that large-scale disorder is ubiquitous in nanocomposites regardless of the level of dispersion, leading to substantial reduction of mechanical properties (modulus) compared to predictions based on idealized filler morphology (Schaefer and Justice 2007). This problem should also be addressed when developing starch-based nano-biocomposites since heterogeneous dispersion of the nanofiller and phase separation unfortunately also existed in some of the studies examined in the current review. While the manipulation of chemistry might help to some extent, the future research should also address the importance in using processing techniques like extrusion, film blowing, and injection/compression molding, which are more aligned to the efficient industrial production. With such processing, intensive thermomechanical treatment is normally involved, which could possibly play the dominant role in controlling the morphology and structure and thus the performance of starch-based nano-biocomposites. Thus more research is needed regarding how to achieve a well-dispersed structure without adding a detrimental effect to the final properties by starch molecular degradation under thermomechanical treatment.

References

Ajayan PM (1999) Nanotubes from carbon. Chem Rev 99(7):1787–1800

Al E, Güçlü G, Banuİyim T, Emik S, Özgümü S (2008) Synthesis and properties of starch-graft-acrylic acid/Na-montmorillonite superabsorbent nanocomposite hydrogels. J Appl Polym Sci 109(1):16–22

Alexandre M, Dubois P (2000) Polymer-layered silicate nanocomposites: preparation, properties and uses of a new class of materials. Mater Sci Eng R Rep 28(1–2):1–63

Alvarez VA, Fraga AN, Vázquez A (2004) Effects of the moisture and fiber content on the mechanical properties of biodegradable polymer–sisal fiber biocomposites. J Appl Polym Sci 91(6):4007–4016

Angellier H, Choisnard L, Molina-Boisseau S, Ozil P, Dufresne A (2004) Optimization of the preparation of aqueous suspensions of waxy maize starch nanocrystals using a response surface methodology. Biomacromolecules 5(4):1545–1551

Angellier H, Molina-Boisseau S, Dole P, Dufresne A (2006) Thermoplastic starch-waxy maize starch nanocrystals nanocomposites. Biomacromolecules 7(2):531–539

Angles MN, Dufresne A (2000) Plasticized starch/tunicin whiskers nanocomposites. 1. Structural analysis. Macromolecules 33(22):8344–8353

Angles MN, Dufresne A (2001) Plasticized starch/tunicin whiskers nanocomposite materials. 2. Mechanical behavior. Macromolecules 34(9):2921–2931

Arroyo OH, Huneault MA, Favis BD, Bureau MN (2010) Processing and properties of PLA/thermoplastic starch/montmorillonite nanocomposites. Polym Compos 31(1):114–127

Atwell WA, Hood LF, Lineback DR, Varrianomarston E, Zobel HF (1988) The terminology and methodology associated with basic starch phenomena. Cereal Foods World 33(3):306–311

Avella M, De Vlieger JJ, Errico ME, Fischer S, Vacca P, Volpe MG (2005) Biodegradable starch/clay nanocomposite films for food packaging applications. Food Chem 93(3):467–474

DOI 10.1007/978-3-319-03751-6_50-1

Avérous L (2002) Interactions between cellulose and plasticized wheat starch – properties of biodegradable multiphase systems. In: Renard D, Della G, Popineau Y (eds) Plant biopolymer science: food and non-food applications. Royal Society of Chemistry, London, pp 253–259

Avérous L (2004) Biodegradable multiphase systems based on plasticized starch: a review. Polym Rev 44(3):231–274

Averous L (2007) Cellulose-based biocomposites: comparison of different multiphasic systems. Compos Interfaces 14:787–805

Averous L, Boquillon N (2004) Biocomposites based on plasticized starch: thermal and mechanical behaviours. Carbohydr Polym 56(2):111–122

Avérous L, Halley PJ (2009) Biocomposites based on plasticized starch. Biofuels Bioprod Biorefin 3(3):329–343

Avérous LR, Halley PJ (2014) Starch polymers: from the field to industrial products. In: Halley PJ, Avérous LR (eds) Starch polymers: from genetic engineering to green applications. Elsevier, Amsterdam, pp 3–10

Avérous L, Fringant C, Moro L (2001) Plasticized starch-cellulose interactions in polysaccharide composites. Polymer 42(15):6565–6572

Azizi Samir MAS, Alloin F, Sanchez J-Y, El Kissi N, Dufresne A (2004) Preparation of cellulose whiskers reinforced nanocomposites from an organic medium suspension. Macromolecules 37(4):1386–1393

Azizi Samir MAS, Alloin F, Dufresne A (2005) Review of recent research into cellulosic whiskers, their properties and their application in nanocomposite field. Biomacromolecules 6(2):612–626

Bagdi K, Müller P, Pukánszky B (2006) Thermoplastic starch/layered silicate composites: structure, interaction, properties. Compos Interfaces 13:1–17

Barron C, Bouchet B, Della Valle G, Gallant DJ, Planchot V (2001) Microscopical study of the destructuring of waxy maize and smooth pea starches by shear and heat at low hydration. J Cereal Sci 33(3):289–300

Baumberger S (2002) Starch-lignin films. In: Thomas QH (ed) Chemical modification, properties, and usage of lignin. Springer, London, pp 1–19

Baumberger S, Lapierre C, Monties B (1998a) Utilization of pine kraft lignin in starch composites: impact of structural heterogeneity. J Agric Food Chem 46(6):2234–2240

Baumberger S, Lapierre C, Monties B, Valle GD (1998b) Use of kraft lignin as filler for starch films. Polym Degrad Stab 59(1–3):273–277

Bélard L, Dole P, Avérous L (2009) Study of pseudo-multilayer structures based on starch-polycaprolactone extruded blends. Polym Eng Sci 49(6):1177–1186

Bergaya F, Jaber M, Lambert J-F (2012) Clays and clay minerals as layered nanofillers for (bio) polymers. In: Avérous L, Pollet E (eds) Environmental silicate nano-biocomposites (green energy and technology). Springer, London, pp 41–75

Bocchini S, Battegazzore D, Frache A (2010) Poly (butylensuccinate co-adipate)-thermoplastic starch nanocomposite blends. Carbohydr Polym 82(3):802–808

Böhm GGA, Nguyen MN (1995) Flocculation of carbon black in filled rubber compounds. I. Flocculation occurring in unvulcanized compounds during annealing at elevated temperatures. J Appl Polym Sci 55(7):1041–1050

Bondeson D, Mathew A, Oksman K (2006) Optimization of the isolation of nanocrystals from microcrystalline cellulose by acid hydrolysis. Cellulose 13(2):171–180

Bonnet P, Albertini D, Bizot H, Bernard A, Chauvet O (2007) Amylose/SWNT composites: from solution to film – synthesis, characterization and properties. Compos Sci Technol 67(5):817–821

Božanić DK, Djoković V, Bibić N, Sreekumari Nair P, Georges MK, Radhakrishnan T (2009) Biopolymer-protected CdSe nanoparticles. Carbohydr Res 344(17):2383–2387

Breuer O, Tchoudakov R, Narkis M, Siegmann A (1997) Segregated structures in carbon black-containing immiscible polymer blends: HIPS/LLDPE systems. J Appl Polym Sci 64(6):1097–1106

Buléon A, Colonna P, Planchot V, Ball S (1998) Starch granules: structure and biosynthesis. Int J Biol Macromol 23(2):85–112

Bulkin BJ, Kwak Y, Dea ICM (1987) Retrogradation kinetics of waxy-corn and potato starches; a rapid, Raman-spectroscopic study. Carbohydr Res 160:95–112

Burros BC, Young LA, Carroad PA (1987) Kinetics of corn meal gelatinization at high temperature and low moisture. J Food Sci 52(5):1372–1376

Cai J, Zhang L (2005) Unique gelation behavior of cellulose in NaOH/urea aqueous solution. Biomacromolecules 7(1):183–189

Cao X, Chen Y, Chang PR, Huneault MA (2007) Preparation and properties of plasticized starch/multiwalled carbon nanotubes composites. J Appl Polym Sci 106(2):1431–1437

Cao X, Chen Y, Chang PR, Muir AD, Falk G (2008a) Starch-based nanocomposites reinforced with flax cellulose nanocrystals. Express Polym Lett 2(7):502–510

Cao X, Chen Y, Chang PR, Stumborg M, Huneault MA (2008b) Green composites reinforced with hemp nanocrystals in plasticized starch. J Appl Polym Sci 109(6):3804–3810

Carvalho AJF, Zambon MD, Curvelo AAS, Gandini A (2003) Size exclusion chromatography characterization of thermoplastic starch composites 1. Influence of plasticizer and fibre content. Polym Degrad Stab 79(1):133–138

Cases JM, Berend I, Besson G, Francois M, Uriot JP, Thomas F, Poirier JE (1992) Mechanism of adsorption and desorption of water vapor by homoionic montmorillonite. 1. The sodium-exchanged form. Langmuir 8(11):2730–2739

Casey A, Farrell GF, McNamara M, Byrne HJ, Chambers G (2005) Interaction of carbon nanotubes with sugar complexes. Synth Met 153(1–3):357–360

Chairam S, Poolperm C, Somsook E (2009) Starch vermicelli template-assisted synthesis of size/shape-controlled nanoparticles. Carbohydr Polym 75(4):694–704

Chang PR, Yu J, Ma X (2009) Fabrication and characterization of Sb_2O_3/carboxymethyl cellulose sodium and the properties of plasticized starch composite films. Macromol Mater Eng 294(11):762–767

Chang PR, Jian R, Yu J, Ma X (2010a) Fabrication and characterisation of chitosan nanoparticles/plasticised-starch composites. Food Chem 120(3):736–740

Chang PR, Jian R, Yu J, Ma X (2010b) Starch-based composites reinforced with novel chitin nanoparticles. Carbohydr Polym 80(2):421–426

Chang PR, Jian R, Zheng P, Yu J, Ma X (2010c) Preparation and properties of glycerol plasticized-starch (GPS)/cellulose nanoparticle (CN) composites. Carbohydr Polym 79(2):301–305

Chatterjee A, Deopura BL (2006) Thermal stability of polypropylene/carbon nanofiber composite. J Appl Polym Sci 100(5):3574–3578

Chaudhary DS (2008) Understanding amylose crystallinity in starch-clay nanocomposites. J Polym Sci B Polym Phys 46(10):979–987

Chaudhary AL, Miler M, Torley PJ, Sopade PA, Halley PJ (2008) Amylose content and chemical modification effects on the extrusion of thermoplastic starch from maize. Carbohydr Polym 74(4):907–913

Chaudhary D, Liu H, John J, Tadé MO (2011) Morphological investigation into starch bio-nanocomposites via synchrotron radiation and differential scanning calorimetry. J Nanotechnol, Article 924582/1–14

Chaudhary DS, Adhikari BP, Kasapis S (2011b) Glass-transition behaviour of plasticized starch biopolymer system – a modified Gordon-Taylor approach. Food Hydrocoll 25(1):114–121

Chen B, Evans JRG (2005) Thermoplastic starch-clay nanocomposites and their characteristics. Carbohydr Polym 61(4):455–463

Chen M, Chen B, Evans JRG (2005) Novel thermoplastic starch-clay nanocomposite foams. Nanotechnology 16(10):2334

Chen P, Yu L, Kealy T, Chen L, Li L (2007) Phase transition of starch granules observed by microscope under shearless and shear conditions. Carbohydr Polym 68(3):495–501

Chen Y, Liu C, Chang PR, Anderson DP, Huneault MA (2009a) Pea starch-based composite films with pea hull fibers and pea hull fiber-derived nanowhiskers. Polym Eng Sci 49(2):369–378

Chen Y, Liu C, Chang PR, Cao X, Anderson DP (2009b) Bionanocomposites based on pea starch and cellulose nanowhiskers hydrolyzed from pea hull fibre: effect of hydrolysis time. Carbohydr Polym 76(4):607–615

Chiou B-S, Yee E, Glenn GM, Orts WJ (2005) Rheology of starch-clay nanocomposites. Carbohydr Polym 59(4):467–475

Chiou BS, Yee E, Wood D, Shey J, Glenn G, Orts W (2006) Effects of processing conditions on nanoclay dispersion in starch-clay nanocomposites. Cereal Chem 83(3):300–305

Chiou B-S, Wood D, Yee E, Imam SH, Glenn GM, Orts WJ (2007) Extruded starch-nanoclay nanocomposites: effects of glycerol and nanoclay concentration. Polym Eng Sci 47(11):1898–1904

Chivrac F, Gueguen O, Pollet E, Ahzi S, Makradi A, Averous L (2008a) Micromechanical modeling and characterization of the effective properties in starch-based nano-biocomposites. Acta Biomater 4(6):1707–1714

Chivrac F, Pollet E, Schmutz M, Avérous L (2008b) New approach to elaborate exfoliated starch-based nanobiocomposites. Biomacromolecules 9(3):896–900

Chivrac F, Pollet E, Avérous L (2009a) Progress in nano-biocomposites based on polysaccharides and nanoclays. Mater Sci Eng R Rep 67(1):1–17

Chivrac F, Pollet E, Avérous L (2009b) Shear induced clay organo-modification: application to plasticized starch nano-biocomposites. Polym Adv Technol 21(8):578–583

Chivrac F, Angellier-Coussy H, Guillard V, Pollet E, Avérous L (2010a) How does water diffuse in starch/montmorillonite nano-biocomposite materials? Carbohydr Polym 82(1):128–135

Chivrac F, Gueguen O, Pollet E, Avérous L, Ahzi S, Belouettar S (2010b) Micromechanically-based formulation of the cooperative model for the yield behavior of starch-based nano-biocomposites. J Nanosci Nanotechnol 10:2949–2955

Chivrac F, Pollet E, Dole P, Avérous L (2010c) Starch-based nano-biocomposites: plasticizer impact on the montmorillonite exfoliation process. Carbohydr Polym 79(4):941–947

Chivrac F, Pollet E, Schmutz M, Avérous L (2010d) Starch nano-biocomposites based on needle-like sepiolite clays. Carbohydr Polym 80(1):145–153

Chung Y-L, Lai H-M (2010) Preparation and properties of biodegradable starch-layered double hydroxide nanocomposites. Carbohydr Polym 80(2):526–533

Chung Y-L, Ansari S, Estevez L, Hayrapetyan S, Giannelis EP, Lai H-M (2010) Preparation and properties of biodegradable starch-clay nanocomposites. Carbohydr Polym 79(2):391–396

DOI 10.1007/978-3-319-03751-6_50-1

Clearfield A, Berman JR (1981) On the mechanism of ion exchange in zirconium phosphates – XXXIV. Determination of the surface areas of α-$Zr(HPO_4)_2 \cdot H_2O$ by surface exchange. J Inorg Nucl Chem 43(9):2141–2142

Clearfield A, Duax WL, Garces JM, Medina AS (1972) On the mechanism of ion exchange in crystalline zirconium phosphates – IV potassium ion exchange of α-zirconium phosphate. J Inorg Nucl Chem 34(1):329–337

Crosby AJ, Lee JY (2007) Polymer nanocomposites: the “nano” effect on mechanical properties. Polym Rev 47(2):217–229

Curran SA, Ajayan PM, Blau WJ, Carroll DL, Coleman JN, Dalton AB, Davey AP, Drury A, McCarthy B, Maier S, Strevens A (1998) A composite from poly(*m*-phenylenevinylene-*co*-2,5-dioctoxy-*p*-phenylenevinylene) and carbon nanotubes: a novel material for molecular optoelectronics. Adv Mater 10(14):1091–1093

Curvelo AAS, de Carvalho AJF, Agnelli JAM (2001) Thermoplastic starch-cellulosic fibers composites: preliminary results. Carbohydr Polym 45(2):183–188

Cyras VP, Manfredi LB, Ton-That M-T, Vazquez A (2008) Physical and mechanical properties of thermoplastic starch/montmorillonite nanocomposite films. Carbohydr Polym 73(1):55–63

Da Róz AL, Carvalho AJF, Gandini A, Curvelo AAS (2006) The effect of plasticizers on thermoplastic starch compositions obtained by melt processing. Carbohydr Polym 63(3):417–424

Dai JC, Huang JT (1999) Surface modification of clays and clay–rubber composite. Appl Clay Sci 15(1–2):51–65

Dai H, Chang P, Geng F, Yu J, Ma X (2009a) Preparation and properties of thermoplastic starch/montmorillonite nanocomposite using *N*-(2-hydroxyethyl)formamide as a new additive. J Polym Environ 17(4):225–232

Dai H, Chang PR, Peng F, Yu J, Ma X (2009b) *N*-(2-hydroxyethyl)formamide as a new plasticizer for thermoplastic starch. J Polym Res 16(5):529–535

Dai H, Chang PR, Geng F, Yu J, Ma X (2010a) Preparation and properties of starch-based film using *N*,*N*-bis(2-hydroxyethyl)formamide as a new plasticizer. Carbohydr Polym 79(2):306–311

Dai H, Chang PR, Yu J, Geng F, Ma X (2010b) *N*-(2-hydroxypropyl)formamide and *N*-(2-hydroxyethyl)-*N*-methylformamide as two new plasticizers for thermoplastic starch. Carbohydr Polym 80(1):139–144

de Carvalho AJF, Curvelo AAS, Agnelli JAM (2001) A first insight on composites of thermoplastic starch and kaolin. Carbohydr Polym 45(2):189–194

Dean K, Yu L, Wu DY (2007) Preparation and characterization of melt-extruded thermoplastic starch/clay nanocomposites. Compos Sci Technol 67(3–4):413–421

Dean KM, Do MD, Petinakis E, Yu L (2008) Key interactions in biodegradable thermoplastic starch/poly(vinyl alcohol)/montmorillonite micro- and nanocomposites. Compos Sci Technol 68(6):1453–1462

Dean KM, Petinakis E, Goodall L, Miller T, Yu L, Wright N (2011) Nanostabilization of thermally processed high amylose hydroxylpropylated starch films. Carbohydr Polym 86(2):652–658

Dennis HR, Hunter DL, Chang D, Kim S, White JL, Cho JW, Paul DR (2001) Effect of melt processing conditions on the extent of exfoliation in organoclay-based nanocomposites. Polymer 42(23):9513–9522

Dong XM, Kimura T, Revol J-F, Gray DG (1996) Effects of ionic strength on the isotropic−chiral nematic phase transition of suspensions of cellulose crystallites. Langmuir 12(8):2076–2082

Donnet J-B, Bansal RC, Wang M-J (1993) Carbon black: science and technology, 2nd edn. Marcel Decker, New York (revised and expanded)

Donovan JW (1979) Phase transitions of the starch-water system. Biopolymers 18(2):263–275

Dufresne A (2008) Polysaccharide nano crystal reinforced nanocomposites. Can J Chem 86(6):484–494

Dufresne A, Dupeyre D, Vignon MR (2000) Cellulose microfibrils from potato tuber cells: processing and characterization of starch-cellulose microfibril composites. J Appl Polym Sci 76(14):2080–2092

Duquesne E, Moins S, Alexandre M, Dubois P (2007) How can nanohybrids enhance polyester/sepiolite nanocomposite properties? Macromol Chem Phys 208(23):2542–2550

Dutta PK, Tripathi S, Mehrotra GK, Dutta J (2009) Perspectives for chitosan based antimicrobial films in food applications. Food Chem 114(4):1173–1182

Enrione J, Osorio F, Pedreschi F, Hill S (2010) Prediction of the glass transition temperature on extruded waxy maize and rice starches in presence of glycerol. Food Bioprocess Technol 3(6):791–796

Falvo MR, Clary GJ, Taylor RM, Chi V, Brooks FP, Washburn S, Superfine R (1997) Bending and buckling of carbon nanotubes under large strain. Nature 389(6651):582–584

Famá LM, Pettarin V, Goyanes SN, Bernal CR (2011) Starch/multi-walled carbon nanotubes composites with improved mechanical properties. Carbohydr Polym 83(3):1226–1231

Famá L, Rojo PG, Bernal C, Goyanes S (2012) Biodegradable starch based nanocomposites with low water vapor permeability and high storage modulus. Carbohydr Polym 87(3):1989–1993

Fischer HR, Gielgens LH, Koster TPM (1999) Nanocomposites from polymers and layered minerals. Acta Polym 50(4):122–126

Fornes TD, Yoon PJ, Keskkula H, Paul DR (2001) Nylon 6 nanocomposites: the effect of matrix molecular weight. Polymer 42(25):09929–09940

Forssell PM, Mikkilä JM, Moates GK, Parker R (1997) Phase and glass transition behaviour of concentrated barley starch-glycerol-water mixtures, a model for thermoplastic starch. Carbohydr Polym 34(4):275–282

Fringant C, Desbrières J, Rinaudo M (1996) Physical properties of acetylated starch-based materials: relation with their molecular characteristics. Polymer 37(13):2663–2673

Fringant C, Rinaudo M, Foray MF, Bardet M (1998) Preparation of mixed esters of starch or use of an external plasticizer: two different ways to change the properties of starch acetate films. Carbohydr Polym 35(1–2):97–106

Frost K, Barthes J, Kaminski D, Lascaris E, Niere J, Shanks R (2011) Thermoplastic starch-silica-polyvinyl alcohol composites by reactive extrusion. Carbohydr Polym 84(1):343–350

Fu C, Meng L, Lu Q, Zhang X, Gao C (2007) Large-scale production of homogeneous helical amylose/SWNTs complexes with good biocompatibility. Macromol Rapid Commun 28(22):2180–2184

Funke U, Bergthaller W, Lindhauer MG (1998) Processing and characterization of biodegradable products based on starch. Polym Degrad Stab 59(1–3):293–296

Gallant DJ, Bouchet B, Baldwin PM (1997) Microscopy of starch: evidence of a new level of granule organization. Carbohydr Polym 32(3–4):177–191

Gao W, Dong H, Hou H, Zhang H (2012) Effects of clays with various hydrophilicities on properties of starch–clay nanocomposites by film blowing. Carbohydr Polym 88(1):321–328

García NL, Ribba L, Dufresne A, Aranguren MI, Goyanes S (2009) Physico-mechanical properties of biodegradable starch nanocomposites. Macromol Mater Eng 294(3):169–177

García NL, Ribba L, Dufresne A, Aranguren M, Goyanes S (2011) Effect of glycerol on the morphology of nanocomposites made from thermoplastic starch and starch nanocrystals. Carbohydr Polym 84(1):203–210

DOI 10.1007/978-3-319-03751-6_50-1

Gaudin S, Lourdin D, Le Botlan D, Ilari JL, Colonna P (1999) Plasticisation and mobility in starch-sorbitol films. J Cereal Sci 29(3):273–284

Geim AK, Novoselov KS (2007) The rise of graphene. Nat Mater 6(3):183–191

Giannelis EP (1996) Polymer layered silicate nanocomposites. Adv Mater 8(1):29–35

Godovsky DY (2000) Device applications of polymer-nanocomposites, Biopolymers – PVA hydrogels, anionic polymerisation nanocomposites. Springer, Berlin, pp 163–205

Gopalan Nair K, Dufresne A, Gandini A, Belgacem MN (2003) Crab shell chitin whiskers reinforced natural rubber nanocomposites. 3. Effect of chemical modification of chitin whiskers. Biomacromolecules 4(6):1835–1842

Grande CJ, Torres FG, Gomez CM, Troncoso OP, Canet-Ferrer J, Martinez-Pastor J (2008) Morphological characterisation of bacterial cellulose-starch nanocomposites. Polym Polym Compos 16(3):181–185

Grande CJ, Torres FG, Gomez CM, Troncoso OP, Canet-Ferrer J, Martínez-Pastor J (2009) Development of self-assembled bacterial cellulose-starch nanocomposites. Mater Sci Eng C 29(4):1098–1104

Gudmundsson M (1994) Retrogradation of starch and the role of its components. Thermochim Acta 246(2):329–341

Harrison BS, Atala A (2007) Carbon nanotube applications for tissue engineering. Biomaterials 28(2):344–353

Hassan Nejad M, Ganster J, Bohn A, Volkert B, Lehmann A (2011) Nanocomposites of starch mixed esters and MMT: improved strength, stiffness, and toughness for starch propionate acetate laurate. Carbohydr Polym 84(1):90–95

He Y, Kong W, Wang W, Liu T, Liu Y, Gong Q, Gao J (2012) Modified natural halloysite/potato starch composite films. Carbohydr Polym 87(4):2706–2711

Helland A, Wick P, Koehler A, Schmid K, Som C (2007) Reviewing the environmental and human health knowledge base of carbon nanotubes. Environ Health Perspect 115(8):1125–1131

Hendricks SB (1942) Lattice structure of clay minerals and some properties of clays. J Geol 50(3):276–290

Hofmeister W, Platen HV (1992) Crystal chemistry and atomic order in brucite-related double-layer structures. Crystallogr Rev 3(1):3–26

Huang M, Yu J (2006) Structure and properties of thermoplastic corn starch/montmorillonite biodegradable composites. J Appl Polym Sci 99(1):170–176

Huang M-F, Yu J-G, Ma X-F (2004) Studies on the properties of montmorillonite-reinforced thermoplastic starch composites. Polymer 45(20):7017–7023

Huang M-F, Yu J-G, Ma X-F, Jin P (2005a) High performance biodegradable thermoplastic starch-EMMT nanoplastics. Polymer 46(9):3157–3162

Huang MF, Yu JG, Ma XF (2005b) Preparation of the thermoplastic starch/montmorillonite nanocomposites by melt-intercalation. Chin Chem Lett 16(4):561–564

Huang M, Yu J, Ma X (2006) High mechanical performance MMT-urea and formamide-plasticized thermoplastic cornstarch biodegradable nanocomposites. Carbohydr Polym 63(3):393–399

Ibrahim SM (2011) Characterization, mechanical, and thermal properties of gamma irradiated starch films reinforced with mineral clay. J Appl Polym Sci 119(2):685–692

Ikeo Y, Aoki K, Kishi H, Matsuda S, Murakami A (2006) Nano clay reinforced biodegradable plastics of PCL starch blends. Polym Adv Technol 17(11–12):940–944

Imberty A, Perez S (1988) A revisit to the three-dimensional structure of B-type starch. Biopolymers 27(8):1205–1221

Imberty A, Chanzy H, Pérez S, Bulèon A, Tran V (1988) The double-helical nature of the crystalline part of A-starch. J Mol Biol 201(2):365–378

Jane J-l (2009) Structural features of starch granules II. In: James B, Roy W (eds) Starch, 3rd edn. Academic, San Diego, pp 193–236

Jarowenko W (1986) Acetylated starch and miscellaneous organic esters. In: Wurzburg OB (ed) Modified starches: properties and uses. CRC Press, Boca Raton, pp 55–77

Jiang L, Shen X-P, Wu J-L, Shen K-C (2010) Preparation and characterization of graphene/poly (vinyl alcohol) nanocomposites. J Appl Polym Sci 118(1):275–279

Jozja N, Baillif P, Touray J-C, Pons C-H, Muller F, Burgevin C (2003) Impacts « multi-échelle » d'un échange (Mg, Ca)–Pb et ses conséquences sur l'augmentation de la perméabilité d'une bentonite. Compt Rendus Geosci 335(9):729–736

Kalambur SB, Rizvi SS (2004) Starch-based nanocomposites by reactive extrusion processing. Polym Int 53(10):1413–1416

Kalambur S, Rizvi SSH (2005) Biodegradable and functionally superior starch-polyester nanocomposites from reactive extrusion. J Appl Polym Sci 96(4):1072–1082

Kalambur S, Rizvi SSH (2006a) An overview of starch-based plastic blends from reactive extrusion. J Plast Film Sheeting 22(1):39–58

Kalambur S, Rizvi SSH (2006b) Rheological behavior of starch-polycaprolactone (PCL) nanocomposite melts synthesized by reactive extrusion. Polym Eng Sci 46(5):650–658

Kampeerapappun P, Aht-ong D, Pentrakoon D, Srikulkit K (2007) Preparation of cassava starch/ montmorillonite composite film. Carbohydr Polym 67(2):155–163

Kaushik A, Singh M, Verma G (2010) Green nanocomposites based on thermoplastic starch and steam exploded cellulose nanofibrils from wheat straw. Carbohydr Polym 82(2):337–345

Ke G (2010) A novel strategy to functionalize carbon nanotubes with cellulose acetate using triazines as intermediated functional groups. Carbohydr Polym 79(3):775–782

Ke Y, Lü J, Yi X, Zhao J, Qi Z (2000) The effects of promoter and curing process on exfoliation behavior of epoxy/clay nanocomposites. J Appl Polym Sci 78(4):808–815

Kim H, Macosko CW (2009) Processing-property relationships of polycarbonate/graphene composites. Polymer 50(15):3797–3809

Kim O-K, Je J, Baldwin JW, Kooi S, Pehrsson PE, Buckley LJ (2003) Solubilization of single-wall carbon nanotubes by supramolecular encapsulation of helical amylose. J Am Chem Soc 125(15):4426–4427

Kirby AR, Clark SA, Parker R, Smith AC (1993) The deformation and failure behaviour of wheat starch plasticized with water and polyols. J Mater Sci 28(21):5937–5942

Kis A, Zettl A (2008) Nanomechanics of carbon nanotubes. Philos Trans R Soc A Math Phys Eng Sci 366(1870):1591–1611

Klaine SJ, Alvarez PJJ, Batley GE, Fernandes TF, Handy RD, Lyon DY, Mahendra S, McLaughlin MJ, Lead JR (2008) Nanomaterials in the environment: behavior, fate, bioavailability, and effects. Environ Toxicol Chem 27(9):1825–1851

Kluüppel M, Schroüder A, Heinrich G (2007) Carbon black. In: Mark JE (ed) Physical properties of polymers handbook. Springer, New York, pp 539–550

Kraus G (1965) Reinforcement of elastomers. Interscience Publishers, New York

Kumar AP, Depan D, Singh Tomer N, Singh RP (2009) Nanoscale particles for polymer degradation and stabilization – trends and future perspectives. Prog Polym Sci 34(6):479–515

Kvien I, Sugiyama J, Votrubec M, Oksman K (2007) Characterization of starch based nanocomposites. J Mater Sci 42(19):8163–8171

Lafargue D, Pontoire B, Buléon A, Doublier JL, Lourdin D (2007) Structure and mechanical properties of hydroxypropylated starch films. Biomacromolecules 8(12):3950–3958

Lagaly G (1986) Interaction of alkylamines with different types of layered compounds. Solid State Ionics 22(1):43–51

Lagaly G (1999) Introduction: from clay mineral-polymer interactions to clay mineral-polymer nanocomposites. Appl Clay Sci 15(1–2):1–9

Lahiff E, Lynam C, Gilmartin N, O'Kennedy R, Diamond D (2010) The increasing importance of carbon nanotubes and nanostructured conducting polymers in biosensors. Anal Bioanal Chem 398(4):1575–1589

Lai LS, Kokini JL (1991) Physicochemical changes and rheological properties of starch during extrusion. Biotechnol Prog 7(3):251–266

Lam C-w, James JT, McCluskey R, Arepalli S, Hunter RL (2006) A review of carbon nanotube toxicity and assessment of potential occupational and environmental health risks. Crit Rev Toxicol 36(3):189–217

Lawton JW, Shogren RL, Tiefenbacher KF (2004) Aspen fiber addition improves the mechanical properties of baked cornstarch foams. Ind Crop Prod 19(1):41–48

Le Corre D b, Bras J, Dufresne A (2010) Starch nanoparticles: a review. Biomacromolecules 11(5):1139–1153

Lee S-Y, Hanna MA (2008) Preparation and characterization of tapioca starch-poly(lactic acid)-Cloisite Na^+ nanocomposite foams. J Appl Polym Sci 110(4):2337–2344

Lee SY, Hanna MA (2009) Tapioca starch-poly(lactic acid)-Cloisite 30B nanocomposite foams. Polym Compos 30(5):665–672

Lee SH, Cho E, Jeon SH, Youn JR (2007a) Rheological and electrical properties of polypropylene composites containing functionalized multi-walled carbon nanotubes and compatibilizers. Carbon 45(14):2810–2822

Lee SY, Xu YX, Hanna MA (2007b) Tapioca starch-poly (lactic acid)-based nanocomposite foams as affected by type of nanoclay. Int Polym Process 22(5):429–435

Lee SY, Chen H, Hanna MA (2008a) Preparation and characterization of tapioca starch-poly(lactic acid) nanocomposite foams by melt intercalation based on clay type. Ind Crop Prod 28(1):95–106

Lee SY, Hanna MA, Jones DD (2008b) An adaptive neuro-fuzzy inference system for modeling mechanical properties of tapioca starch-poly(lactic acid) nanocomposite foams. Starch-Starke 60(3–4):159–164

Lelievre J (1974) Starch gelatinization. J Appl Polym Sci 18(1):293–296

Leroux F, Besse J-P (2001) Polymer interleaved layered double hydroxide: a new emerging class of nanocomposites. Chem Mater 13(10):3507–3515

Li JH, Ren CL, Liu X, De Hu Z, Xue DS (2007) "Green" synthesis of starch capped CdSe nanoparticles at room temperature. Mater Sci Eng A 458(1–2):319–322

Li M, Liu P, Zou W, Yu L, Xie F, Pu H, Liu H, Chen L (2011a) Extrusion processing and characterization of edible starch films with different amylose contents. J Food Eng 106(1):95–101

Li R, Liu C, Ma J (2011b) Studies on the properties of graphene oxide-reinforced starch biocomposites. Carbohydr Polym 84(1):631–637

Li M, Hasjim J, Xie F, Halley PJ, Gilbert RG (2014) Shear degradation of molecular, crystalline, and granular structures of starch during extrusion. Starch-Stärke (in press). 10.1002/star.201300201

Liao H-T, Wu C-S (2008) New biodegradable blends prepared from polylactide, titanium tetraisopropylate, and starch. J Appl Polym Sci 108(4):2280–2289

Lii C-y, Stobinski L, Tomasik P, Liao C-d (2003) Single-walled carbon nanotube – potato amylose complex. Carbohydr Polym 51(1):93–98

DOI 10.1007/978-3-319-03751-6_50-1

Lilichenko N, Maksimov R, Zicans J, Merijs Meri R, Plume E (2008) A biodegradable polymer nanocomposite: mechanical and barrier properties. Mech Compos Mater 44(1):45–56

Lin C-A, Tung C-C (2009) The preparation of glycerol pseudo-thermoplastic starch (GTPS) via gelatinization and plasticization. Polym Plast Technol Eng 48(5):509–515

Liu Q, Thompson DB (1998) Effects of moisture content and different gelatinization heating temperatures on retrogradation of waxy-type maize starches. Carbohydr Res 314(3–4):221–235

Liu H, Xie F, Chen L, Yu L, Dean K, Bateman S (2005) Thermal behaviour of high amylose cornstarch studied by DSC. Int J Food Eng 1(1), Article 3/1–6

Liu H, Yu L, Xie F, Chen L (2006) Gelatinization of cornstarch with different amylose/amylopectin content. Carbohydr Polym 65(3):357–363

Liu X, Yu L, Liu H, Chen L, Li L (2008) In situ thermal decomposition of starch with constant moisture in a sealed system. Polym Degrad Stab 93(1):260–262

Liu H, Xie F, Yu L, Chen L, Li L (2009a) Thermal processing of starch-based polymers. Prog Polym Sci 34(12):1348–1368

Liu P, Yu L, Liu H, Chen L, Li L (2009b) Glass transition temperature of starch studied by a high-speed DSC. Carbohydr Polym 77(2):250–253

Liu P, Yu L, Wang X, Li D, Chen L, Li X (2010a) Glass transition temperature of starches with different amylose/amylopectin ratios. J Cereal Sci 51(3):388–391

Liu W-C, Halley PJ, Gilbert RG (2010b) Mechanism of degradation of starch, a highly branched polymer, during extrusion. Macromolecules 43(6):2855–2864

Liu D, Chang PR, Deng S, Wang C, Zhang B, Tian Y, Huang S, Yao J, Ma X (2011a) Fabrication and characterization of zirconium hydroxide-carboxymethyl cellulose sodium/plasticized *Trichosanthes Kirilowii* starch nanocomposites. Carbohydr Polym 86(4):1699–1704

Liu H, Chaudhary D, Ingram G, John J (2011b) Interactions of hydrophilic plasticizer molecules with amorphous starch biopolymer – an investigation into the glass transition and the water activity behavior. J Polym Sci B Polym Phys 49(14):1041–1049

Liu H, Chaudhary D, Yusa S-i, Tadé MO (2011c) Glycerol/starch/Na^+-montmorillonite nanocomposites: a XRD, FTIR, DSC and ^1H NMR study. Carbohydr Polym 83(4):1591–1597

Liu P, Xie F, Li M, Liu X, Yu L, Halley PJ, Chen L (2011d) Phase transitions of maize starches with different amylose contents in glycerol-water systems. Carbohydr Polym 85(1):180–187

Liu Z, Zhao L, Chen M, Yu J (2011e) Effect of carboxylate multi-walled carbon nanotubes on the performance of thermoplastic starch nanocomposites. Carbohydr Polym 83(2):447–451

Lourdin D, Coignard L, Bizot H, Colonna P (1997) Influence of equilibrium relative humidity and plasticizer concentration on the water content and glass transition of starch materials. Polymer 38(21):5401–5406

Lu Y, Weng L, Cao X (2006) Morphological, thermal and mechanical properties of ramie crystallites – reinforced plasticized starch biocomposites. Carbohydr Polym 63(2):198–204

Luckham PF, Rossi S (1999) The colloidal and rheological properties of bentonite suspensions. Adv Colloid Interf Sci 82(1–3):43–92

Luo W, Zhang W a, Chen P, Fang Y e (2005) Synthesis and properties of starch grafted poly [acrylamide-*co*-(acrylic acid)]/montmorillonite nanosuperabsorbent via γ-ray irradiation technique. J Appl Polym Sci 96(4):1341–1346

Luo HL, Lian JJ, Wan YZ, Huang Y, Wang YL, Jiang HJ (2006) Moisture absorption in VARTMed three-dimensional braided carbon-epoxy composites with different interface conditions. Mater Sci Eng A 425(1–2):70–77

Ma X, Yu J (2004a) Formamide as the plasticizer for thermoplastic starch. J Appl Polym Sci 93(4):1769–1773

Ma X, Yu J (2004b) The plasticizers containing amide groups for thermoplastic starch. Carbohydr Polym 57(2):197–203

Ma X, Yu J (2004c) The effects of plasticizers containing amide groups on the properties of thermoplastic starch. Starch-Starke 56(11):545–551

Ma X, Yu J, Feng J (2004) Urea and formamide as a mixed plasticizer for thermoplastic starch. Polym Int 53(11):1780–1785

Ma XF, Yu JG, Ma YB (2005) Urea and formamide as a mixed plasticizer for thermoplastic wheat flour. Carbohydr Polym 60:111–116

Ma XF, Yu JG, Wan JJ (2006) Urea and ethanolamine as a mixed plasticizer for thermoplastic starch. Carbohydr Polym 64(2):267–273

Ma X, Yu J, He K, Wang N (2007a) The effects of different plasticizers on the properties of thermoplastic starch as solid polymer electrolytes. Macromol Mater Eng 292(4):503–510

Ma X, Yu J, Wang N (2007b) Production of thermoplastic starch/MMT-sorbitol nanocomposites by dual-melt extrusion processing. Macromol Mater Eng 292(6):723–728

Ma X, Chang PR, Yu J, Lu P (2008a) Characterizations of glycerol plasticized-starch (GPS)/carbon black (CB) membranes prepared by melt extrusion and microwave radiation. Carbohydr Polym 74(4):895–900

Ma X, Chang PR, Yu J, Lu P (2008b) Electrically conductive carbon black (CB)/glycerol plasticized-starch (GPS) composites prepared by microwave radiation. Starch-Starke 60(7):373–375

Ma X, Jian R, Chang PR, Yu J (2008c) Fabrication and characterization of citric acid-modified starch nanoparticles/plasticized-starch composites. Biomacromolecules 9(11):3314–3320

Ma X, Yu J, Wang N (2008d) Glycerol plasticized-starch/multiwall carbon nanotube composites for electroactive polymers. Compos Sci Technol 68(1):268–273

Ma X, Chang PR, Yang J, Yu J (2009) Preparation and properties of glycerol plasticized-pea starch/zinc oxide-starch bionanocomposites. Carbohydr Polym 75(3):472–478

Magalhães NF, Andrade CT (2009) Thermoplastic corn starch/clay hybrids: effect of clay type and content on physical properties. Carbohydr Polym 75(4):712–718

Magalhães NF, Andrade CT (2010) Calcium bentonite as reinforcing nanofiller for thermoplastic starch. J Braz Chem Soc 21:202–208

Majdzadeh-Ardakani K, Nazari B (2010) Improving the mechanical properties of thermoplastic starch/poly(vinyl alcohol)/clay nanocomposites. Compos Sci Technol 70(10):1557–1563

Majdzadeh-Ardakani K, Navarchian AH, Sadeghi F (2010) Optimization of mechanical properties of thermoplastic starch/clay nanocomposites. Carbohydr Polym 79(3):547–554

Maksimov RD, Lagzdins A, Lilichenko N, Plume E (2009) Mechanical properties and water vapor permeability of starch/montmorillonite nanocomposites. Polym Eng Sci 49(12):2421–2429

Mallapragada SK, Narasimhan B (2006) Handbook of biodegradable polymeric materials and applications: volume 1. materials. American Scientific Publishers, Stevenson Rance, California, USA

Martin O, Averous L, Della Valle G (2003) In-line determination of plasticized wheat starch viscoelastic behavior: impact of processing. Carbohydr Polym 53(2):169–182

Mathew AP, Dufresne A (2002a) Plasticized waxy maize starch: effect of polyols and relative humidity on material properties. Biomacromolecules 3(5):1101–1108

Mathew AP, Dufresne A (2002b) Morphological investigation of nanocomposites from sorbitol plasticized starch and tunicin whiskers. Biomacromolecules 3(3):609–617

Mathew AP, Thielemans W, Dufresne A (2008) Mechanical properties of nanocomposites from sorbitol plasticized starch and tunicin whiskers. J Appl Polym Sci 109(6):4065–4074

Matsui KN, Larotonda FDS, Paes SS, Luiz DB, Pires ATN, Laurindo JB (2004) Cassava bagasse-Kraft paper composites: analysis of influence of impregnation with starch acetate on tensile strength and water absorption properties. Carbohydr Polym 55(3):237–243

Mbey JA, Hoppe S, Thomas F (2012) Cassava starch–kaolinite composite film. Effect of clay content and clay modification on film properties. Carbohydr Polym 88(1):213–222

Mbougueng PD, Tenin D, Scher J, Tchiégang C (2012) Influence of acetylation on physicochemical, functional and thermal properties of potato and cassava starches. J Food Eng 108(2):320–326

McGlashan SA, Halley PJ (2003) Preparation and characterisation of biodegradable starch-based nanocomposite materials. Polym Int 52(11):1767–1773

Mering J (1946) On the hydration of montmorillonite. Trans Faraday Soc 42:B205–B219

Meskinfam M, Sadjadi MAS, Jazdarreh H, Zare K (2011) Biocompatibility evaluation of nano hydroxyapatite-starch biocomposites. J Biomed Nanotechnol 7(3):455–459

Meyer WH (1998) Polymer electrolytes for lithium-ion batteries. Adv Mater 10(6):439–448

Miyasaka K, Watanabe K, Jojima E, Aida H, Sumita M, Ishikawa K (1982) Electrical conductivity of carbon-polymer composites as a function of carbon content. J Mater Sci 17(6):1610–1616

Mohanty AK, Misra M, Drzal LT (2005) Natural fibers, biopolymers, and their biocomposites. CRC Press, Boca Raton

Mondragón M, Mancilla JE, Rodríguez-González FJ (2008) Nanocomposites from plasticized high-amylopectin, normal and high-amylose maize starches. Polym Eng Sci 48(7):1261–1267

Mondragón M, Hernández EM, Rivera-Armenta JL, Rodríguez-González FJ (2009) Injection molded thermoplastic starch/natural rubber/clay nanocomposites: morphology and mechanical properties. Carbohydr Polym 77(1):80–86

Morin A, Dufresne A (2002) Nanocomposites of chitin whiskers from Riftia tubes and poly (caprolactone). Macromolecules 35(6):2190–2199

Müller CMO, Laurindo JB, Yamashita F (2011) Effect of nanoclay incorporation method on mechanical and water vapor barrier properties of starch-based films. Ind Crop Prod 33(3):605–610

Murugan R, Ramakrishna S (2004) Crystallographic study of hydroxyapatite bioceramics derived from various sources. Cryst Growth Des 5(1):111–112

Namazi H, Mosadegh M, Dadkhah A (2009) New intercalated layer silicate nanocomposites based on synthesized starch-*g*-PCL prepared via solution intercalation and in situ polymerization methods: as a comparative study. Carbohydr Polym 75(4):665–669

Nashed G, Rutgers RPG, Sopade PA (2003) The plasticisation effect of glycerol and water on the gelatinisation of wheat starch. Starch-Starke 55(3–4):131–137

Nayak SK (2010) Biodegradable PBAT/starch nanocomposites. Polym Plast Technol Eng 49(14):1406–1418

Nejad MH, Ganster J, Volkert B (2010) Starch esters with improved mechanical properties through melt compounding with nanoclays. J Appl Polym Sci 118(1):503–510

Nicole G (2007) Carbon nanotubes – becoming clean. Mater Today 10(1–2):28–35

Norman RH (1970) Conductive rubbers and plastics: their production, application and test methods. Elsevier, Amsterdam

Oberdörster G, Stone V, Donaldson K (2007) Toxicology of nanoparticles: a historical perspective. Nanotoxicology 1(1):2–25

Paakko M, Ankerfors M, Kosonen H, Nykanen A, Ahola S, Osterberg M, Ruokolainen J, Laine J, Larsson PT, Ikkala O, Lindstrom T (2007) Enzymatic hydrolysis combined with mechanical shearing and high-pressure homogenization for nanoscale cellulose fibrils and strong gels. Biomacromolecules 8(6):1934–1941

DOI 10.1007/978-3-319-03751-6_50-1

Paillet M, Dufresne A (2001) Chitin whisker reinforced thermoplastic nanocomposites. Macromolecules 34(19):6527–6530

Pandey JK, Singh RP (2005) Green nanocomposites from renewable resources: effect of plasticizer on the structure and material properties of clay-filled starch. Starch-Starke 57(1):8–15

Park H-M, Li X, Jin C-Z, Park C-Y, Cho W-J, Ha C-S (2002) Preparation and properties of biodegradable thermoplastic starch/clay hybrids. Macromol Mater Eng 287(8):553–558

Park H-M, Lee W-K, Park C-Y, Cho W-J, Ha C-S (2003) Environmentally friendly polymer hybrids. Part I: mechanical, thermal, and barrier properties of thermoplastic starch/clay nanocomposites. J Mater Sci 38(5):909–915

Park H-M, Kim G-H, Ha C-S (2007) Preparation and characterization of biodegradable aliphatic polyester/thermoplastic starch/organoclay ternary hybrid nanocomposites. Compos Interfaces 14:427–438

Paul DR, Robeson LM (2008) Polymer nanotechnology: nanocomposites. Polymer 49(15):3187–3204

Pavlidou S, Papaspyrides CD (2008) A review on polymer–layered silicate nanocomposites. Prog Polym Sci 33(12):1119–1198

Pawlak A, Mucha M (2003) Thermogravimetric and FTIR studies of chitosan blends. Thermochim Acta 396(1–2):153–166

Payne AR (1962) The dynamic properties of carbon black-loaded natural rubber vulcanizates. Part I. J Appl Polym Sci 6(19):57–63

Payne AR (1963) Dynamic properties of heat-treated butyl vulcanizates. J Appl Polym Sci 7(3):873–885

Payne AR (1964) Strainwork dependence of filler-loaded vulcanizates. J Appl Polym Sci 8(6):2661–2686

Payne AR (1965a) Dynamic properties of natural rubber containing heat-treated carbon blacks. J Appl Polym Sci 9(10):3245–3254

Payne AR (1965b) Effect of dispersion on the dynamic properties of filler-loaded rubbers. J Appl Polym Sci 9(6):2273–2284

Pérez S, Bertoft E (2010) The molecular structures of starch components and their contribution to the architecture of starch granules: a comprehensive review. Starch-Starke 62(8):389–420

Pérez CJ, Alvarez VA, Mondragón I, Vázquez A (2007) Mechanical properties of layered silicate/starch polycaprolactone blend nanocomposites. Polym Int 56(5):686–693

Perez C, Vázquez A, Alvarez V (2008) Isothermal crystallization of layered silicate/starch-polycaprolactone blend nanocomposites. J Therm Anal Calorim 91(3):749–757

Pérez CJ, Alvarez VA, Mondragón I, Vázquez A (2008a) Water uptake behavior of layered silicate/starch-polycaprolactone blend nanocomposites. Polym Int 57(2):247–253

Pérez CJ, Alvarez VA, Vázquez A (2008b) Creep behaviour of layered silicate/starch-polycaprolactone blends nanocomposites. Mater Sci Eng A 480(1–2):259–265

Pérez S, Baldwin PM, Gallant DJ (2009) Structural features of starch granules I. In: James B, Roy W (eds) Starch, 3rd edn. Academic, San Diego, pp 149–192

Pinnavaia TJ, Beall GW (2000) Polymer-clay nanocomposites, Wiley series in polymer science. Wiley, Chichester

Powell DH, Tongkhao K, Kennedy SJ, Slade PG (1997) Interlayer water structure in Na- and Li-montmorillonite clays. Phys B Condens Matter 241–243:387–389

Powell DH, Fischer HE, Skipper NT (1998) The structure of interlayer water in Li−montmorillonite studied by neutron diffraction with isotopic substitution. J Phys Chem B 102(52):10899–10905

DOI 10.1007/978-3-319-03751-6_50-1

Pushpadass HA, Hanna MA (2009) Age-induced changes in the microstructure and selected properties of extruded starch films plasticized with glycerol and stearic acid. Ind Eng Chem Res 48(18):8457–8463

Pushpadass HA, Kumar A, Jackson DS, Wehling RL, Dumais JJ, Hanna MA (2009) Macromolecular changes in extruded starch-films plasticized with glycerol, water and stearic acid. Starch-Starke 61(5):256–266

Putaux J-L, Molina-Boisseau S, Momaur T, Dufresne A (2003) Platelet nanocrystals resulting from the disruption of waxy maize starch granules by acid hydrolysis. Biomacromolecules 4(5):1198–1202

Qi HJ, Teo KBK, Lau KKS, Boyce MC, Milne WI, Robertson J, Gleason KK (2003) Determination of mechanical properties of carbon nanotubes and vertically aligned carbon nanotube forests using nanoindentation. J Mech Phys Solids 51(11–12):2213–2237

Qiao X, Jiang W, Sun K (2005) Reinforced thermoplastic acetylated starch with layered silicates. Starch-Starke 57(12):581–586

Qiao X, Tang Z, Sun K (2011) Plasticization of corn starch by polyol mixtures. Carbohydr Polym 83(2):659–664

Radhakrishnan T, Georges MK, Nair PS, Luyt AS, Djokovi V (2007) Study of sago starch-CdS nanocomposite films: fabrication, structure, optical and thermal properties. J Nanosci Nanotechnol 7(3):986–993

Rao Y, Pochan JM (2006) Mechanics of polymer−clay nanocomposites. Macromolecules 40(2):290–296

Raquez J-M, Nabar Y, Narayan R, Dubois P (2011) Preparation and characterization of maleated thermoplastic starch-based nanocomposites. J Appl Polym Sci 122(1):639–647

Ratnayake WS, Jackson DS, Steve LT (2008) Starch gelatinization. Adv Food Nutr Res 55:221–268

Raveendran P, Fu J, Wallen SL (2003) Completely “green” synthesis and stabilization of metal nanoparticles. J Am Chem Soc 125(46):13940–13941

Reis RL, Cunha AM, Allan PS, Bevis MJ (1997) Structure development and control of injection-molded hydroxylapatite-reinforced starch/EVOH composites. Adv Polym Technol 16(4):263–277

Remsen CH, Clark JP (1978) A viscosity model for a cooking dough. J Food Process Eng 2(1):39–64

Ren P, Shen T, Wang F, Wang X, Zhang Z (2009) Study on biodegradable starch/OMMT nanocomposites for packaging applications. J Polym Environ 17(3):203–207

Rinaudo M (2006) Chitin and chitosan: properties and applications. Prog Polym Sci 31(7):603–632

Rodriguez P, Muñoz-Aguirre N, San-Martín Martinez E, González de la Cruz G, Tomas SA, Zelaya Angel O (2008) Synthesis and spectral properties of starch capped CdS nanoparticles in aqueous solution. J Cryst Growth 310(1):160–164

Rodriguez-Gonzalez FJ, Ramsay BA, Favis BD (2004) Rheological and thermal properties of thermoplastic starch with high glycerol content. Carbohydr Polym 58(2):139–147

Roman M, Winter WT (2004) Effect of sulfate groups from sulfuric acid hydrolysis on the thermal degradation behavior of bacterial cellulose. Biomacromolecules 5(5):1671–1677

Romhány G, Karger-Kocsis J, Czigány T (2003) Tensile fracture and failure behavior of thermoplastic starch with unidirectional and cross-ply flax fiber reinforcements. Macromol Mater Eng 288(9):699–707

Ruan SL, Gao P, Yang XG, Yu TX (2003) Toughening high performance ultrahigh molecular weight polyethylene using multiwalled carbon nanotubes. Polymer 44(19):5643–5654

Russell PL (1987) Gelatinisation of starches of different amylose/amylopectin content. A study by differential scanning calorimetry. J Cereal Sci 6(2):133–145

Russo MAL, O'Sullivan C, Rounsefell B, Halley PJ, Truss R, Clarke WP (2009) The anaerobic degradability of thermoplastic starch: polyvinyl alcohol blends: potential biodegradable food packaging materials. Bioresour Technol 100(5):1705–1710

Sadjadi MS, Meskinfam M, Sadeghi B, Jazdarreh H, Zare K (2010) In situ biomimetic synthesis, characterization and in vitro investigation of bone-like nanohydroxyapatite in starch matrix. Mater Chem Phys 124(1):217–222

Saito Y, Putaux JL, Okano T, Gaill F, Chanzy H (1997) Structural aspects of the swelling of β chitin in HCl and its conversion into α chitin. Macromolecules 30(13):3867–3873

Schadler LS (2003) Polymer-based and polymer-filled nanocomposites. In: Ajayan PM, Schadler LS, Braun PV (eds) Nanocomposite science and technology. Wiley-VCH, Weinheim, pp 55–70

Schaefer DW, Justice RS (2007) How nano are nanocomposites? Macromolecules 40(24):8501–8517

Shen Z, Simon GP, Cheng Y-B (2002) Comparison of solution intercalation and melt intercalation of polymer–clay nanocomposites. Polymer 43(15):4251–4260

Shi R, Liu Q, Ding T, Han Y, Zhang L, Chen D, Tian W (2007a) Ageing of soft thermoplastic starch with high glycerol content. J Appl Polym Sci 103(1):574–586

Shi R, Zhang Z, Liu Q, Han Y, Zhang L, Chen D, Tian W (2007b) Characterization of citric acid/glycerol co-plasticized thermoplastic starch prepared by melt blending. Carbohydr Polym 69(4):748–755

Shogren RL, Swanson CL, Thompson AR (1992) Extrudates of cornstarch with urea and glycols: structure/mechanical property relations. Starch-Starke 44(9):335–338

Shu XZ, Zhu KJ (2000) A novel approach to prepare tripolyphosphate/chitosan complex beads for controlled release drug delivery. Int J Pharm 201(1):51–58

Sinha Ray S, Bousmina M (2005) Biodegradable polymers and their layered silicate nanocomposites: in greening the 21st century materials world. Prog Mater Sci 50(8):962–1079

Sinha Ray S, Okamoto M (2003) Polymer/layered silicate nanocomposites: a review from preparation to processing. Prog Polym Sci 28(11):1539–1641

Sinha Ray S, Okamoto K, Okamoto M (2003) Structure−property relationship in biodegradable poly(butylene succinate)/layered silicate nanocomposites. Macromolecules 36(7):2355–2367

Siqueira G, Bras J, Dufresne A (2008) Cellulose whiskers versus microfibrils: influence of the nature of the nanoparticle and its surface functionalization on the thermal and mechanical properties of nanocomposites. Biomacromolecules 10(2):425–432

Smits ALM, Kruiskamp PH, van Soest JJG, Vliegenthart JFG (2003) Interaction between dry starch and plasticisers glycerol or ethylene glycol, measured by differential scanning calorimetry and solid state NMR spectroscopy. Carbohydr Polym 53(4):409–416

Spitalsky Z, Tasis D, Papagelis K, Galiotis C (2010) Carbon nanotube-polymer composites: chemistry, processing, mechanical and electrical properties. Prog Polym Sci 35(3):357–401

Sposito G, Grasso D (1999) Electrical double layer structure, forces, and fields at the clay-water interface. In: Hsu J-P (ed) Interfacial forces and fields: theory and applications, vol 85, Surfactant science. Marcel Dekker, New York, pp 207–249

Sreekala MS, Goda K, Devi PV (2008) Sorption characteristics of water, oil and diesel in cellulose nanofiber reinforced corn starch resin/ramie fabric composites. Compos Interfaces 15:281–299

Sriupayo J, Supaphol P, Blackwell J, Rujiravanit R (2005) Preparation and characterization of α-chitin whisker-reinforced chitosan nanocomposite films with or without heat treatment. Carbohydr Polym 62(2):130–136

Star A, Steuerman DW, Heath JR, Stoddart JF (2002) Starched carbon nanotubes. Angew Chem Int Ed 41(14):2508–2512

Stobinski L, Tomasik P, Lii C-Y, Chan H-H, Lin H-M, Liu H-L, Kao C-T, Lu K-S (2003) Single-walled carbon nanotube-amylopectin complexes. Carbohydr Polym 51(3):311–316

Sumita M, Sakata K, Asai S, Miyasaka K, Nakagawa H (1991) Dispersion of fillers and the electrical conductivity of polymer blends filled with carbon black. Polym Bull 25(2):265–271

Sun L, Boo WJ, Browning RL, Sue H-J, Clearfield A (2005) Effect of crystallinity on the intercalation of monoamine in α-zirconium phosphate layer structure. Chem Mater 17(23):5606–5609

Sundaram J, Durance TD, Wang R (2008) Porous scaffold of gelatin-starch with nanohydroxyapatite composite processed via novel microwave vacuum drying. Acta Biomater 4(4):932–942

Svagan AJ, Hedenqvist MS, Berglund L (2009) Reduced water vapour sorption in cellulose nanocomposites with starch matrix. Compos Sci Technol 69(3–4):500–506

Tako M, Hizukuri S (2002) Gelatinization mechanism of potato starch. Carbohydr Polym 48(4):397–401

Tan I, Wee CC, Sopade PA, Halley PJ (2004a) Investigation of the starch gelatinisation phenomena in water-glycerol systems: application of modulated temperature differential scanning calorimetry. Carbohydr Polym 58(2):191–204

Tan I, Wee CC, Sopade PA, Halley PJ (2004b) Estimating the specific heat capacity of starch-water-glycerol systems as a function of temperature and compositions. Starch-Starke 56(1):6–12

Tan I, Flanagan BM, Halley PJ, Whittaker AK, Gidley MJ (2007) A method for estimating the nature and relative proportions of amorphous, single, and double-helical components in starch granules by ^{13}C CP/MAS NMR. Biomacromolecules 8(3):885–891

Tang X, Alavi S (2011) Recent advances in starch, polyvinyl alcohol based polymer blends, nanocomposites and their biodegradability. Carbohydr Polym 85(1):7–16

Tang S, Zou P, Xiong H, Tang H (2008a) Effect of nano-SiO_2 on the performance of starch/polyvinyl alcohol blend films. Carbohydr Polym 72(3):521–526

Tang X, Alavi S, Herald TJ (2008b) Effects of plasticizers on the structure and properties of starch-clay nanocomposite films. Carbohydr Polym 74(3):552–558

Tang X, Alavi S, Herald TJ (2008c) Barrier and mechanical properties of starch-clay nanocomposite films. Cereal Chem 85(3):433–439

Tang H, Xiong H, Tang S, Zou P (2009) A starch-based biodegradable film modified by nano silicon dioxide. J Appl Polym Sci 113(1):34–40

Taubert A, Wegner G (2002) Formation of uniform and monodisperse zincite crystals in the presence of soluble starch. J Mater Chem 12(4):805–807

Tchoudakov R, Breuer O, Narkis M, Siegmann A (1996) Conductive polymer blends with low carbon black loading: polypropylene/polyamide. Polym Eng Sci 36(10):1336–1346

Teixeira EM, Pasquini D, Curvelo AAS, Corradini E, Belgacem MN, Dufresne A (2009) Cassava bagasse cellulose nanofibrils reinforced thermoplastic cassava starch. Carbohydr Polym 78(3):422–431

Tettenhorst R (1962) Cation migration in montmorillonites. Am Mineral 47(5–6):769–773

Thomas F, Michot LJ, Vantelon D, Montargès E, Prélot B, Cruchaudet M, Delon JF (1999) Layer charge and electrophoretic mobility of smectites. Colloids Surf A Physicochem Eng Asp 159(2–3):351–358

Thostenson ET, Ren Z, Chou T-W (2001) Advances in the science and technology of carbon nanotubes and their composites: a review. Compos Sci Technol 61(13):1899–1912

Tigau N, Ciupina V, Prodan G (2005) The effect of substrate temperature on the optical properties of polycrystalline Sb_2O_3 thin films. J Cryst Growth 277(1–4):529–535

Tsai Y-C, Chen S-Y, Liaw H-W (2007) Immobilization of lactate dehydrogenase within multiwalled carbon nanotube-chitosan nanocomposite for application to lactate biosensors. Sensors Actuators B Chem 125(2):474–481

Tsai ML, Bai SW, Chen RH (2008) Cavitation effects versus stretch effects resulted in different size and polydispersity of ionotropic gelation chitosan–sodium tripolyphosphate nanoparticle. Carbohydr Polym 71(3):448–457

Tung C-C, Ku T-H, Lin C-A (2011) The effect of plasticizers and characterization on formamide pseudo-thermoplastic potato starch films using solution casting method. Polym Plast Technol Eng 50(14):1452–1457

Vaia RA, Giannelis EP (1997) Polymer melt intercalation in organically-modified layered silicates: model predictions and experiment. Macromolecules 30(25):8000–8009

Valdés M, Valdés González A, García Calzón J, Díaz-García M (2009) Analytical nanotechnology for food analysis. Microchim Acta 166(1):1–19

Van Soest JJG, Knooren N (1997) Influence of glycerol and water content on the structure and properties of extruded starch plastic sheets during aging. J Appl Polym Sci 64(7):1411–1422

van Soest JJG, de Wit D, Tournois H, Vliegenthart JFG (1994) The influence of glycerol on structural changes in waxy maize starch as studied by Fourier transform infra-red spectroscopy. Polymer 35(22):4722–4727

van Soest JJG, Bezemer RC, de Wit D, Vliegenthart JFG (1996) Influence of glycerol on the melting of potato starch. Ind Crop Prod 5(1):1–9

Vertuccio L, Gorrasi G, Sorrentino A, Vittoria V (2009) Nano clay reinforced PCL/starch blends obtained by high energy ball milling. Carbohydr Polym 75(1):172–179

Vigneshwaran N, Sampath K, Kathe AA, Varadarajan PV, Prasad V (2006) Functional finishing of cotton fabrics using zinc oxide–soluble starch nanocomposites. Nanotechnology 17(20):5087–5095

Viguié J, Molina-Boisseau S, Dufresne A (2007) Processing and characterization of waxy maize starch films plasticized by sorbitol and reinforced with starch nanocrystals. Macromol Biosci 7(11):1206–1216

Volkert B, Lehmann A, Greco T, Nejad MH (2010) A comparison of different synthesis routes for starch acetates and the resulting mechanical properties. Carbohydr Polym 79(3):571–577

Vorwerg W, Dijksterhuis J, Borghuis J, Radosta S, Kröger A (2004) Film properties of hydroxypropyl starch. Starch-Starke 56(7):297–306

Wan YZ, Luo H, He F, Liang H, Huang Y, Li XL (2009) Mechanical, moisture absorption, and biodegradation behaviours of bacterial cellulose fibre-reinforced starch biocomposites. Compos Sci Technol 69(7–8):1212–1217

Wang J (2005) Carbon-nanotube based electrochemical biosensors: a review. Electroanalysis 17(1):7–14

Wang B-X, Zhao X-P (2006) The influence of intercalation rate and degree of substitution on the electrorheological activity of a novel ternary intercalated nanocomposite. J Solid State Chem 179(3):949–954

Wang SS, Zheng X (1995) Tribological shear conversion of starch. J Food Sci 60(3):520–522

Wang SS, Chiang WC, Zhao B, Zheng XG, Kim IH (1991) Experimental analysis and computer simulation of starch-water interactions during phase transition. J Food Sci 56(1):121–124

Wang X-L, Yang K-K, Wang Y-Z (2003) Properties of starch blends with biodegradable polymers. Polym Rev 43(3):385–409

Wang N, Yu J, Chang PR, Ma X (2007) Influence of citric acid on the properties of glycerol-plasticized dry starch (DTPS) and DTPS/poly(lactic acid) blends. Starch-Starke 59(9):409–417

Wang N, Jiugao Y, Xiaofei M, Chunmei H (2009a) An investigation of the physical properties of extruded glycerol- and formamide-plasticized cornstarch. J Thermoplast Compos Mater 22(3):273–291

Wang N, Zhang X, Han N, Bai S (2009b) Effect of citric acid and processing on the performance of thermoplastic starch/montmorillonite nanocomposites. Carbohydr Polym 76(1):68–73

Wang N, Zhang X, Wang X, Liu H (2009c) Communications: ionic liquids modified montmorillonite/thermoplastic starch nanocomposites as ionic conducting biopolymer. Macromol Res 17(5):285–288

Wang X, Zhang X, Liu H, Wang N (2009d) Impact of pre-processing of montmorillonite on the properties of melt-extruded thermoplastic starch/montmorillonite nanocomposites. Starch-Starke 61(9):489–494

Wang J, Yu L, Xie F, Chen L, Li X, Liu H (2010a) Rheological properties and phase transition of cornstarches with different amylose/amylopectin ratios under shear stress. Starch-Starke 62(12):667–675

Wang N, Zhang X, Han N, Liu H (2010b) A facile method for preparation of thermoplastic starch/urea modified montmorillonite nanocomposites. J Compos Mater 44(1):27–39

Wei Q, Kang S-Z, Mu J (2004) "Green" synthesis of starch capped CdS nanoparticles. Colloids Surf A Physicochem Eng Asp 247(1–3):125–127

Wei T, Luo G, Fan Z, Zheng C, Yan J, Yao C, Li W, Zhang C (2009) Preparation of graphene nanosheet/polymer composites using in situ reduction–extractive dispersion. Carbon 47(9):2296–2299

Wilder JWG, Venema LC, Rinzler AG, Smalley RE, Dekker C (1998) Electronic structure of atomically resolved carbon nanotubes. Nature 391(6662):59–62

Wilhelm H-M, Sierakowski M-R, Souza GP, Wypych F (2003a) The influence of layered compounds on the properties of starch/layered compound composites. Polym Int 52(6):1035–1044

Wilhelm HM, Sierakowski MR, Souza GP, Wypych F (2003b) Starch films reinforced with mineral clay. Carbohydr Polym 52(2):101–110

Wilkie CA, Zhu J, Uhl F (2001) How do nanocomposites enhance the thermal stability of polymer. Polym Prepr 42(1):392

Woehl MA, Canestraro CD, Mikowski A, Sierakowski MR, Ramos LP, Wypych F (2010) Bionanocomposites of thermoplastic starch reinforced with bacterial cellulose nanofibres: effect of enzymatic treatment on mechanical properties. Carbohydr Polym 80(3):866–873

Wollerdorfer M, Bader H (1998) Influence of natural fibres on the mechanical properties of biodegradable polymers. Ind Crop Prod 8(2):105–112

Wu C-S, Liao H-T (2007) Study on the preparation and characterization of biodegradable polylactide/multi-walled carbon nanotubes nanocomposites. Polymer 48(15):4449–4458

Wu J, Lin J, Zhou M, Wei C (2000) Synthesis and properties of starch-*graft*-polyacrylamide/clay superabsorbent composite. Macromol Rapid Commun 21(15):1032–1034

Wu Z, Feng W, Feng Y, Liu Q, Xu X, Sekino T, Fujii A, Ozaki M (2007) Preparation and characterization of chitosan-grafted multiwalled carbon nanotubes and their electrochemical properties. Carbon 45(6):1212–1218

Wu H, Liu C, Chen J, Chang PR, Chen Y, Anderson DP (2009a) Structure and properties of starch/$\alpha-$zirconium phosphate nanocomposite films. Carbohydr Polym 77(2):358–364

Wu M, Wang M, Ge M (2009b) Investigation into the performance and mechanism of SiO_2 nanoparticles and starch composite films. J Text Inst 100(3):254–259

DOI 10.1007/978-3-319-03751-6_50-1

Wu D, Chang PR, Ma X (2011) Preparation and properties of layered double hydroxide-carboxymethylcellulose sodium/glycerol plasticized starch nanocomposites. Carbohydr Polym 86(2):877–882

Xiao Y, Li CM (2008) Nanocomposites: from fabrications to electrochemical bioapplications. Electroanalysis 20(6):648–662

Xie F, Liu H, Chen P, Xue T, Chen L, Yu L, Corrigan P (2006) Starch gelatinization under shearless and shear conditions. Int J Food Eng 2(5), Article 6/1–29

Xie F, Yu L, Chen L, Li L (2008) A new study of starch gelatinization under shear stress using dynamic mechanical analysis. Carbohydr Polym 72(2):229–234

Xie F, Yu L, Su B, Liu P, Wang J, Liu H, Chen L (2009) Rheological properties of starches with different amylose/amylopectin ratios. J Cereal Sci 49(3):371–377

Xie Y, Chang PR, Wang S, Yu J, Ma X (2011) Preparation and properties of halloysite nanotubes/plasticized *Dioscorea opposita* Thunb. Starch composites. Carbohydr Polym 83(1):186–191

Xie F, Halley PJ, Avérous L (2012) Rheology to understand and optimize processibility, structures and properties of starch polymeric materials. Prog Polym Sci 37(4):595–623

Xie F, Pollet E, Halley PJ, Avérous L (2013) Starch-based nano-biocomposites. Prog Polym Sci 38(10–11):1590–1628

Xie F, Liu P, Yu L (2014) Processing of plasticized starch-based materials: state of art and perspectives. In: Halley PJ, Avérous LR (eds) Starch polymers: from genetic engineering to green applications. Elsevier, Amsterdam, pp 257–289

Xiong H, Tang S, Tang H, Zou P (2008) The structure and properties of a starch-based biodegradable film. Carbohydr Polym 71(2):263–268

Xu Y, Zhou J, Hanna MA (2005) Melt-intercalated starch acetate nanocomposite foams as affected by type of organoclay. Cereal Chem 82(1):105–110

Xue T, Yu L, Xie F, Chen L, Li L (2008) Rheological properties and phase transition of starch under shear stress. Food Hydrocoll 22(6):973–978

Yan L, Chang PR, Zheng P (2011) Preparation and characterization of starch-grafted multiwall carbon nanotube composites. Carbohydr Polym 84(4):1378–1383

Yan Q, Hou H, Guo P, Dong H (2012) Effects of extrusion and glycerol content on properties of oxidized and acetylated corn starch-based films. Carbohydr Polym 87(1):707–712

Yang J, Lin Y, Wang J, Lai M, Li J, Liu J, Tong X, Cheng H (2005) Morphology, thermal stability, and dynamic mechanical properties of atactic polypropylene/carbon nanotube composites. J Appl Polym Sci 98(3):1087–1091

Yang J-H, Yu J-G, Ma X-F (2006a) Study on the properties of ethylenebisformamide and sorbitol plasticized corn starch (ESPTPS). Carbohydr Polym 66(1):110–116

Yang J-H, Yu J-G, Ma X-F (2006b) Preparation of a novel thermoplastic starch (TPS) material using ethylenebisformamide as the plasticizer. Starch-Starke 58(7):330–337

Yang J-H, Yu J-G, Ma X-F (2006c) Preparation and properties of ethylenebisformamide plasticized potato starch (EPTPS). Carbohydr Polym 63(2):218–223

Yang J-H, Yu J-G, Feng Y, Ma X-F (2007) Study on the properties of ethylenebisformamide plasticized corn starch (EPTPS) with various original water contents of corn starch. Carbohydr Polym 69(2):256–261

Yang L, Zhang B, Liang Y, Yang B, Kong T, Zhang L-M (2008) In situ synthesis of amylose/single-walled carbon nanotubes supramolecular assembly. Carbohydr Res 343(14):2463–2467

Yao K, Cai J, Liu M, Yu Y, Xiong H, Tang S, Ding S (2011) Structure and properties of starch/PVA/nano-SiO_2 hybrid films. Carbohydr Polym 86(4):1784–1789

DOI 10.1007/978-3-319-03751-6_50-1

Yu J, Wang N, Ma X (2005a) The effects of citric acid on the properties of thermoplastic starch plasticized by glycerol. Starch-Starke 57(10):494–504

Yu J, Zhang LQ, Rogunova M, Summers J, Hiltner A, Baer E (2005b) Conductivity of polyolefins filled with high-structure carbon black. J Appl Polym Sci 98(4):1799–1805

Yu L, Dean K, Li L (2006a) Polymer blends and composites from renewable resources. Prog Polym Sci 31(6):576–602

Yu L, Kealy T, Chen P (2006b) Study of starch gelatinization in a flow field using simultaneous rheometric data collection and microscopic observation. Int Polym Process 21(3):283–289

Yu J, Yang J, Liu B, Ma X (2009) Preparation and characterization of glycerol plasticized-pea starch/ZnO-carboxymethylcellulose sodium nanocomposites. Bioresour Technol 100(11):2832–2841

Yun Y-H, Hwang K-J, Wee Y-J, Yoon S-D (2011) Synthesis, physical properties, and characterization of starch-based blend films by adding nano-sized TiO_2/poly(methyl metacrylate-*co*-acrylamide). J Appl Polym Sci 120(3):1850–1858

Zamudio-Flores PB, Torres AV, Salgado-Delgado R, Bello-Pérez LA (2010) Influence of the oxidation and acetylation of banana starch on the mechanical and water barrier properties of modified starch and modified starch/chitosan blend films. J Appl Polym Sci 115(2):991–998

Zeng M, Huang Y, Lu L, Fan L, Lourdin D (2011) Effects of filler-matrix morphology on mechanical properties of corn starch-zein thermo-moulded films. Carbohydr Polym 84(1):323–328

Zeppa C, Gouanvé, Espuche E (2009) Effect of a plasticizer on the structure of biodegradable starch/clay nanocomposites: thermal, water-sorption, and oxygen-barrier properties. J Appl Polym Sci 112(4):2044–2056

Zhang X, Golding J, Burgar I (2002) Thermal decomposition chemistry of starch studied by ^{13}C high-resolution solid-state NMR spectroscopy. Polymer 43(22):5791–5796

Zhang Q-X, Yu Z-Z, Xie X-L, Naito K, Kagawa Y (2007) Preparation and crystalline morphology of biodegradable starch/clay nanocomposites. Polymer 48(24):7193–7200

Zhang J-s, Chang PR, Wu Y, Yu J-g, Ma X-f (2008) Aliphatic amidediol and glycerol as a mixed plasticizer for the preparation of thermoplastic starch. Starch-Starke 60(11):617–623

Zhao X, Wang B, Li J (2008) Synthesis and electrorheological activity of a modified kaolinite/carboxymethyl starch hybrid nanocomposite. J Appl Polym Sci 108(5):2833–2839

Zheng X, Wang SS (1994) Shear induced starch conversion during extrusion. J Food Sci 59(5):1137–1143

Zheng X, Chiang W-C, Wang SS (1995) Effect of shear energy on size reduction of starch granules in extrusion. Starch-Starke 47(4):146–151

Zheng P, Chang PR, Yu J, Ma X (2009a) Preparation of Sb_2O_3-carboxymethyl cellulose sodium nanoparticles and their reinforcing action on plasticized starch. Starch-Starke 61(11):665–668

Zheng P, Chang PR, Yu J, Ma X (2009b) Formamide and 2-hydroxy-*N*-[2-(2-hydroxy-propionylamino)-ethyl] propionamide (HPEP) as a mixed plasticizer for thermoplastic starch. Carbohydr Polym 78(2):296–301

Zhou M, Zhao J, Zhou L (2011) Utilization of starch and montmorrilonite for the preparation of superabsorbent nanocomposite. J Appl Polym Sci 121(4):2406–2412

Zobel HF (1988) Molecules to granules: a comprehensive starch review. Starch-Starke 40(2):44–50